"In presenting the dissertation as a partial fulfillment of the requirements for an advanced degree from the Georgia Institute of Technology, I agree that the Library of the Institution shall make it available for inspection and circulation in accordance with its regulations governing materials of this type. I agree that permission to copy from, or to publish from, this dissertation may be granted by the professor under whose direction it was written, or, in his absence, by the dean of the Graduate Division when such copying or publication is solely for scholarly purposes and does not involve potential financial gain. It is understood that any copying from, or publication of, this dissertation which involves potential financial gain will not be allowed without written permission."

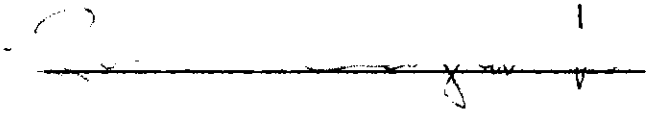

MOLECULAR CONSTANTS OF NITRYL CHLORIDE FROM MICROWAVE SPECTRUM ANALYSIS

A THESIS

Presented to

the Faculty of the Graduate Division

by

Lorimer Clayton, Jr.

In Partial Fulfillment

of the Requirements for the Degree

Doctor of Philosophy in the School

of Physics

Georgia Institute of Technology

June, 1961

MOLECULAR CONSTANTS OF NITRYL CHLORIDE

FROM MICROWAVE SPECTRUM ANALYSIS

Approved:

Date Approved by Chairman: 26 May 1961

ACKNOWLEDGEMENTS

The author is deeply indebted to his advisors, Dr. J. Q. Williams and Dr. T. L. Weatherly, for their guidance and encouragement throughout this investigation. He also greatly appreciates the very helpful advice of Dr. W. H. Eberhardt in matters concerning the chemistry and optical spectra of the molecule.

Major parts of this work were supported by the Office of Ordnance Research and by the Engineering Experiment Station of the Georgia Institute of Technology. The writer's subsequent employer, Scientific-Atlanta, Inc., was also most generous in making time and facilities available for the completion and reproduction of the thesis.

Sincere thanks are extended to Mrs. Margaret Holliman and Mrs. Carolyn Lambert for their painstaking work in typing and illustrating the thesis.

TABLE OF CONTENTS

Page

ACKNOWLEDGEMENTS ii

LIST OF TABLES. v

LIST OF ILLUSTRATIONS vi

SUMMARY vii

Chapter

I. INTRODUCTION 1

Nature of the Spectrum 1
Theoretical Background 3
Published Work on Nitryl Chloride. 8

II. INSTRUMENTATION AND EQUIPMENT 11

Absorption Cell and Vacuum System 13
85-Kilocycle Amplifiers and Detector 13
Spectrum Display System. 15
Frequency Measurement Equipment 15
Square Wave Generator. 18

III. EXPERIMENTAL PROCEDURE AND OBSERVED SPECTRUM. 21

Sample Preparation 21
Spectrum Observation and Measurement 21

IV. ANALYSIS OF THE SPECTRUM. 23

Pure Rotational Spectrum; Rotational Constants 23
Molecular Dimensions 36
Hyperfine Structure; Quadrupole Coupling Constants . . . 39
Stark Effect; Dipole Moment of NO_2Cl^{35} 44

V. DISCUSSION OF RESULTS 53

VI. CONCLUSIONS 62

TABLE OF CONTENTS (Continued)

Page

Appendix

A. THEORY OF THE RIGID ASYMMETRIC ROTOR 66

The Wave Equation 67
Technique of Solution 76
Evaluation of the Hamiltonian Matrix Elements 79
Calculation of Energy Levels 90
Symmetry Properties of the Eigenfunctions 94
Transition Probabilities and Selection Rules 98
Restrictions Imposed by Identical Nuclei. 107

B. THEORY OF NUCLEAR QUADRUPOLE INTERACTIONS IN ASYMMETRIC ROTOR MOLECULES 113

Origin of the Interaction: Classical Viewpoint 113
Quantum Mechanical Treatment. 115
First-Order Theory. 116
Limitations of First-Order Theory 123
Characteristics of Hyperfine Structure 124
Maximum-Likelihood Calculation of Quadrupole Couplings 126
Illustration of Maximum-Likelihood Data Reduction . . . 131

C. THEORY OF THE STARK EFFECT IN ASYMMETRIC-ROTOR MOLECULES 135

Stark Effect in the Absence of Quadrupole Interaction . . 135
Stark Effect in the Presence of Quadrupole Interaction . 145

D. SPECTRUM OF NITRYL CHLORIDE: 25,000-40,600 MC 149

E. EXCITED VIBRATION SPECTRUM 154

BIBLIOGRAPHY 157

VITA 164

LIST OF TABLES

Table		Page
1.	Transition Frequency Relations	25
2.	Rotational Constants Resulting from Application of Planar Rotor Restriction to J: $2 \rightarrow 3$ Transitions	33
3.	Calculated Rotational Energy Levels	34
4.	Difference between Measured and Calculated Group-Center Frequencies	36
5.	Moments of Inertia	39
6.	Quadrupole Coupling Constants from Successive Maximum-Likelihood Fittings	41
7.	Quadrupole Coupling Constants of Nitryl Chloride	44
8.	Measured and Calculated Stark Component Frequencies	47
9.	Measured and Calculated Stark Component Frequencies	48
10.	Stark Effect of $M_F = 7/2$ Component, $2_1 \rightarrow 3_0$ Transition of NO_2Cl^{35}	51
11.	Characteristics of Contributing Bond Structures	59
12.	Symmetry Classification of Asymmetric Rotor Eigenfunctions	97
13.	Symmetry Selection Rules	105
14.	Coefficients for Evaluation of Quadrupole Interaction Energies in Asymmetric-Rotor Molecules	120
15.	Spectrum of Nitryl Chloride; 25,000 - 40,600 Mc	150

LIST OF ILLUSTRATIONS

Figure		Page
1.	Block Diagram of Spectrograph	12
2.	Apparatus for Admitting Gas into the Cell at a Controlled Pressure	14
3.	Circuit Diagram of Phase-Sensitive Detector	16
4.	Diagram of Waveform Clamping Circuit for Square-Wave Generator	19
5.	Functional Constraints upon the Rotational Constants of NO_2Cl^{35}	28
6.	Functional Constraints upon the Rotational Constants of NO_2Cl^{37}	29
7.	Molecular Geometry	37
8.	The $J = 2_1 \rightarrow 3_0$ Transition of NO_2Cl^{35} Showing the Stark Components for an Electric Field of 515 Volts/cm	45
9.	Behavior of $M_F = 7/2$ Stark Component for $J = 2_1 \rightarrow 3_0$ Transition of NO_2Cl^{35}	50
10.	Euler Angles Relating a Body-Fixed Coordinate System to Space-Fixed Axis	68
11.	Normal Modes of Vibration of Nitryl Chloride	111

SUMMARY

The microwave spectrum of nitryl chloride has been studied in the region 25,000 to 40,600 Mc. Three J: 2 → 3 and three J: 3 → 4 transitions were examined for each of the two abundant molecular isotopic species; the J_τ: $4_{-4} \rightarrow 5_{-5}$ transition of NO_2Cl^{37} was observed in addition. The following molecular parameters were established.

	NO_2Cl^{35}	NO_2Cl^{37}
Rotational Constants (Mc)		
A	13,250	13,250
B	5,173.77	5,018.97
C	3,721.13	3,640.35
Quadrupole Coupling Constants (Mc)		
χ_{aa}	-94.70	-74.58
χ_{bb}	52.4	41.3
χ_{cc}	42.3	33.3
Dipole Moment (debye)		
μ	0.533 ± 0.01	

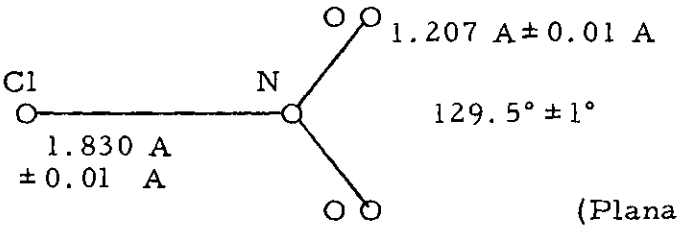

(Planar)

Implications of these results are discussed. The molecule may be of interest to bond theorists because of its rather large N-Cl distance, large quadrupole coupling constants, and small dipole moment. These features restrict the latitude of bond parameter adjustment to a greater degree than in most other compounds.

CHAPTER I

INTRODUCTION

In recent years the refinement of apparatus for generation, transmission, and detection of microwave radiation has made possible spectroscopic studies in a frequency region in which many molecular gases exhibit pure rotational absorption spectra. Analyses of these spectra and their hyperfine structures permit determination of important molecular constants, including bond distances and angles, molecular dipole moments, and electric field gradients at the positions of certain nuclei. Widespread activity has been directed toward amassing a large body of such experimental data, which as a testing ground for theory is expected to lead to a better understanding of the chemical bond. This thesis reports a determination of these constants for nitryl chloride (NO_2Cl) through compilation and analysis of its microwave spectrum in the region 25,000 to 40,600 megacycles.

Nature of the Spectrum

Nitryl chloride is a planar, Y-shaped molecule in which a central nitrogen nucleus is bonded to a chlorine and two oxygen nuclei. The gross features of its microwave absorption spectrum can be predicted by regarding the molecular structure as a rigid framework and applying the quantum-mechanical treatment of the rotation of an asymmetric top. Absorptions are attributed to transitions induced between quantized

rotational energy levels by interaction of the molecular electric dipole moment with the radiation electric field. Selection rules governing such interactions prescribe particular pairs of energy levels between which transitions are allowed; the absorption frequency corresponding to each transition is related to the energy difference between levels by the Bohr rule, $\Delta E = h\nu$. Fitting of calculated transition frequencies to the observed spectrum permits evaluation of the moments of inertia of the molecular framework, and from them, bond distances and angles.

Prediction of the more detailed features of the spectrum requires consideration of the electric quadrupole moment of the chlorine nucleus, which interacts with the electric field gradient produced at the nucleus by all other charges in the molecule. Each allowed orientation of the chlorine nuclear spin relative to the molecular rotational angular momentum is characterized by a unique interaction energy, which adds algebraically to the rotational energy. Because of this splitting of rotational levels the spectrum exhibits a hyperfine structure; each rotational transition appears as a group of several lines. Fitting of the hyperfine splitting permits calculation of quantities proportional to the electric field gradient at the chlorine nucleus.

When an external electric field is applied to the gas there is an additional interaction between the applied field and the molecular electric dipole moment, the Stark effect. The different values of the interaction energy for the various allowed average orientations of the molecule relative to the field cause futher splitting and displacement of the hyperfine component lines. Fitting of this Stark spectrum permits evaluation of the molecular electric dipole moment.

Theoretical Background

The theoretical basis for analysis of the field-free rotational spectrum of an asymmetric-top molecule with nuclear quadrupole interaction is now well established. The Stark effect for such molecules, however, has not yet been worked out completely for all cases. In the following sections the history of applicable theoretical work is reviewed and symbols used in the sequel are introduced. Results of theory and their applications are discussed in greater detail in Appendices A, B, and C.

Rotational energy of an asymmetric top.--The Hamiltonian for a rigid rotor is $H_r = \frac{1}{2}(P_a^2/I_a + P_b^2/I_b + P_c^2/I_c)$, where P_a, P_b, P_c are the components of the total angular momentum along the principal axes of inertia, and $I_a \leq I_b \leq I_c$ are the moments of inertia about these axes. The wave equation $(H_r - E_r)\psi_r = 0$ can be solved in a straightforward manner for the symmetric rotor, where two of the moments of inertia are equal. The resulting states are characterized by three quantum numbers: J, corresponding to the total rotational angular momentum; K, corresponding to the component of angular momentum along the molecular symmetry axis, and M, corresponding to the component of angular momentum along a space-fixed axis. Solution for the asymmetric rotor, however, is complicated by the fact that the wave equation does not separate in simple coordinate systems.

A comprehensive treatment of the asymmetric rotor was given in 1929 by Wang (1), who developed simple expressions for matrix elements of H_r evaluated with symmetric-rotor wavefunctions. The resulting H_r matrix is independent of M and is diagonal in J; for each

J there is a (2J + 1) by (2J + 1) submatrix which may be diagonalized to find allowed energies. No quantum number with physical meaning distinguishes among the (2J + 1) roots; in one commonly used notation they are identified by the symbol J_τ, where the index integer τ runs from -J to +J in order of increasing energy.

The problem of solving the secular determinant for given J can always be simplified by factoring it into smaller determinants (four, for $J \geq 2$). That this can be done is a consequence of symmetry properties of the rotational wavefunctions, which must remain unchanged or at most change sign when the momental ellipsoid is subjected to a 180° rotation about a principal axis; each smaller determinant involves states whose wavefunctions have the same behavior with respect to such rotations. For $J \leq 3$ the resulting equations, of second degree at most, can be solved exactly for all allowed energies in terms of three rotational constants: $A = h/(8\pi^2 I_a)$, $B = h/(8\pi^2 I_b)$, and $C = h/(8\pi^2 I_c)$. Certain roots for J = 4, 5 can be found similarly, but for larger J the increasing degree of the equations leads to computational difficulties.

It was shown by Ray (2) in 1932 that the energy levels of any asymmetric rotor can be expressed in terms of dimensionless "reduced energies" calculated from secular equations involving only the asymmetry parameter $\kappa = (2B - A - C)/(A - C)$. In 1942 King, Hainer, and Cross (3) expressed the roots of these equations in the form of continued fractions, suitable for numerical evaluation. They published tables from which the reduced energies of any asymmetric rotor for $J \leq 10$ may be determined approximately by interpolation.

Nuclear quadrupole interaction energy.--A quantum-mechanical treatment of the interaction between a nuclear electric quadrupole and a surrounding charge distribution was given in 1936 by Casimir (4), who analyzed the hyperfine structure of atomic spectra. His characteristic values of the first-order interaction energy can be written $E_q = eq_J Q\, f(I, J, F)$, where e is the electronic charge and Q is the quadrupole moment of the nucleus. The quantity q_J is the second derivative of the electric potential at the nucleus with respect to distance along the axis of electronic angular momentum, averaged over the motion of the atomic electrons. The "Casimir function" f(I,J, F) is a tabulated quantity, a dimensionless rational fraction involving the nuclear spin quantum number I, the total electronic angular momentum quantum number J, and the quantum number of their resultant, F.

The situation considered by Casimir is identical to that encountered in molecular rotational spectra, except that the angular momentum represented by J becomes that of the rotation, and q_J must be evaluated by averaging over the molecular motion. Several methods of determining q_J for an asymmetric-top molecule were developed by Bragg and Golden (5, 6) in 1948. Their theory expresses quadrupole interaction energies in terms of three quadrupole coupling constants: $\chi_{aa} = eQ(\partial^2 V/\partial a^2)$, $\chi_{bb} = eQ(\partial^2 V/\partial b^2)$, $\chi_{cc} = eQ(\partial V^2/\partial c^2)$. The derivatives are those of the electric potential at the nuclear position, taken with respect to the principal axes. These χ's, generally expressed in megacycles, are measured experimentally by analysis of the hyperfine structure.

Stark-effect interaction energy.--The Hamiltonian operator for a molecule in an external electric field includes the perturbation term $H_s = -\mu\mathcal{E}\cos\alpha$, representing the energy of an electric dipole moment μ oriented at an angle α with respect to a field of strength $\mathcal{E}$. The resulting level-splitting for an asymmetric-top molecule without quadrupole interaction was worked out by Golden and Wilson (7) in 1948. The matrix of H_s, evaluated with asymmetric-rotor wavefunctions, is diagonal in M. Because the submatrix for each M has no elements on the diagonal, there is no first-order energy perturbation. Off-diagonal elements connect all states $J_\tau M$, J'_τ, M between which radiation-induced transitions are allowed. Application of the second-order energy expression of conventional nondegenerate perturbation theory gives, for each M of a selected J_τ, a Stark-effect interaction energy proportional to the square of the electric field strength.

An extension of the theory of asymmetric-rotor Stark effect to include nuclear quadrupole interaction was carried out by Mizushima (8) in 1952. When Stark and hyperfine splittings are of the same order of magnitude it is necessary to construct and diagonalize the matrix of the combined perturbation $H_s + H_q$, where H_q is the Hamiltonian operator of Casimir. The perturbation matrix proposed by Mizushima is diagonal in J_τ. Elements of H_q are evaluated with the unperturbed wavefunctions of the rotor and the nucleus for no coupling between $\underline{J}$ and $\underline{I}$; such wavefunctions are characterized by J, τ, M, I, and the quantum number m representing the component of $\underline{I}$ along a space-fixed axis. Only diagonal matrix elements of H_s are included, and these are taken to be simply the second-order Stark-effect energies of the rotor without

$\underline{J} - \underline{I}$ coupling. The justification for this procedure has been discussed in detail by Eagle (9). The resulting matrix is further diagonal in the sum M + m, so that it may be factored into submatrices for convenience in numerical evaluation of the perturbation energies.

A complication arises in the evaluation of the Stark-effect splitting of a rotational level whose energy is not greatly different from that of an adjacent level. Even in the most asymmetric rotors there are numerous pairs of such near-degenerate states, states which would be completely degenerate in a symmetric rotor. Application of an electric field causes a relatively large intermixing of the wavefunctions of the closely spaced states, and the second-order perturbation treatment becomes inaccurate. The importance of the near-degenerate case was correctly assessed by Golden and Wilson in their analysis of the rotor without quadrupole interaction. However, the situation was not considered by Mizushima, and no discussion of near-degeneracy in the presence of quadrupole interaction appears in the literature. To avoid the labor involved in the direct diagonalization of the entire matrix of $H_r + H_s$, Golden and Wilson developed a contact transformation which may be applied to the matrix to separate the strong interactions between neighboring states from the weaker interactions with more remote states. The weaker interactions can then be handled by the second-order theory, leaving only the strong interactions to be treated by matrix diagonalization. Adaptation of this procedure to the quadrupole-interaction problem has been undertaken recently by Eagle (10).

Published Work on Nitryl Chloride

Early chemical investigations of nitryl chloride have been reviewed by W. A. Noyes (11). Although its discovery was claimed in 1862 by Müller (12), it remained an obscure compound of questioned existence until 1929, when high-yield preparation processes were developed by Dachlauer (13) and by Schumacher and Sprenger (14). Even recent chemical work, however, gave ambiguous evidence as to the structure of the molecule. Schmeisser (15), for example, interpreted the formation of chloramine in the reaction of nitryl chloride with ammonia as an indication of the existence of the irregular structure O=N-O-Cl, but this conclusion was contested by Batey and Sisler (16).

The infrared and ultraviolet absorption spectra of nitryl chloride have been investigated by Athey and Eberhardt (17, 18), and the infrared absorption and the Raman spectra have been studied by Ryason and Wilson (19). The analysis by Ryason and Wilson established that the chlorine bond is to the nitrogen nucleus, but did not indicate whether the structure is planar or pyramidal.

In 1955 Millen and Sinnott (20) reported a determination of the rotational constants of NO_2Cl^{35} from its $0_0 \rightarrow 1_{-1}$, $1_{-1} \rightarrow 2_{-2}$, and $2_{-2} \rightarrow 3_{-3}$ microwave transitions, and mentioned observation of numerous other lines in the region from 8500 to 27, 500 megacycles. A planar molecular form with oxygen atoms situated symmetrically with respect to the axis of least moment of inertia was established conclusively by the absence of transitions involving energy levels antisymmetric with

respect to π-rotation about that axis.[†] From the infrared data it was inferred that the molecule is Y-shaped. Rotational constants were reported to be A = 13,012 Mc, B = 5,164.7 Mc, C = 3,730.5 Mc. These values are inaccurate; it appears that they were determined from the three reported transitions alone, which allow a latitude of several hundred megacycles in the choice of the constant A.

Early results of the present investigation were reported in 1956 (21). The quadrupole coupling constants $\chi_{aa} = -94.7$ Mc, $\chi_{bb} = 52.2$ Mc, $\chi_{cc} = 42.5$ Mc, (NO_2Cl^{35}), and $\chi_{aa} = -74.6$ Mc, $\chi_{bb} = 41.1$ Mc, $\chi_{cc} = 33.5$ Mc (NO_2Cl^{37}), were determined by statistical fitting of the three J: 2 → 3 transitions of each isotope. They predicted accurately the observed splittings of the J: 3 → 4 transitions also. The inadequacy of the microwave data for determining rotational constants was pointed out, and it was proposed that the planar-rotor approximation $I_c - I_a - I_b = 0$ be imposed as an additional restriction. A 1957 report (22) covering the government-supported phase of the study gave the following rotational constants, determined in that manner: A = 13,250 Mc, B = 5173.8 Mc, C = 3721.1 Mc (NO_2Cl^{35}), and A = 13,250 Mc, B = 5,019.0 Mc, C = 3,640.4 Mc (NO_2Cl^{37}). From these constants the molecular dimensions d(N-O) = 1.21 A, d(N-Cl) = 1.83 A, ∠ ONO = 129.5° were calculated. Analysis of the Stark effect of the J_τ: $2_1 \rightarrow 3_0$ transition of NO_2Cl^{35} established a dipole moment of 0.53 debye.

In 1958 Millen and Sinnott reported their work in greater detail (23). Rotational constants were given as A = 13,239.96 Mc, B =

[†] The nature of this exclusion is discussed in Appendix A.

5,173.78 Mc, C = 3,721.37 Mc (NO_2Cl^{35}), and A = 13,240.0 Mc, B = 5,019.00 Mc, C = 3,640.49 Mc (NO_2Cl^{37}). The revision was attributed to their identification of the J_τ: $6_{-3} \rightarrow 6_{-2}$ transition of NO_2Cl^{35} at approximately 9,975 Mc. However, this transition still allows a latitude of several tens of megacycles in the choice of the constant A; the planar rotor restriction seems preferable. Molecular dimensions and quadrupole coupling constants were also reported; they are in general agreement with those found in the present study, but here also a difference of opinion exists as to the number of significant figures justifiably retained in the result. A dipole moment of 0.42 ± 0.01 debye was surmised from application of weak-field theory to the Stark effect of the J_τ: $0 \rightarrow 1_{-1}$ transition of NO_2Cl^{35}. This result appears erroneous; it was obtained from a single Stark line, consisting of two unresolved components, whose maximum displacement from its parent line was 2.9 Mc. The measured displacements reported do not exhibit the quadratic dependence upon the field strength required by the theory employed.

A more nearly complete account of the present work was given in 1959 (24). Final values of the quadrupole coupling constants were $\chi_{aa} = -94.70$ Mc, $\chi_{bb} = 52.4$ Mc, $\chi_{cc} = 42.3$ Mc (NO_2Cl^{35}), and $\chi_{aa} = -74.58$ Mc, $\chi_{bb} = 41.3$ Mc, $\chi_{cc} = 33.3$ Mc (NO_2Cl^{37}). Other constants were the same as those reported earlier. Transitions attributed to molecules in an excited vibration state were discussed briefly. Features of the N–Cl bond were pointed out that might make it of interest to those concerned with overlap effects in molecular bond theory.

CHAPTER II

INSTRUMENTATION AND EQUIPMENT

Figure 1 shows a block diagram of the Stark-modulation spectrograph used for observation and measurement of absorption lines. It is similar to one described by Hughes and Wilson (25).

Microwave energy from a klystron signal source is directed through a waveguide absorption cell, cooled by dry ice and filled with the sample gas under low pressure. An 85-kilocycle square-wave voltage, applied to a flat strip electrode centered within the waveguide, produces an electric field parallel to that of the microwave radiation. The alternate presence and absence of Stark splitting causes intensity modulation of the absorption which occurs when the klystron frequency coincides with that of a molecular transition. This modulation is detected by a crystal diode mounted at the end of the absorption cell. After amplification it is applied to a phase-sensitive second detector, where its phase is compared with that of the square-wave voltage. Absorptions which occur during the field-on half-period produce a negative output signal, while those occurring during the field-off interval produce a positive output; the Stark spectrum is thus distinguished from the unperturbed spectrum.

Absorption lines may be displayed either by sweeping the klystron frequency electrically and viewing the detector output on an oscilloscope, or by tuning the klystron slowly with an electric motor while recording the output signal on a recording milliammeter.

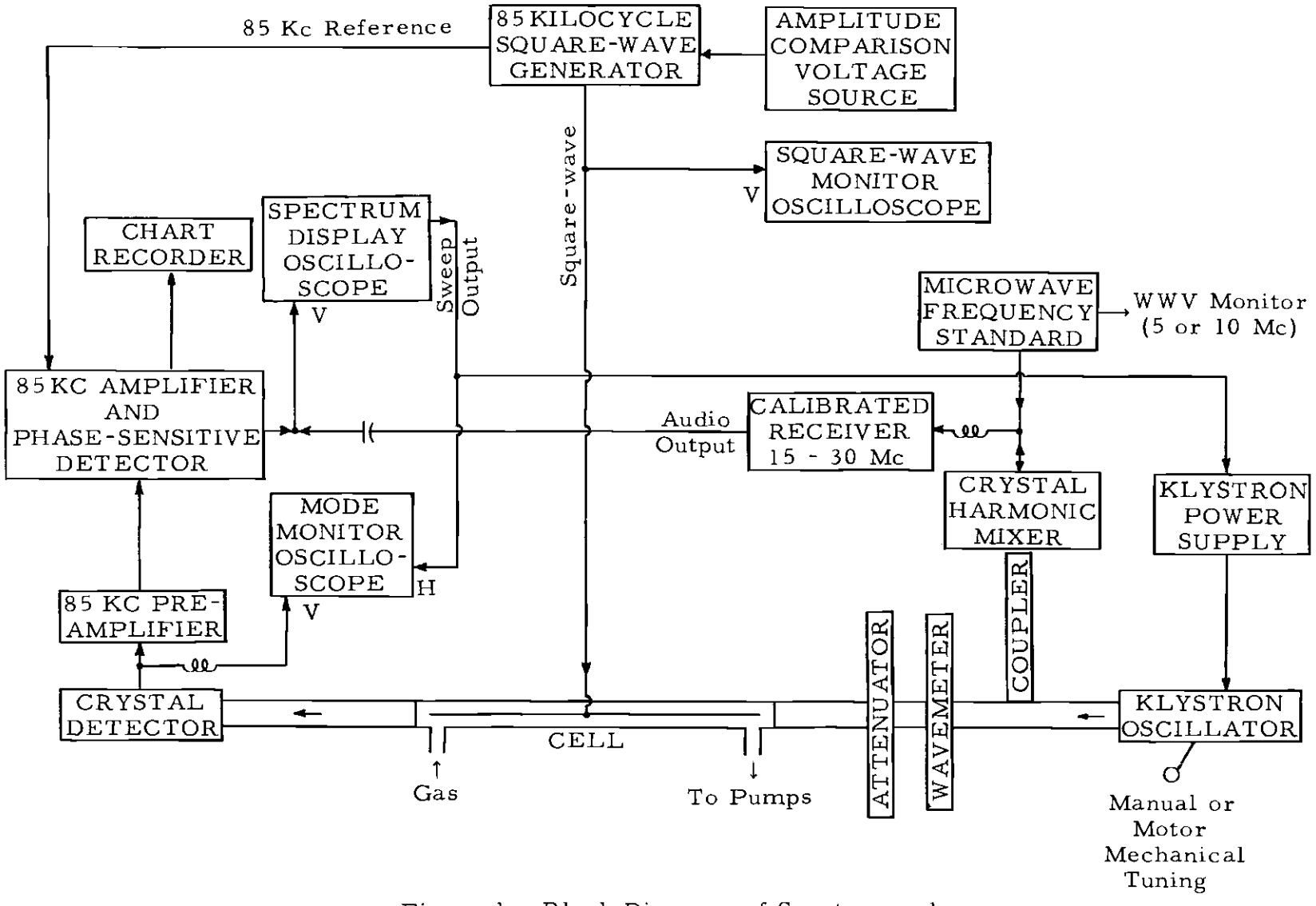

Figure 1. Block Diagram of Spectrograph.

For measurement of absorption line frequencies, marker signals are generated at 30 Mc intervals throughout the microwave region by a crystal-controlled frequency standard; the frequency separation between the klystron signal and a nearby marker is determined by a calibrated communications receiver.

Important components of the microwave spectrograph are discussed in greater detail in the following sections.

Absorption cell and vacuum system.--The absorption cell consists of a seventeen-foot section of X-band waveguide, sealed at each end by mica windows and connected to the glass tubing of the vacuum system through sylphon bellows couplings. A wooden trough surrounding the cell is filled with dry ice for cooling.

Gas is admitted continuously at the detector end of the cell through the pressure-reducing capillary constriction shown in Figure 2. An oil-diffusion pump at the other end maintains a constant low pressure, which can be varied over the range from about four to fifty microns by adjusting the depth of immersion of the liquefied gas sample in the cooling bath.

The Stark field electrode is supported within the waveguide by grooved teflon strips at its edges. The effective spacing between the electrode and the walls of the guide, as determined by measurements of the Stark effect in carbonyl sulfide, is 0.467 centimeters.

85-kilocycle amplifiers and detector.--The absorption modulation signal is applied to a cascode preamplifier developed by Good (26), followed by a tuned lock-in amplifier designed by Williams and described by Gordy, et al. (27). The phase-sensitive detector in the latter instrument has

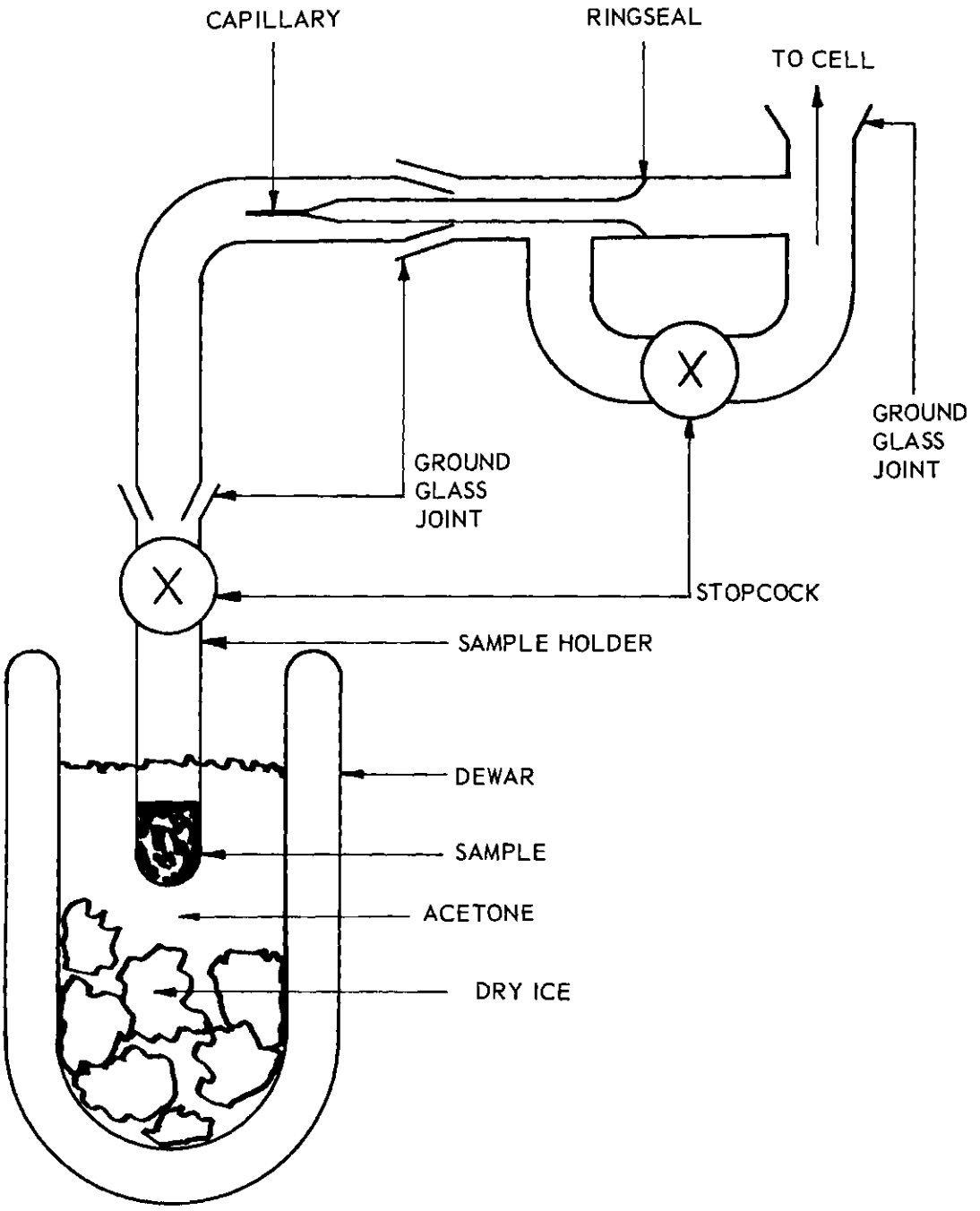

Figure 2. Apparatus for Admitting Gas into the Cell at a Controlled Pressure.

been replaced by the circuit shown in Figure 3, which provides greater sensitivity and stability.

Spectrum display system.--Lines of moderate intensity are most conveniently observed by applying the output of the phase-sensitive detector to the vertical deflection amplifier of an oscilloscope, while sweeping the klystron frequency with a sample of the oscilloscope sawtooth waveform applied to the repeller electrode. For weaker lines the signal-to-noise ratio can be greatly enhanced by using an external capacitor to increase the time-constant of the detector filter and sweeping very slowly. However, the extent to which this procedure can be pressed is limited by the persistence of the phosphor screen. Where greatest sensitivity is required the output of the detector is recorded on an Esterline-Angus graphic milliammeter while the klystron is slowly tuned mechanically by an electric motor drive. Filter time-constants on the order of several seconds can then be used.

Frequency measurement equipment.--Frequency measurements are made in a manner similar to that described by Unterberger and Smith (28). The microwave frequency standard employs a 5.0 megacycle crystal-controlled oscillator, followed by vacuum tube multipliers which generate harmonic frequencies of 30, 90, 270, 540, 1080, and 2160 Mc. A mixture of these frequencies is applied through a coaxial cable to a 1N26 multiplier-mixer diode mounted in a waveguide crystal holder, producing standard marker signals at 30-megacycle intervals throughout the microwave region. A sample of the klystron signal, impressed across the crystal through the waveguide, heterodynes with the marker signals. A heterodyne component in the frequency range 15 to 30 Mc,

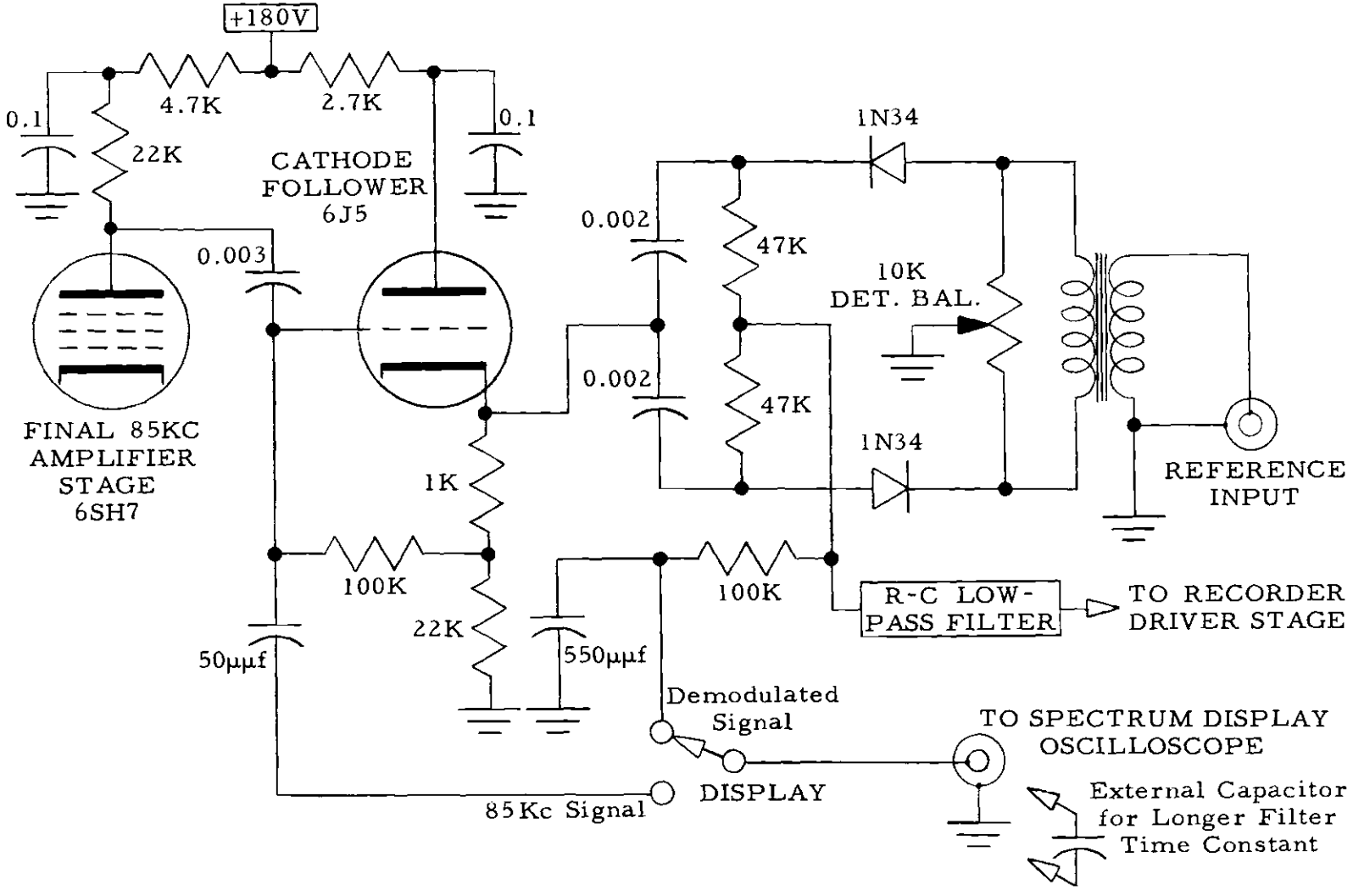

Figure 3. Circuit Diagram of Phase-Sensitive Detector.

recovered from the coaxial crystal terminal through a small isolating inductance, is detected and measured with a calibrated National HRO Sixty communications receiver. The particular marker involved is identified by measuring the klystron frequency approximately with an absorption-type cavity wavemeter. If necessary for positive identification, the 30-megacycle standard frequency may be switched off to increase the marker spacing to 90 megacycles.

Measurement of the frequency of a line displayed on the oscilloscope is accomplished by superimposing the audio output signal of the receiver upon the detector signal at the oscilloscope terminals. When the heterodyne signal sweeps through the passband of the receiver a sharp spike appears on the oscilloscope trace. The receiver tuning is adjusted so that the spike occurs at the peak of the absorption and the heterodyne frequency is noted from the receiver calibration chart. In this operation the slight time delay suffered by the absorption line in the detector output filter causes a small displacement of the line peak from its true position; consequently, a switch is provided to invert the sawtooth sweep waveform so that the absorption is traversed from the opposite direction. The apparent displacement of the line is then of the same magnitude but opposite in sign. The average of ten or more measurements made for alternate sweep directions is recorded as the frequency separation between line and marker.

Spectrum recordings made on the graphic milliammeter can be calibrated by actuating a relay-operated marking pen at one-megacycle intervals. The operator tunes the receiver manually to successive

integral-megacycle frequencies and depresses the pen switch when he hears the heterodyne signal in the monitor loudspeaker. The primary use of such calibrated recordings is in the measurement of Stark spectra.

Square wave generator.--The 85-kilocycle square wave generator is one constructed by Mauldin (29) following the circuit design of Hedrick and Williams (30). It is capable of developing a waveform amplitude of up to 1000 volts across a Stark cell and cable capacity of about 1800 $\mu\mu$f.

To facilitate accurate measurement of Stark voltages, the waveform clamping circuit of this instrument has been modified to that shown in Figure 4. It consists of a type 8020 clamping diode, a regulated power supply delivering a variable reference voltage, a precision voltmeter, and a monitor oscilloscope whose vertical deflection plates are connected directly across the Stark cell. The diode clamps the positive excursion of the square wave to a potential substantially equal to that of its cathode. In normal operation the cathode is returned to a small potential, adjustable about ground by means of the ZERO potentiometer, which cancels a slight potential difference between the diode electrodes. The control is adjusted so that the top of the square wave coincides with a horizontal ruling on the oscilloscope screen which represents ground potential, the position of the trace with the deflection plates shorted. For measurement of the waveform amplitude the reference voltage source is connected in series with the cathode return circuit. The magnitude of the reference voltage is adjusted to shift the position of the waveform upward on the oscilloscope screen so that its negative excursion coincides with the ground-potential ruling. The

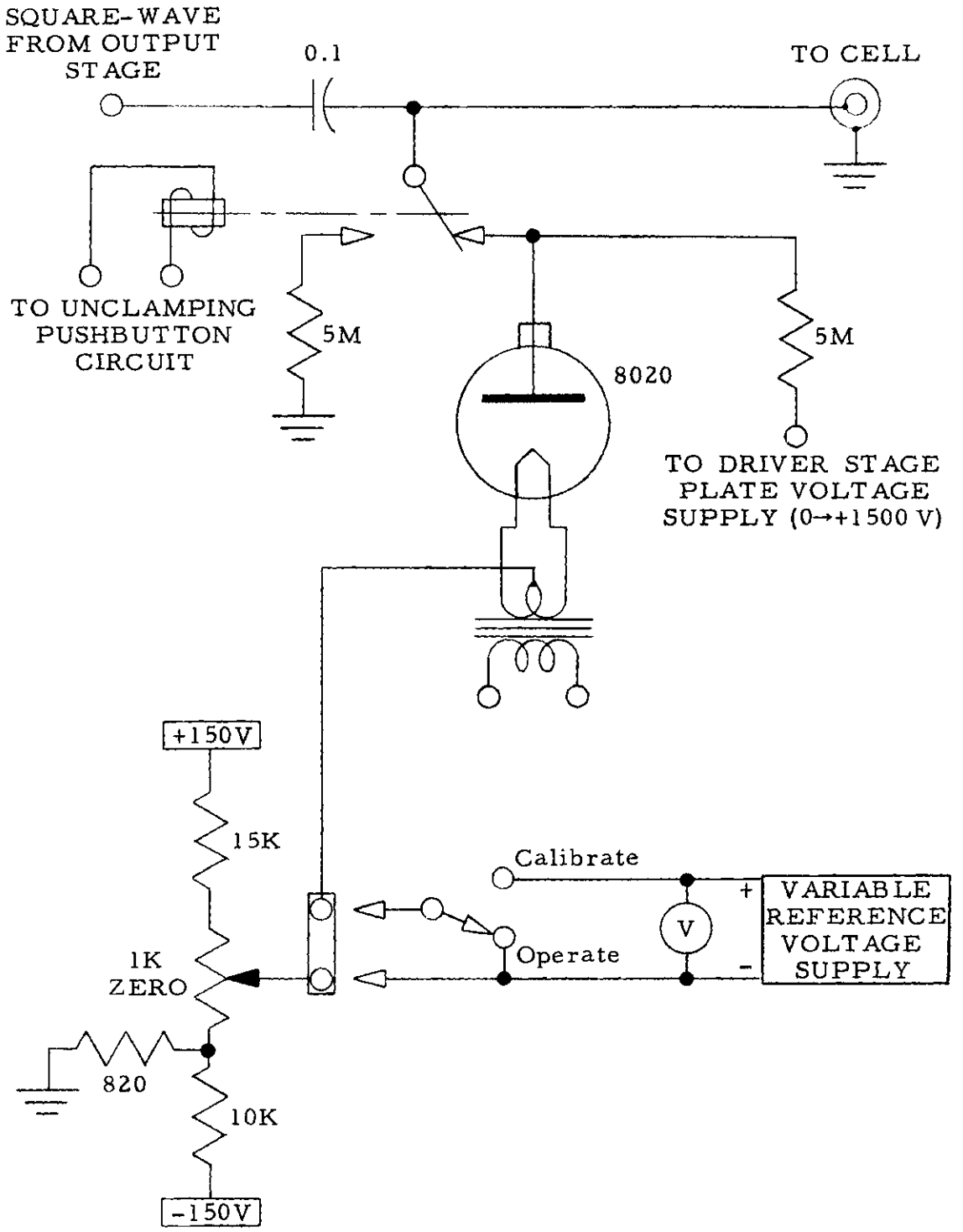

Figure 4. Diagram of Waveform Clamping Circuit for Square-Wave Generator.

waveform amplitude is then equal to the reference voltage, as indicated by the precision voltmeter.

A pushbutton-operated relay to disconnect the clamping circuit is retained from the Williams design. By allowing the square wave to become balanced about ground, it removes the Stark modulation of absorption lines without changing the waveform amplitude. This arrangement is helpful in distinguishing a weak line from background noise and stray pickup of the square-wave signal; operation of the relay causes a line to disappear while the noise remains the same.

CHAPTER III

EXPERIMENTAL PROCEDURE AND OBSERVED SPECTRUM

Sample preparation.--Nitryl chloride was prepared through the reaction of chlorosulfonic acid and anhydrous nitric acid, as in the Dachlauer process (13). A mixture of freshly distilled nitric acid and an equal amount of fuming sulfuric acid was added dropwise to distilled chlorosulfonic acid in a flask cooled by an ice bath. The nitryl chloride gas evolved was collected in a receiver cooled by dry ice in alcohol. A similar procedure is described in detail by Schechter, et al. (31).

The sample, a pale yellow liquid, was allowed to distill into a previously evacuated sample holder (Figure 2) immersed in liquid nitrogen. After the transfer was complete residual air was pumped away from the frozen sample. The holder was stored in a dry ice-acetone bath.

Spectrum observation and measurement.--Searches of the region 25,000 to 41,000 Mc were made at Pirani-gauge pressures on the order of 50 microns, with the cell cooled by dry ice. The oscilloscope spectrum display was used. Thirteen groups of lines were observed, identified by the methods discussed in the next chapter as the $2_{-2} \rightarrow 3_{-3}$, $2_{1} \rightarrow 3_{0}$, $2_{2} \rightarrow 3_{1}$, $3_{-3} \rightarrow 4_{-4}$, $3_{0} \rightarrow 4_{-1}$, and $3_{1} \rightarrow 4_{0}$ transitions of the isotopic species NO_2Cl^{35} and NO_2Cl^{37}, and the $4_{-4} \rightarrow 5_{-5}$ transition of NO_2Cl^{37}. These transitions exhibit quadrupole-interaction hyperfine structure due to the chlorine nucleus only; splittings due to the nitrogen nucleus

were too small to resolve. Each transition has four strong principal lines, and several have three additional weak lines. The measured frequencies of 65 lines are listed in Appendix D.

Frequency measurements were made at pressures of 4 to 15 microns, using the oscilloscope display system. Line widths were approximately 4.0 Mc between the half-amplitude points. Where frequencies are listed to 0.01 Mc, it is estimated that measurement errors seldom exceed 0.05 Mc and are more often around 0.02 Mc. Where difficulty was encountered in resolving weak lines from noise or from adjacent strong lines, frequencies are listed to 0.1 Mc.

Sensitivity to Stark-effect splitting varies markedly among transitions. Transitions involving the 2_1 and 2_2 levels exhibit the greatest sensitivity; electric fields of 200 to 300 volts cm are sufficient to cause complete displacement of all Stark components from their parent lines. The $3_0 \rightarrow 4_{-1}$ and $3_1 \rightarrow 4_0$ transitions are intermediate in sensitivity; they show splitting at less than 200 volts/cm, yet resolution of components is not complete at 1500 volts/cm. The remaining transitions are quite insensitive, requiring fields of around 1500 volts/cm to produce sufficient splitting for observation and accurate measurement of their lines. Calibrated recordings were made of the $2_1 \rightarrow 3_0$ transition of NO_2Cl^{35} for the Stark-effect analysis presented in the next chapter.

In addition to the strong absorption lines of the primary spectrum, a careful search with the recording milliammeter disclosed eight groups of weaker lines. These lines, attributed to absorptions by molecules in an excited vibration state, are listed and discussed in Appendix E.

CHAPTER IV

ANALYSIS OF THE SPECTRUM

Theoretical work upon which the following analysis is based has been reviewed briefly in Chapter I. Results of theory and methods of application are presented in greater detail in Appendix A (pure rotational spectra), Appendix B (hyperfine structure), and Appendix C (Stark effect), to which the reader may refer as necessary.

Pure rotational spectrum; rotational constants.--To facilitate identification of lines observed in a preliminary search of the region from 25,000 to 30,000 megacycles, a predicted spectrum was first compiled from rotational constants estimated for an assumed Y-shaped planar structure with internuclear distances comparable to those found in other compounds. The observed lines fell in a pattern resembling that predicted for the J: 2 → 3 transitions, but their frequencies were roughly 1000 Mc lower than predicted. Before sufficient data had been gathered to permit an adjustment of rotational constants, Millen and Sinnott reported (in 1955) the values listed on page 9 for NO_2Cl^{35}. A revised NO_2Cl^{35} spectrum calculated from these constants was found to be in quite accurate agreement with experiment, permitting ready identification of the J: 3 → 4 transitions subsequently observed.

An improved prediction of the NO_2Cl^{37} spectrum was obtained by using the NO_2Cl^{35} constants to refine the assumed molecular structure. Estimates of d(N - O) = 1.22 A and ∠(ONO) = 127.5 degrees were

considered reliable because they are close to the corresponding dimensions in CH_3NO_2 (32) and in other compounds; the greatest uncertainty was in the N-Cl distance. The assumed configuration of the O-N-O group was therefore retained, and the value d(N-Cl) = 1.81 A was calculated from equation 9, using I_b^{35} = 97.882 amu A^2 from Millen and Sinnott (20). Substitution of the Cl^{37} nuclear mass in the resulting structure gave the rotational constants A^{37} = 13,012 Mc, B^{37} = 5,010.5 Mc, and C^{37} = 3,649.5 Mc. Group-center (pure rotational) frequencies of the J: 2 → 3 and J: 3 → 4 transitions calculated from these constants were within eight megacycles of the measured frequencies.

The determination of rotational constants was re-examined after treatment of the hyperfine splitting had permitted accurate evaluation of group-center frequencies for all J: 2 → 3 and J: 3 → 4 transitions. These "measured group-center frequencies" are listed in Appendix D; they were obtained by subtracting the calculated quadrupole-interaction shift of each hyperfine component from its measured frequency and averaging. Relationships between transition frequencies and rotational constants can be established from the expressions given by Gordy, Smith, and Trambarulo (33) for low-J rotational energies as explicit functions of A, B, and C. These expressions lead to those in Table 1 for the frequencies of pertinent nitryl chloride transitions. Rotational constants can be obtained by substitution of observed group-center frequencies and simultaneous solution of appropriate sets of the equations.

Table 1. Transition Frequency Relations

(a) $\nu(0_0 \rightarrow 1_{-1}) = B + C$

(b) $\nu(1_{-1} \rightarrow 2_{-2}) = 2A + B + C - 2\left[(B - C)^2 + (A - C)(A - B) \right]^{\frac{1}{2}}$

(c) $\nu(2_{-2} \rightarrow 3_{-3}) = 3(B + C) - 2 \left\{ \left[4(B - C)^2 + (A - B)(A - C) \right]^{\frac{1}{2}} - \left[(B - C)^2 + (A - B)(A - C) \right]^{\frac{1}{2}} \right\}$

(d) $\nu(2_1 \rightarrow 3_0) = 3(B + C)$

(e) $\nu(2_2 \rightarrow 3_1) = 3(B + C) + 2 \left\{ \left[4(B - C)^2 + (A - B)(A - C) \right]^{\frac{1}{2}} - \left[(B - C)^2 + (A - B)(A - C) \right]^{\frac{1}{2}} \right\}$

(f) $\nu(3_0 \rightarrow 4_{-1}) = 6A + B + C - 2\left[4(B - C)^2 + 9(A - B)(A - C) \right]^{\frac{1}{2}}$

The expressions listed in Table 1 include two linear-combination interrelations among transition frequencies which must hold for any rigid rotor with arbitrary rotational constants: from (a) and (d), $\nu(2_1 \rightarrow 3_0) = 3\nu(0_0 \rightarrow 1_{-1})$; from (c), (d), and (e), $\nu(2_{-2} \rightarrow 3_{-3}) + \nu(2_2 \rightarrow 3_1) = 2\nu(2_1 \rightarrow 3_0)$. From the six transitions one therefore can extract only four separate constraints upon A, B, and C. The following form a convenient set. From (d),

$$(B + C) = \frac{1}{3}\nu(2_1 \rightarrow 3_0) , \tag{1}$$

or for better statistical data-smoothing, from (c), (d), and (e),

$$(B + C) = \frac{1}{9}[\nu(2_1 \rightarrow 3_0) + \nu(2_{-2} \rightarrow 3_{-3}) + \nu(2_2 \rightarrow 3_1)] . \tag{1'}$$

From (b),

$$(B - C) = \left[\frac{1}{3}(2\nu_o - \nu_1)(4A - \nu_1)\right]^{\frac{1}{2}} \tag{2}$$

where $\nu_o = (B + C)$

$$\nu_1 = \nu(1_{-1} \rightarrow 2_{-2}) .$$

From (c) and (e),

$$(B - C) = \left[\frac{1}{2}\nu_2^2 + \frac{1}{6}\nu_2\left\{(4A - 2\nu_o)^2 + 5\nu_2^2\right\}^{\frac{1}{2}}\right]^{\frac{1}{2}} \tag{3}$$

where $\nu_2 = \frac{1}{4}[\nu(2_2 \rightarrow 3_1) - \nu(2_{-2} \rightarrow 3_{-3})]$.

From (f),

$$(B - C) = \left[\frac{1}{7}(4\nu_o - \nu_3)(12A - 2\nu_o - \nu_3)\right]^{\frac{1}{2}} \qquad (4)$$

where $\nu_3 = \nu(3_0 \rightarrow 4_{-1})$.

Any three of these equations are, in principle, sufficient for a solution. The fourth can be expected to be slightly inconsistent, both because of experimental frequency-measurement errors and because the actual molecule is not strictly a rigid rotor, for which the equations are derived. Centrifugal stretching of the molecular framework causes it to exhibit slightly different effective rotational constants in different rotational states (34).

In order to effect solution of these equations in a manner that would indicate clearly the degree of inconsistency and the strength of the determination of the rotational constants, a digital computer (Univac Scientific 1101) was employed to tabulate numerically equations 2, 3, and 4, with $\nu_o = B + C$ inserted from equation 1'. (Equation 2 was tabulated for NO_2Cl^{35} only, using $\nu(1_{-1} \rightarrow 2_{-2}) = 17,611.15$ Mc from the frequencies published by Millen and Sinnott.) It was intended to find the simultaneous solution of any pair of equations by noting the value of A for which (B - C) was the same in the two corresponding tabulations. However, the tables exhibited no meaningful "intersections." This result is indicated graphically in Figures 5 and 6, where the functional constraints plot as almost-parallel lines. The six transitions of Table 1 therefore afford only a very weak determination of the rotational constants. Small displacements of the plots by centrifugal distortion are

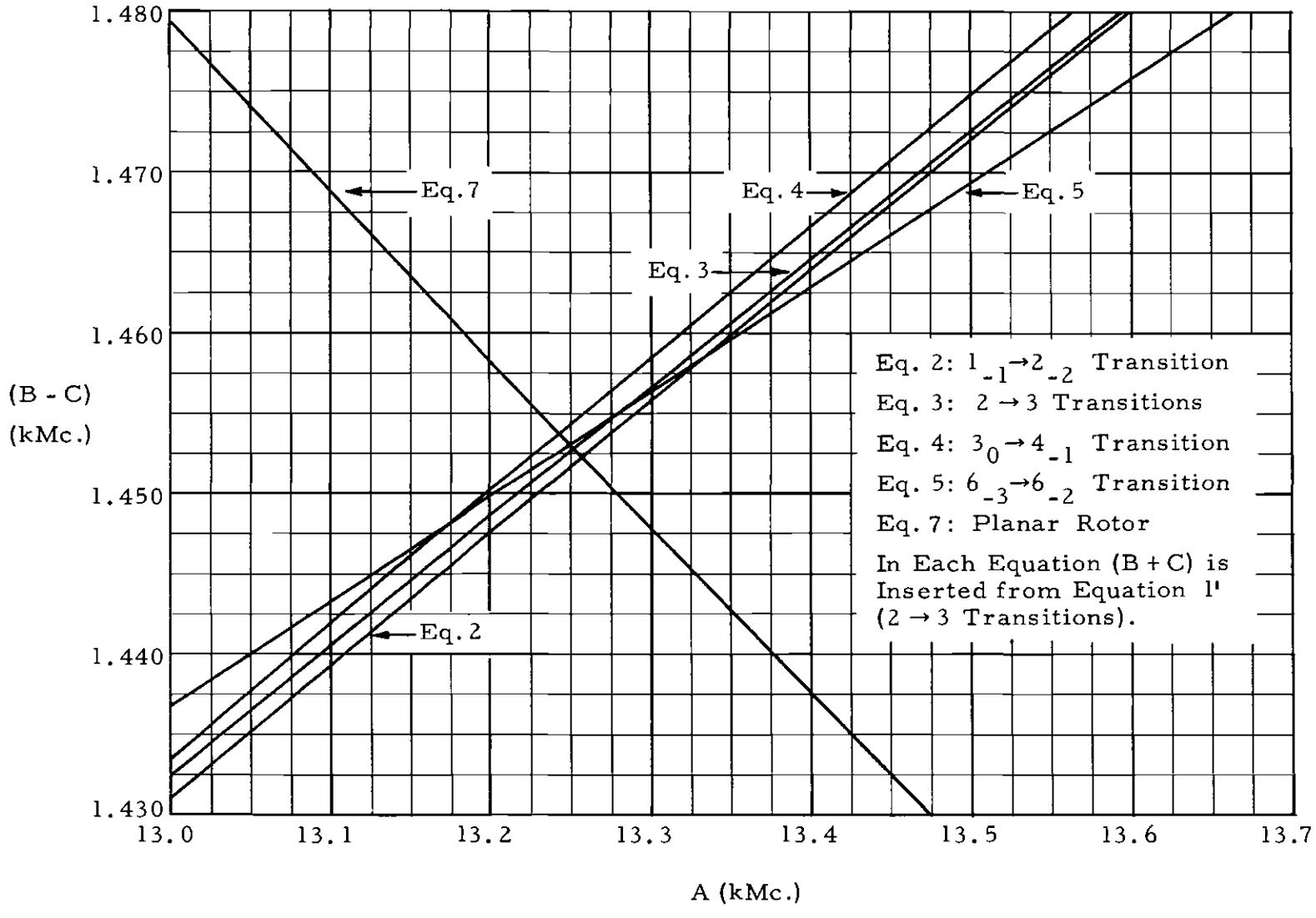

Figure 5. Functional Constraints upon the Rotational Constants of NO_2Cl^{35}.

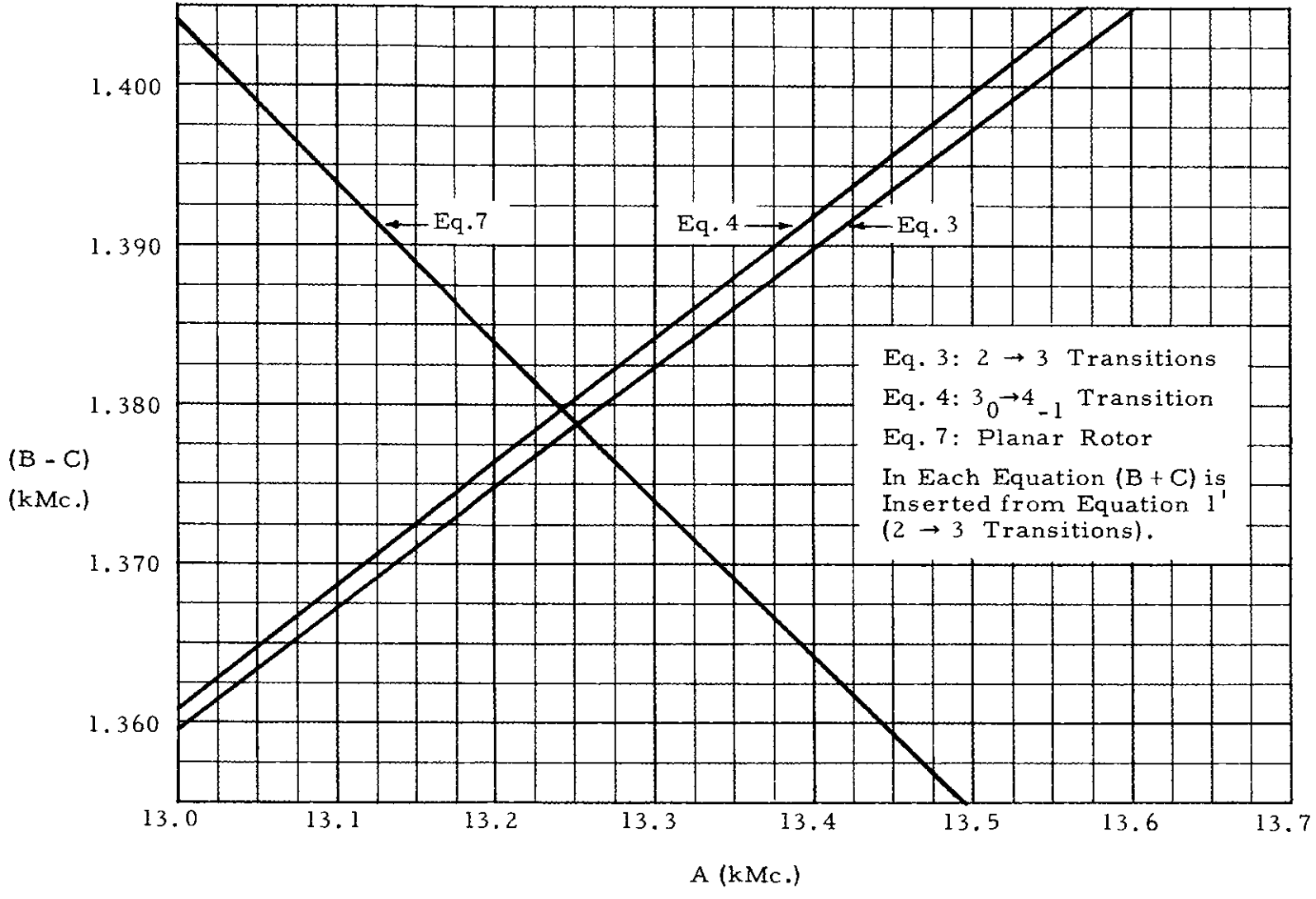

Figure 6. Functional Constraints upon the Rotational Constants of NO_2Cl^{37}

sufficient to shift the value of A at intersection by several hundred megacycles. Furthermore, since the frequencies of the J_τ: $3_1 \rightarrow 4_0$ and $3_{-3} \rightarrow 4_{-4}$ transitions are predicted well by any set of constants obtained from the parallel plots, it is clear that they can impose no strong additional restriction.

Molecular microwave spectra do not usually leave such a wide latitude in the determination of rotational constants. In nitryl chloride, however, two types of transitions which would provide strong additional constraints are not observed. First, one half of the transitions ordinarily ascribed to an asymmetric rotor are missing altogether because of the exclusion, discussed in Appendix A, which applies to a planar molecule with two identical nuclei of spin zero. Only those rotational states are allowed whose wavefunctions do not change sign when the molecule is subjected to a π-rotation about the a axis, the axis of the "Y". Second, certain $\Delta J=0$ or "Q-branch" transitions (e.g., $2_{-2} \rightarrow 2_1$, $3_{-3} \rightarrow 3_0$) often observable in asymmetric-top molecules have not been observed in nitryl chloride. An inspection of tables of line intensities (35) shows that such transitions should be quite weak because the molecule ($\kappa \approx -0.7$) is too nearly a prolate symmetric rotor ($\kappa = -1$), for which the transitions are completely forbidden.

In their 1958 article (23), Millen and Sinnott supposed that this difficulty had been overcome by their identification of the $6_{-3} \rightarrow 6_{-2}$ transition of NO_2Cl^{35} at approximately 9975 Mc. However, this is not one of the strongly constraining Q-branch transitions. Although the restriction imposed by the transition cannot be put in closed algebraic

form, it can be calculated numerically from equation A-84 (Appendix A) with the aid of tables of the reduced energy $E(\kappa)$. Equations A-84 and A-85 can be combined to give the following parametric equations:

$$(B - C) = \frac{1 + \kappa}{\Delta E(\kappa)} \nu(6_{-3} \rightarrow 6_{-2}) \quad , \tag{5}$$

$$A = \frac{3 - \kappa}{2\Delta E(\kappa)} \nu(6_{-3} \rightarrow 6_{-2}) + \frac{1}{2}(B + C) \quad ,$$

where $\Delta E(\kappa)$ is the difference in the reduced energies of the two levels. These equations were evaluated for κ ranging from -0.690 to -0.705 by interpolation in the reduced-energy tables of Turner, Hicks, and Reitwiesner (36). The resulting restriction is included in Figure 5. The latitude in A is still several tens of megacycles and the retention of significant figures to 0.01 Mc by Millen and Sinnott is unwarranted.

If the molecule is treated as a rigid planar rotor, an additional constraint may be imposed for a stronger determination of the rotational constants. The moments of inertia of such a body are related by the equation

$$I_c - I_a - I_b = 0 \tag{6}$$

which requires

$$(B - C) = \left[4A^2 + \nu_o^2\right]^{\frac{1}{2}} - 2A. \tag{7}$$

It should be recognized that an approximation is made when this restriction is applied to an actual molecule, which is not strictly rigid. In certain planar molecules for which all three moments of inertia can be

obtained from their spectra, it has been found that equation 6 is not satisfied exactly (37, 38). The amount by which $I_c - I_a - I_b$ differs from zero has been called the "inertial defect"; it is attributed to zero-point vibrations of molecules in their ground vibrational states. This defect is quite small in comparison to the moments of inertia, but like centrifugal distortion it limits the ultimate precision possible in a rigid-rotor analysis.

Plots of equation 7 in Figures 5 and 6 have sharply defined intersections with the plots of the other equations at $A \approx 13,250$ Mc. However, because the functional constraints obtained from the spectrum do not coincide exactly, the rotational constants at the points of precise intersection with the planar-rotor constraint are slightly different for different transitions. One therefore has the choice of fitting any one transition, or of taking an average. If experimental frequency-measurement errors were the primary source of inconsistency, then averaging would be justified. However, an inspection of spectrum prediction errors will show presently that this can hardly be so, and that centrifugal distortion effects predominate. Because an average over such effects would have no clearly defined meaning, constants used in further work were obtained from the J: $2 \rightarrow 3$ transitions alone. These constants, read from the computer tabulations of equation 3, are listed in Table 2. They can be regarded as effective rotational constants exhibited by the molecule in its $2 \rightarrow 3$ transitions, assuming zero inertial defect. Values of B and C are retained to 0.01 Mc in this table to preserve the accuracy of the sum (B + C) for later calculations.

Table 2. Rotational Constants Resulting From Application of Planar Rotor Restriction to J: 2 → 3 Transitions

Rotational Constants	NO_2Cl^{35}	NO_2Cl^{37}
A	13,250 Mc	13,250 Mc
B	5,173.77	5,018.97
C	3,721.13	3,640.35

Calculated pure rotational energies for states associated with observed transtions are listed in Table 3. Energies for the J = 1, 2, 3 levels and for $J_\tau = 4_{-1}$ were obtained by direct substitution of A, B, and C in the explicit energy expressions given by Gordy, Smith, and Trambarulo (33). Energies for the 4_{-4} and 4_0 levels were evaluated by numerical solution of their cubic secular equation. The energy of the NO_2Cl^{37} 5_{-5} level was determined by three-point interpolation in the reduced-energy tables of Turner, Hicks, and Reitwiesner (36). An indication of the adequacy of such interpolation was obtained by making additional calculations of the 4_0-level energy of NO_2Cl^{37} from the reduced-energy tables. A three-point interpolation led to a figure only 0.004 Mc different from that obtained through solution of the secular equation, while a simple linear interpolation resulted in an error of 0.5 Mc.

The calculated group-center frequencies ν_o^c included in Appendix D are the differences $\Delta E_r/h$ between the energies of the initial and the final states in each observed transition. The spectrum thus predicted

Table 3. Calculated Rotational Energy Levels

State J	Symmetry*	Rotational Energy E_r/h, Mc NO_2Cl^{35}	NO_2Cl^{37}
1_{-1}	-+	8,894.90	8,659.32
2_2	++	62,073.78	61,818.41
2_1	-+	61,894.90	61,659.32
2_{-2}	++	26,505.82	25,818.87
3_1	-+	89,456.71	88,419.13
3_0	++	88,579.60	87,637.28
3_{-3}	-+	52,492.29	51,174.07
4_0	++	126,542.06	124,409.39
4_{-1}	-+	124,019.55	122,150.42
4_{-4}	++	86,425.59	84,333.53
5_{-5}	-+		124,936.32

*Symmetries are indicated according to the convention of Dennison (61). See Appendix A.

is in quite close agreement with experimental measurements; differences between the calculated frequencies and those measured are listed in Table 4. These discrepancies, although small, are of significance in speculation as to the cause of the slight inconsistencies found among the rotational-constant tabulations for different transitions (Figures 5 and 6). Because the nearly-parallel plots do not coincide, the measured frequencies of all corresponding transitions cannot be fitted precisely by any single set of rotational constants, whether or not the condition $I_c - I_a - I_b = 0$ is imposed. Possible sources of inconsistency include (1) measurement errors in the frequencies of individual transitions, (2) an error in the experimental value of (B + C) used in all three tabulations, and (3) a fundamental limitation of the rigid-rotor theory. Effects due to experimental errors should differ for NO_2Cl^{35} and NO_2Cl^{37} because the determinations of their rotational constants are based upon entirely independent measurements; yet the spectrum prediction errors in Table 4 are almost identical for the two isotopic species. Especially interesting is the 0.23-Mc error in the prediction of the $0_0 \rightarrow 1_{-1}$ transition frequency of NO_2Cl^{35}; the frequency of this transition must be precisely one-third that of the $2_1 \rightarrow 3_0$ transition for any rigid rotor, regardless of its rotational constants. It is concluded that the spectrum prediction errors in Table 4 (except those for the fitted $2 \rightarrow 3$ transitions) and the relative displacements of the rotational-constant plots are manifestations of slight centrifugal distortion of the molecular framework.

Table 4. Differences between Measured and Calculated Group-Center Frequencies

Transition	$\nu_o^m - \nu_o^c$ (Mc) NO_2Cl^{35}	NO_2Cl^{37}
$4_{-4} \rightarrow 5_{-5}$		-2.22
$3_1 \rightarrow 4_0$	0.10	0.10
$3_0 \rightarrow 4_{-1}$	-0.32	-0.31
$3_{-3} \rightarrow 4_{-4}$	-0.59	-0.58
$2_2 \rightarrow 3_1$	0.00	0.01
$2_1 \rightarrow 3_0$	-0.03	-0.03
$2_{-2} \rightarrow 3_{-3}$	0.01	0.03
$1_{-1} \rightarrow 2_{-2}$	0.23†	
$0_0 \rightarrow 1_{-1}$	0.23†	

†Based on measured frequencies published by Millen and Sinnott (20).

Molecular dimensions.--The dimensions of a planar XYZ_2 molecular framework can be expressed in terms of the three parameters u, v, w shown in Figure 7. The moments of inertia of the structure about its principal axes may then be expressed in the following form.

$$I_a = 2 m_3 w^2 \tag{8}$$

$$I_b = \frac{1}{M}\left[m_1 \{(m_2 + 2m_3) u^2 + 4m_3 uv + 2m_3 v^2\} + 2m_2 m_3 v^2 \right] \tag{9}$$

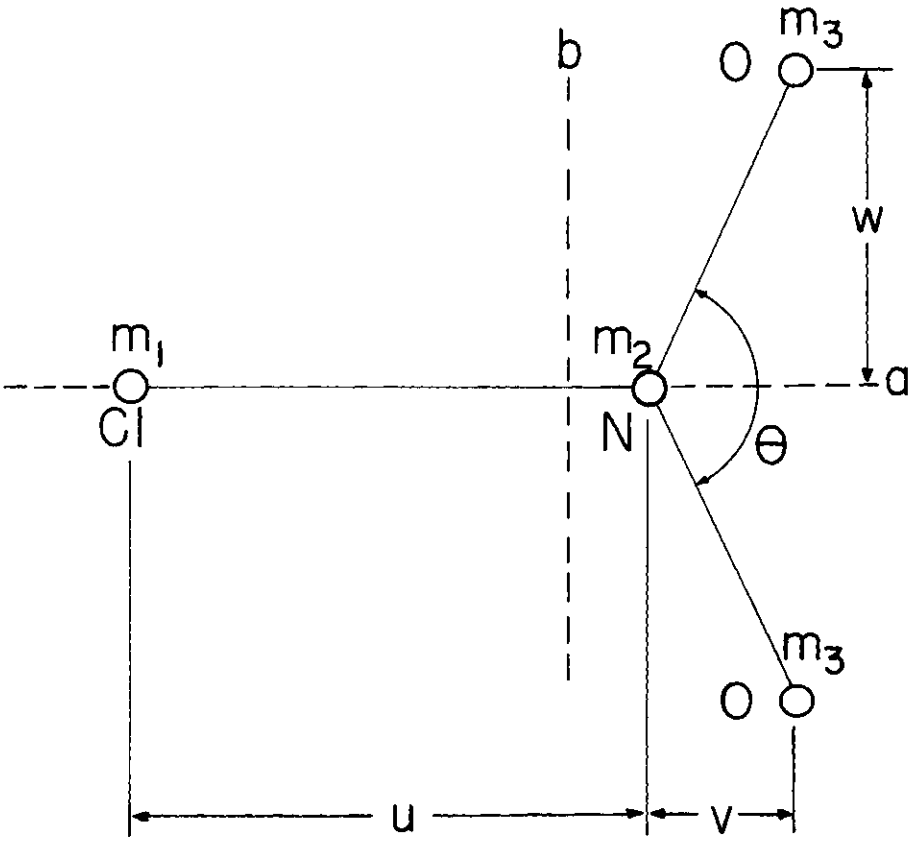

Figure 7. Molecular Geometry.

$$I_c = I_a + I_b \tag{10}$$

where $M = m_1 + m_2 + 2m_3$.

The dimension $\underline{w}$ is given immediately by I_a. To find $\underline{u}$ and $\underline{v}$ in nitryl chloride, one can solve simultaneously the equations for MI_b for NO_2Cl^{35} and NO_2Cl^{37}. Subtraction of the equations for the two isotopes gives a numerical value for the quantity

$$(m_2 + 2m_3)\, u^2 + 4m_3\, uv + 2m_3\, v^2 = \Delta(MI_b)/\Delta m_1 \ , \tag{11}$$

which can be substituted in the sum of the equations to find $\underline{v}^2$. Once $\underline{v}$ is known, equation 11 can be solved for $\underline{u}$. Straightforward trigonometry then gives the N-O distance and the O-N-O angle.

Table 5 lists moments of inertia corresponding to the rotational constants of Table 2. They follow from the relations $I_a = h/(8\pi^2 A)$, $I_b = h/(8\pi^2 B)$, $I_c = h/(8\pi^2 C)$, where $h/(8\pi^2) = 5.0553 \times 10^5$ Mc amu A^2. These moments of inertia lead to the following molecular dimensions: d(N-O) = 1.207 A, d(N-Cl) = 1.830 A, $\angle$ (ONO) = 129.5°. It is estimated that effects of molecular nonrigidity can produce uncertainties in these figures on the order of 0.01 A in distance and one degree in angle.

It should be pointed out that the alternate root of the quadratic equation 11, u = d(N-Cl) = -2.546 A, corresponds to a diamond or "kite" shaped molecular structure in which the chlorine and the oxygen nuclei are on the same side of the nitrogen nucleus. This structure can be rejected on the basis of incompatibility with the infrared spectrum (19),

Table 5. Moments of Inertia

Moments of Inertia	NO_2Cl^{35}	NO_2Cl^{37}
I_a	38.15 amu A^2	38.15 amu A^2
I_b	97.710	100.724
I_c	135.854	138.868

implausibility of the chemical bond, and gross incompatibility with the observed quadrupole coupling constants. Its pure rotational spectrum, however, would be identical to that of the Y-shaped model. This ambiguity could of course be removed if one could observe the rotational spectrum of the N^{15} molecular isotopic species.

Hyperfine structure; quadrupole coupling constants. --The hyperfine splitting produced by the chlorine nucleus was analyzed by the first-order theory of Bragg and Golden (5, 6); quadrupole coupling constants were calculated from a fitting of the hyperfine structures of the $^2_{-2} \rightarrow {}^3_{-3}$, $^2_1 \rightarrow {}^3_0$, and $^2_2 \rightarrow {}^3_1$ transitions. The pertinent results of Bragg and Golden's theoretical analysis are presented in Appendix B, along with a number of algebraic manipulations which have proved convenient in the practical application of the theory.

Quadrupole coupling constants can be determined from as few as two line-spacings in certain hyperfine multiplets, but the extreme sensitivity of such determinations to small frequency-measurement errors dictates instead that the determination be based upon a simultaneous

optimum fitting of as many measured lines as is practicable. Consequently, the "maximum likelihood" statistical fitting procedure described in Appendix B was employed. In order to explore the smoothing effects of data-pooling, three types of determinations were performed in which successively larger numbers of measured line frequencies were fitted simultaneously. The results of these calculations are shown in Table 6, in which the coupling constants obtained are listed without roundoff.

The first three columns of Table 6 show the results of separate maximum-likelihood fittings of the well-resolved lines of each individual transition for each isotope. Values of χ_{aa} determined from different transitions differ by as much as 0.4 Mc and values of χ_{bb} and χ_{cc} by as much as 2.2 Mc. (The splitting of the $2_1 \rightarrow 3_0$ transition is is independent of χ_{bb} and χ_{cc}.) The lack of consistency between isotopic species in the magnitudes of the discrepancies suggests that the variation is due to the sensitivity of single-transition determinations to small experimental errors rather than to possible higher-order effects. In this connection it is noteworthy that for the general asymmetric rotor Bragg's theory indicates that second-order corrections can become important for closely-spaced energy levels such as those of the 2_1 and 2_2 states. However, the terms involved in the corrections for near-degeneracy of this type all include as factors the cross-derivatives of the electric potential at the quadrupolar nucleus: $(\partial^2 V/\partial a \partial b)$, etc. In nitryl chloride the molecular symmetry is such that the inertial principal axes are also principal axes of the field-gradient tensor, so

Table 6. Quadrupole Coupling Constants from Successive Maximum-Likelihood Fittings

Coupling Constant	Constants from Single-Transition Fittings $2_{-2} \rightarrow 3_{-3}$	$2_1 \rightarrow 3_0$	$2_2 \rightarrow 3_1$	Constants from Three-Transition Fittings	Constants from Simultaneous Fittings, Three Transitions of Both Isotopes
	Mc	Mc	Mc	Mc	Mc
χ_{aa}^{35}	-94.81	-94.64	-95.07	-94.70	-94.70
χ_{bb}^{35}	52.35		50.47	52.11	52.21
χ_{cc}^{35}	42.46		44.60	42.59	42.49
χ_{aa}^{37}	-74.38	-74.68	-74.77	-74.58	-74.58
χ_{bb}^{37}	40.67		40.28	41.21	41.12
χ_{cc}^{37}	33.71		34.49	33.37	33.46

that the cross-derivatives vanish. There is therefore no contribution to the quadrupole splitting from the near degeneracy of the 2_1 and 2_2 levels.

To make more efficient use of the data than is afforded by single-transition fittings, simultaneous fittings of all well-resolved lines of all three transitions were next performed for each isotope. The resulting coupling constants are listed in the fourth column of Table 6. Because the hyperfine splitting is more sensitive to χ_{aa} than to χ_{bb} and χ_{cc}, the figures obtained for χ_{aa} are more reliable than those for the other two couplings.

A further restriction may be imposed to refine the determination of the less strongly constrained χ_{bb} and χ_{cc}. If the electronic environments of the chlorine nuclei are assumed to be identical in the two isotopic molecular species, then the ratios of coupling constants $\chi_{xx}^{35}/\chi_{xx}^{37}$ must be equal to the ratio of nuclear quadrupole moments Q^{35}/Q^{37}. It is therefore possible to perform a maximum-likelihood fitting of all well-resolved lines of all transitions of both isotopes simultaneously, subject to this restriction. The measured ratio $\chi_{aa}^{35}/\chi_{aa}^{37} = 1.2697$ is intermediate between the value $Q^{35}/Q^{37} = 1.2688$ listed in a table of nuclear properties in the book by Townes and Schawlow (39) and the ratio 1.2706 of the quadrupole moments in a similar table in the book by Gordy, Smith, and Trambarulo (40). The measured ratio was used in the calculation. The results are shown in the fifth column of Table 6. Values of χ_{bb} and χ_{cc} differ by only 0.1 Mc from the figures obtained in the previous fittings, where the two isotopes were treated independently.

The preceding determinations were based upon tentative rotational constants: for NO_2Cl^{35}, those reported in 1955 by Millen and Sinnott, listed on page 9; for NO_2Cl^{37}, those derived from the NO_2Cl^{35} data as described on page 24. The couplings obtained in the final fitting were used to calculate the predicted quadrupole-interaction shifts of all measured lines, and these shifts were subtracted from the measured frequencies in order to obtain estimates of the group-center frequencies of all transitions. The individual estimates thus obtained for the well-resolved lines were then averaged to obtain the measured group-center frequencies ν_o^m listed in Appendix D. The figures in the columns headed $\nu_o^m + \Delta\nu_q$ (measured group-center frequency plus calculated quadrupole interaction shift) may be compared with the measured frequencies of individual lines as an indication of the adequacy of these coupling constants for predicting the hyperfine structure. They predict the shifts of 58 well-resolved lines (including the higher-J transitions not involved in the fittings) with a standard deviation of approximately 0.02 Mc, confirming the applicability of first-order theory within the limits of experimental measurement capability.

The revised rotational constants listed in Table 2 were obtained after treatment of the hyperfine splitting had permitted accurate evaluation of the group-center frequencies. An examination of the effect of the revision upon the quadrupole coupling constants confirmed that the determination is relatively insensitive to rotational-constant variations which are consistent with the observed pure-rotational spectrum. In a final simultaneous fitting of all J: $2 \rightarrow 3$ transitions of both isotopes,

Table 7. Quadrupole Coupling Constants of Nitryl Chloride

Coupling Constant	NO_2Cl^{35}	NO_2Cl^{37}
	Mc	Mc
χ_{aa}	-94.70	-74.58
χ_{bb}	52.4	41.3
χ_{cc}	42.3	33.3

values of χ_{aa} changed only 0.002 Mc; χ_{bb} and χ_{cc} changed 0.20 Mc for NO_2Cl^{35} and 0.16 Mc for NO_2Cl^{37}. The final coupling constants are shown in Table 7, where χ_{bb} and χ_{cc} are rounded to 0.1 Mc to reflect their greater uncertainty. The effect of the change upon the predicted hyperfine splitting was not considered sufficiently great to warrant recalculation of the complete spectrum; only a few most sensitive line displacements change by as much as 0.02 Mc.

Stark effect; dipole moment of NO_2Cl^{35}.--Determination of the dipole moment of NO_2Cl^{35} was undertaken by analysis of the Stark splitting of the $2_1 \rightarrow 3_0$ transition. In Figure 8, a recording made at an electric field intensity of 515 volts/cm, all ten Stark components of this transition are visible as downward deflections.

The theory of the Stark effect in the asymmetric rotor is discussed in Appendix C. Notable work in this field includes the treatment by Golden and Wilson of the rotor without hyperfine structure and the method of Mizushima for including quadrupole interaction.

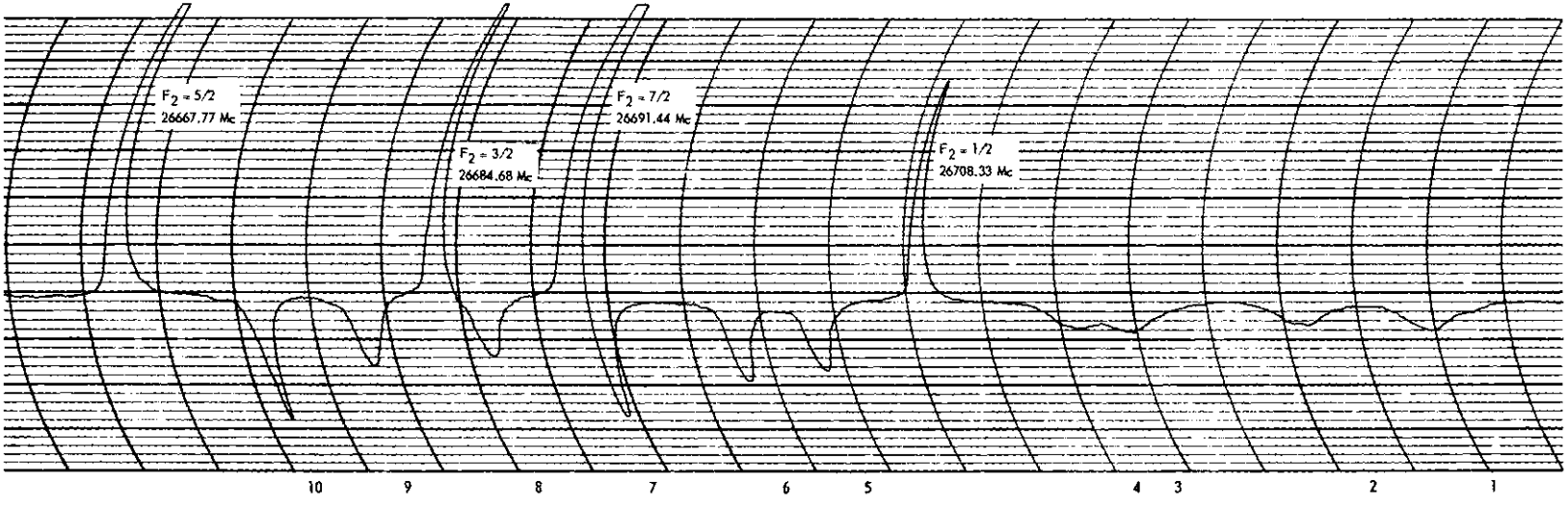

Figure 8. The $J = 2_1 \rightarrow 3_0$ Transition of NO_2Cl^{35} Showing the Stark Components for an Electric Field of 515 Volts/cm. The F_2 Values are for the Lower State. The Values of F in the Upper State are not Identified as the 3_0 Level is Degenerate in F.

Splittings of the 2_1 energy level were first calculated for several values of the quantity $\mu\mathcal{E}$ (the product of the dipole moment and the field intensity), using an IBM 650 computer to diagonalize the Hamiltonian matrices of Mizushima. This procedure was not necessary for the 3_0 level; there the average value of the molecular electric field gradient at the chlorine nucleus vanishes, so that there is no quadrupole interaction and the Stark energies are those for an ordinary asymmetric rotor.

Comparison of recordings with calculated Stark structures showed good qualitative agreement and indicated a dipole moment in the neighborhood of 0.5 debye. There was however a pronounced foreshortening, increasing with field intensity, in the observed shifts of those components which were displaced by more than about 30 Mc from their parent lines. This result is indicated in Tables 8 and 9, which list Stark component frequencies measured from calibrated recordings for $\mathcal{E}$ = 556 v/cm and 750 v/cm respectively. The adjacent columns list frequencies calculated by Mizushima's method for $(\mu\mathcal{E})/h$ = 150 Mc and 200 Mc respectively. The actual and the assumed field conditions are equivalent for $\mu \approx 0.53$ debye. The theory predicts quite accurately the shifts of components 9 and 10 (Figure 8), corresponding to states of dominant character M = 0. It also shows correctly that component 8 overtakes and passes component 7 as the field is increased from 556 v/cm to 750 v/cm. However, the shifts of the most widely displaced components, corresponding to states of dominant character M = 2, fall as much as 27 Mc short of the predicted shifts for $\mathcal{E}$ = 750 v/cm.

Table 8. Measured and Calculated Stark Component Frequencies, NO_2Cl^{35} $2_1 \rightarrow 3_0$ Transition
$\mathcal{E}$ = 556 v/cm ; $(\mu\mathcal{E})/h$ = 150 Mc

Component Number (Figure 8)	Dominant Character M	m	Parent Line Frequency (Mc)	Measured Frequency† (Mc)	Calculated, Mizushima Method (Mc)	Calculated, Degenerate Theory (Mc)
1	2	-3/2	26 708.33	26 738.6 ± 1	26 748.57	
2	2	3/2	26 691.44	26 732.7 ± 1	26 744.01	26 733.24
3	2	1/2	"	26 723.8 ± 1	26 733.81	26 723.95
4	2	-1/2	"	26 722.0 ± 1	26 732.12	
5	1	-1/2	"	26 705.4 ± 0.3	26 707.97	
6	1	1/2	26 684.68	26 701.3 ± 0.3	26 702.11	
7	-1	3/2	"	26 693.3 ± 0.3	26 692.33	
8	1	3/2	26 667.77	26 689.5 ± 0.4	26 691.20	26 689.42
9	0	1/2	"	26 682.5 ± 0.3	26 682.51	
10	0	3/2	"	26 675.7 ± 0.3	26 675.57	

† Limits indicate the breadth of the region in which the line amplitude is not greatly different from the peak amplitude. Measured frequencies are for the centers of this region.

Table 9. Measured and Calculated Stark Component Frequencies, NO_2Cl^{35} $2_1 \rightarrow 3_0$ Transition

$\mathcal{E}$ = 750 v/cm ; $(\mu\mathcal{E})/h$ = 200 Mc

Component Number (Figure 8)	Dominant Character M	m	Parent Line Frequency (Mc)	Measured Frequency† (Mc)	Calculated, Mizushima Method (Mc)	Calculated, Degenerate Theory (Mc)
1	2	-3/2	26 708.33	26 761 ± 2	26 787.60	
2	2	3/2	26 691.44	26 757 ± 2	26 784.91	26 757.42
3	2	1/2	"	} 26 746 ± 1 {	26 773.26	26 746.74
4	2	-1/2	"		26 772.31	
5	1	-1/2	"	26 714.3 ± 0.5	26 719.27	
6	1	1/2	26 684.68	26 710.0 ± 0.5	26 712.20	
7	-1	3/2	"	26 698.0 ± 1	26 697.81	
8	1	3/2	26 667.77	26 699.5 ± 1	26 702.91	26 699.40
9	0	1/2	"	26 688.4 ± 0.2	26 688.28	
9'	*		"	26 687.2 ± 0.2	26 687.07	
10	0	3/2	"	26 676.7 ± 0.2	26 676.57	

† Limits indicate the breadth of the region in which the line amplitude is not greatly different from the peak amplitude. Measured frequencies are for the centers of this region.

* Weak satellite transition to M = 1 state of 3_0 level; attributed to slight M = 1 character of 2_1 Stark level No. 9.

Of particular interest is Component No. 2, for which $M_F = M+m = 7/2$. For this component the splitting of the $J = 2$ level is obtained from a first-degree secular equation. The displacement of the component from the $F_2 = 7/2$ line is found to be identical to the Stark-effect displacement for any asymmetric rotor without quadrupole interaction, which according to second-order perturbation theory should be proportional to $\mathcal{E}^2$. The dashed line in Figure 9 shows this expected behavior, for comparison with the observed shifts.

The failure of the nondegenerate theory can be attributed primarily to the proximity of the 2_1 and 2_2 energy levels, whose calculated separation is 178.89 Mc. For $M \neq 0$ the states are connected by a matrix element of H_s. The solid curve in Figure 9 shows the behavior predicted by the theory of Golden and Wilson for an asymmetric rotor without quadrupole interaction in the case of near degeneracy. The agreement with experiment is very good indeed, even though a nonvanishing influence of quadrupole interaction might be expected in a rigorous treatment of the degenerate case. Also neglected is a similar but much smaller effect resulting from the proximity of the 3_0 and 3_1 levels. A useful indication of the adequacy of the theory is the consistency of the results obtained when it is used to calculate the dipole moment from a number of separate component-shift measurements over a wide range of field strengths. Table 10 lists values of μ thus obtained from fifteen calibrated-recording measurements of the $M_F = 7/2$ component, for $\mathcal{E}$ ranging from 214 v/cm to 1500 v/cm. Differences of the individual solutions from the mean of 0.533 debye are apparently

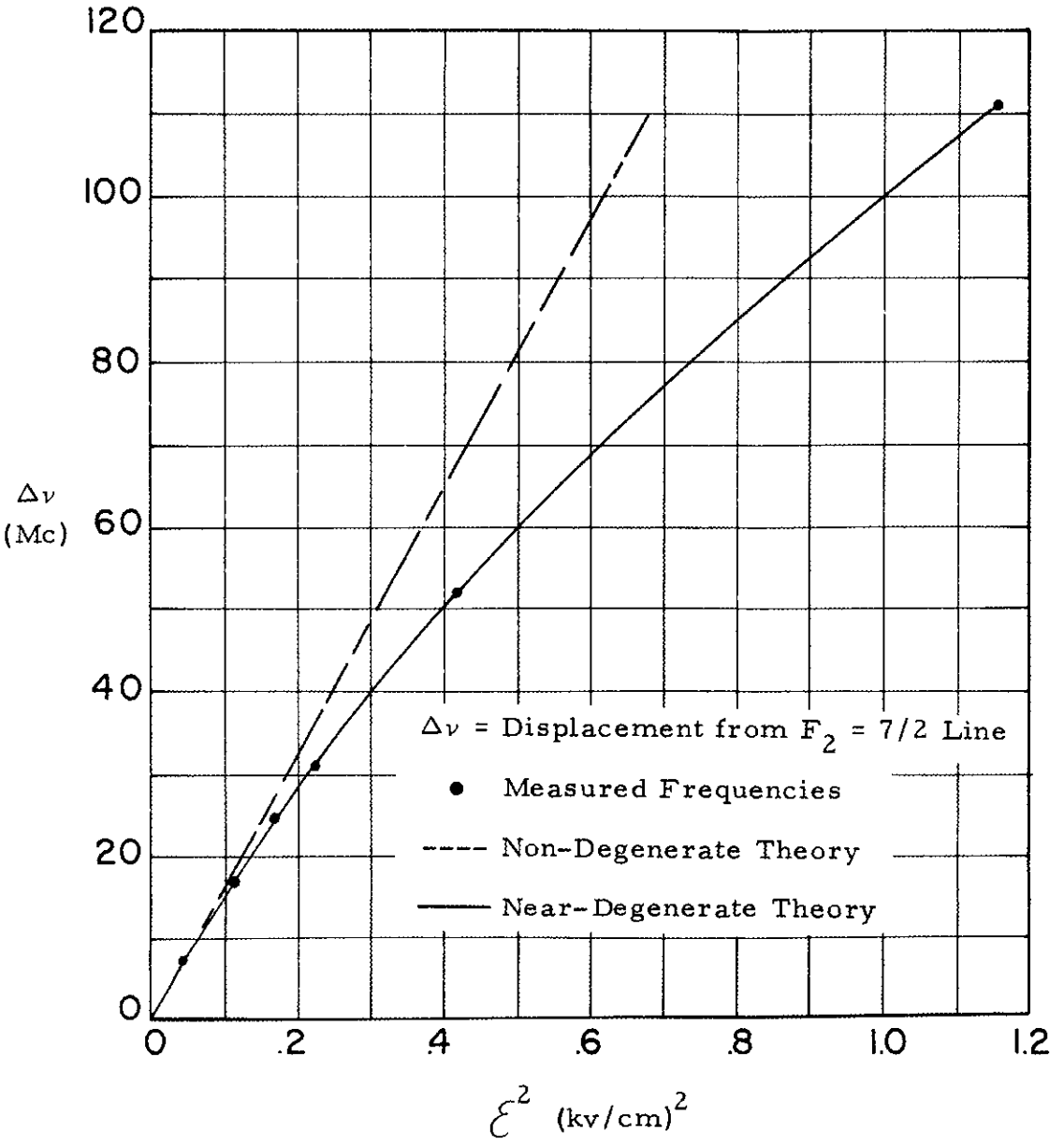

Figure 9. Behavior of $M_F = 7/2$ Stark Component for $J = 2_1 \rightarrow 3_0$ Transition of NO_2Cl^{35}.

Table 10. Stark Effect of $M_F = 7/2$ Component, $2_1 \rightarrow 3_0$ Transition of NO_2Cl^{35}

Electric Field Intensity (v/cm)	Measured Frequency † (Mc)	Shift From $F_2 = 7/2$ Line (Mc)	Calculated Dipole Moment; Degenerate Theory (debye)
214	26 698.9 ± 0.2	7.46	0.5351
321	26 707.2 ± 0.2	15.8	0.5310
364	26 711.4 ± 0.3	20.0	0.5336
407	26 715.8 ± 0.4	24.4	0.5339
428	26 717.8 ± 0.5	26.4	0.5303
471	26 723.3 ± 0.7	31.9	0.5383
514	26 727.7 ± 0.7	36.3	0.5325
556	26 732.7 ± 1	41.3	0.5312
600	26 738.5 ± 1	47.1	0.5346
642	26 744 ± 1	52.6	0.5346
696	26 750.5 ± 1.5	59.1	0.5314
750	26 757 ± 2	65.6	0.5282
856	26 773 ± 1.5	81.6	0.5346
1070	26 802.5 ± 1.5	111.1	0.5318
1500	26 865 ± 3	173.6	0.5346
		Average =	0.5330

† Limits indicate the breadth of the region in which the line amplitude is not greatly different from the peak amplitude. Measured frequencies are for the centers of this region.

random, with a standard deviation of 0.0025 debye. (Possible systematic errors associated with the determination of the effective field intensity in the cell, however, limit the accuracy of the determination to about ± 0.01 debye.)

In Appendix C it is pointed out that certain quadrupole-interaction effects that would otherwise complicate the near-degenerate situation are absent in the case of the 2_1 and 2_2 levels of nitryl chloride; the matrix elements $(2_1|H_q|2_2)$ vanish because the inertial principal axes are also principal axes of the field gradient tensor, and the matrix elements $(2_2|H_q|2_2)$ are almost equal to the elements $(2_1|H_q|2_1)$. This circumstance presumably accounts for the excellent consistency noted in Table 10 for the $M_F = 7/2$ Stark component. It indicates also that the other components should be predicted accurately simply by the use of the correct degenerate-case Stark energies in the diagonal elements of the Mizushima secular determinant. This conclusion was tested for the quadratic $M_F = 5/2$ subfactor, which is readily solved without resort to the digital computer program. The resulting calculated frequencies of components 3 and 8, listed in the right-hand columns of Tables 8 and 9, agree with those observed.

CHAPTER V

DISCUSSION OF RESULTS

Although a theoretical interpretation of the bond structure of nitryl chloride is not within the scope of this investigation, certain interesting features of the molecular data can be pointed out. For comparisons with long-established bond theories and chemical experience, the following commentary by Pauling (32) is particularly pertinent.

> Resonance between the two equivalent structures
>
> 
>
> I
>
> with perhaps a small contribution by
>
> 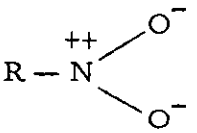
>
> II
>
> is expected for the nitro group. This would lead to the tetrahedral [double-bond plane to single-bond axis] value 125° 16' for the O-N=O bond angle and to the predicted value 1.20 A for the N-O distance, the three atoms of the group being coplanar, with the two oxygen atoms symmetrically related to the R-N axis.... This configuration has been verified by the electron-diffraction study of nitromethane, which led to the values ONO angle = 127° ± 3° and N-O distance 1.21 ± 0.02 A. Moreover, the calculated electric dipole moment for the group, 2.70 debye (corresponding to the average charge distribution
>
> 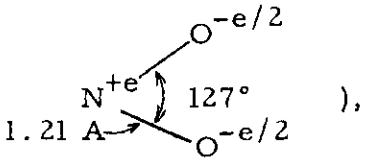
>
>),
>
> agrees satisfactorily with the observed large value of about 3 debye for aliphatic nitro compounds.

The structure of the ONO group in nitryl chloride, d(N-O) = 1.207 ± 0.01 A; ONO angle = 129.5° ± 1°, is evidently just as might have been expected. However, the molecular dipole moment of 0.53 debye is much smaller than is indicated by Pauling's analysis of the ONO group on the basis of structure I. Furthermore, the N-Cl distance 1.830 ± 0.01 A is 0.14 A greater than the sum of the generally accepted covalent single-bond radii (41). In contrast, the N-C distance 1.46 A in nitromethane (42) agrees with the sum of the covalent radii (1.47 A).

It is interesting to compare the gas-phase dipole moments of nitrobenzene, chlorobenzene, and the sequence of chloronitrobenzenes (43):

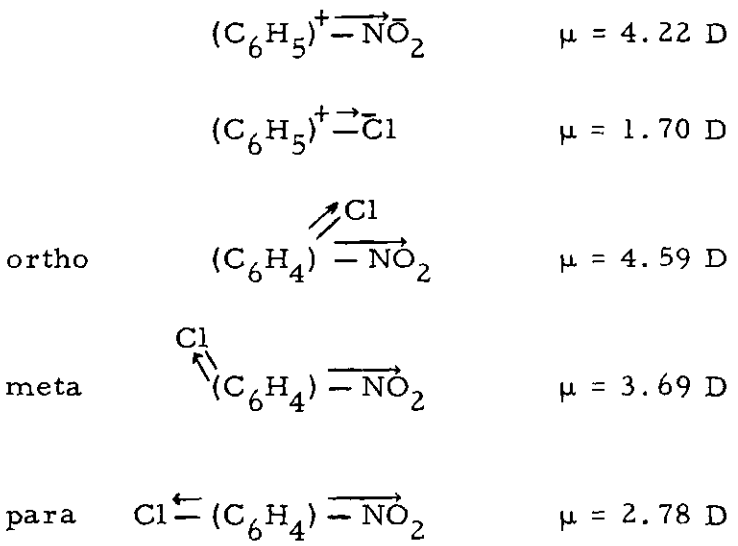

The chlorine atom is clearly negative in these structures; one can account for the net dipole moments fairly well by vector addition of the individual moments indicated. Even in p-chloronitrobenzene, however, where the moments fully oppose, the resultant is about that calculated

by Pauling for the NO_2 structure I. The low dipole moment of nitryl chloride might appear to result from a substantial contribution of the ionic structure

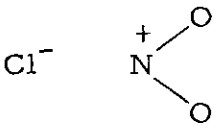

III

The excess N-Cl distance could be regarded as a consequence of such ionic character, to which has been attributed (44) the remarkable d(N-Cl) = 1.98 A in nitrosyl chloride (ClNO). The admission of appreciable character III, however, runs counter to chemical evidence that the chlorine atom is nearly neutral or perhaps slightly positive (16); furthermore, the electronegativities of N and Cl are approximately equal (N: 3.0, N with + formal charge : 3.3, Cl: 3.1). A quantitative limitation is provided by the quadrupole coupling constants.

All molecular charges exterior to the quadrupolar nucleus participate in the production of an electric field gradient at the nucleus; however, treatments such as that by Townes and Schawlow (45) indicate that contributions from the valence-shell electrons held or shared by the nucleus are usually much larger than the direct or induced effects of all other charges. The quadrupole coupling constants therefore indicate the effective electronic occupations of the valence atomic orbitals. The validity of the atomic-orbital concept is hard to judge, but the results of quadrupole-coupling analyses have been generally satisfactory.

The ground-state electronic configuration of chlorine is $1s^2 2s^2 p^6 3s^2 p^5$. The filled inner shells and the symmetrical 3s orbitals contribute nothing to the field at the nucleus. The 3d-state contributions

to the molecular orbitals are presumably small because of their very high energies (46). The states of principal importance are therefore the three orbitals p_a, p_b, and p_c, directed along the respective molecular inertial axes. Let $n(p_i)$ represent the effective number of electrons occupying each orbital. Because the electric potential function due to each electron obeys Laplace's equation, one can write:

$$\chi_{aa} = [\, n(p_a) - \tfrac{1}{2}\, n(p_b) - \tfrac{1}{2}\, n(p_c)]\ \chi_{Cl}$$

$$\chi_{bb} = [\, -\tfrac{1}{2}\, n(p_a) + n(p_b) - \tfrac{1}{2}\, n(p_c)]\ \chi_{Cl}$$

$$\chi_{cc} = [\, -\tfrac{1}{2}\, n(p_a) - \tfrac{1}{2}\, n(p_b) + n(p_c)]\ \chi_{Cl}$$

The quantity χ_{Cl} is a measure of the field gradient produced at the nucleus by one 3p orbital electron; it is 109.7 Mc in atomic Cl^{35} and about 126 Mc in $^{+}Cl^{35}$ (47).

Consider, for example, the following situations: (a) For a pure covalent p bond along the a axis, the average electronic configuration is $3s^2 p_a^1 p_b^2 p_c^2$; consequently $\chi_{aa} = -109.7$ Mc, $\chi_{bb} = \chi_{cc} = 54.84$ Mc. (b) For the Cl^- ion the configuration is $3s^2 p_a^2 p_b^2 p_c^2$, and $\chi_{aa} = \chi_{bb} = \chi_{cc} = 0$. (c) For the Cl^+ ion formed by loss of an electron from the p_a orbital ($3s^2 p_b^2 p_c^2$), $\chi_{aa} = -2(126\ \text{Mc}) = -252$ Mc, $\chi_{bb} = \chi_{cc} = 126$ Mc. (d) For a covalent double bond involving the p_a and p_c orbitals of Cl^+, the average configuration is $3s^2 p_a^1 p_b^2 p_c^1$; therefore $\chi_{aa} = -63$ Mc, $\chi_{bb} = 126$ Mc, $\chi_{cc} = -63$ Mc.

Although the s orbitals themselves produce no field gradient at the nucleus, s-p_a hybridization of a single a-axis covalent bond nevertheless influences the quadrupole coupling constants by changing the average occupation of the p_a orbital. Hybridization produces two sp_a orbitals, one occupied by the two non-bonding electrons which without hybridization would occupy the pure s states; the other is occupied, on the average, by a single bonding electron. If the fractional importance of the s state in the bonding hybrid is x, the effective electronic distribution is $3s^{2-x}p_a^{1+x}p_b^2p_c^2$; consequently $\chi_{aa} = -(1 - x)\chi_{Cl}$; $\chi_{bb} = \chi_{cc} = \frac{1}{2}(1 - x)\chi_{Cl}$.

In most compounds of chlorine the combined effects of s-hybridization and negative ionic character--situation (b)--reduce χ^{35}_{bond} to about -70 to -85 Mc; e.g., in chloromethane to -74.8 Mc. The high value $\chi^{35}_{aa} = -94.7$ Mc in nitryl chloride is unusually close to that of a pure p bond, situation (a); it argues against admission of s-hybridization. This is consistent with Townes' rule (48) of no chlorine-orbital hybridization in a bond with an atom of nearly equal electronegativity, and with the observation that s character shortens rather than lengthens the bond distance (49).

The high value of χ_{aa} does not in fact permit introduction of enough ionic character III to reduce the dipole moment to the observed value, unless the following structure IV is admitted also* to offset the reduction of the χ's.

---

*Even in the molecule H_2 a five per cent contribution is attributed to the structures $H_a^+ {}^-H_b$, $H_a^- {}^+H_b$ (50).

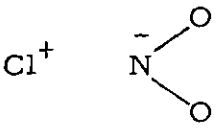

IV

This structure tends to make the dipole moment even higher, but to a much greater degree it increases the χ's through the effect of situation (c).

The inequality of the coupling constants $\chi_{bb}^{35} = 52.4$ Mc, $\chi_{cc}^{35} = 42.3$ Mc can be interpreted as indicative of a contribution from the structure

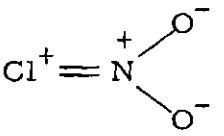

, V

which corresponds to situation (d). Of the four situations considered, only this one gives rise to field asymmetry in the bc plane; this is the basis of J. H. Goldstein's analysis of double-bonding (51). The contribution of structure V should be small because it violates Pauling's adjacent charge rule† (52).

Table 11 summarizes the characteristics of the four structures that are probably the principal participants in the bonding of nitryl chloride. The quadrupole coupling constants are those established in the previous discussion of situations (a) through (d). The "formal"

---

†It is interesting that the dimer O_2NNO_2 is one of the few apparently marked exceptions to this rule (53). However, a new type of "π-only" bond has been attributed to this molecule recently by Coulson and Duchesne (54). The conditions that are believed to give rise to the bond do not exist in the nitryl halides (55), and it is incompatible with the quadrupole coupling constants of nitryl chloride.

Table 11. Characteristics of Contributing Bond Structures

Parameter	Structure I	III	IV	V	Measured Resultant
χ_{aa}^{35} (Mc)	-109.7	0	-252	-63	-94.7
χ_{bb}^{35} (Mc)	54.84	0	126	126	52.4
χ_{cc}^{35} (Mc)	54.84	0	126	-63	42.3
μ (D)	2.47	-8.79	8.79	13.74	0.53

dipole moments were calculated in the manner indicated in Pauling's commentary, with nitryl chloride molecular dimensions.

An analysis of the actual origin of the molecular dipole moment is a most difficult problem in quantum mechanics, complicated by polarization, overlap, and hybridization effects. Syrkin and Dyatkina (56) hold that the dipole moment due to the covalent bond character alone is negligible, even in such dissimilar-atom molecules as HF. (This view is controversial.) When ionic character is included in their analysis, the resultant dipole moment can be written

$$\mu = \tilde{\mu_f}(x_i + 2\sqrt{x_i x_c}\, S)$$

where μ_f is the "formal" dipole moment of the ionic structure, x_i is the fractional contribution of the ionic structure, x_c is the fractional contribution of the covalent structure, and S is the overlap integral. The overlap term will be ignored in the present discussion, with some encouragement from the fact that algebraic and vector additions of dipole

moments appear to give results of the right general magnitude. This procedure is followed also by Pauling (57).

If the measured parameters listed in the last column of Table 11 are regarded as the arithmetic resultants of resonance among the four structures considered, each making an appropriate fractional contribution, four equations in the fractional weights can be obtained from the tabular entries. Three of these are independent; an additional condition is that the sum of the weights be unity. Simultaneous solution of the equations gives the following contributions: structures I, 48.4 per cent; structure III, 31.1 per cent; structure IV, 15.2 per cent; structure V, 5.3 per cent. The net formal charges carried by the atoms are: Cl, -0.106 e; N, +0.696 e; O(each), -0.295 e. The small negativity of chlorine is consistent with the chemical evidence (16).

The concept of resonating structures is of course just an artifice for avoiding quantum-mechanical calculations that are too difficult to be carried out. In modern bond theory effort is being directed toward development of more valid but manageable approximation methods. A molecular-orbital treatment, for example, has been suggested by W. H. Eberhardt (58) as a step toward a realistic interpretation of the bond structure of nitryl chloride. Experimental data for critical tests of theories are not abundant, because for most molecules the simplest bond structures can be made to account for the observed parameters by adjustment of the amount of hybridization and ionic character. It is suggested that nitryl chloride may be of interest in this regard

because the large quadrupole coupling and small dipole moment restrict the latitude of adjustment of these parameters to a greater degree than in most other molecules considered.

CHAPTER VI

CONCLUSIONS

A planar molecular form with oxygen atoms situated symmetrically with respect to the axis of least moment of inertia is established by the absence of transitions involving states antisymmetric with respect to π-rotation about that axis. The remaining allowed transitions do not alone permit accurate measurement of the rotational constants; for a strong determination it is necessary to impose the additional condition $I_c - I_a - I_b = 0$, which holds for a rigid planar rotor. The effective rigid-rotor rotational constants exhibited in the J: 2 → 3 transitions are the following: A = 13,250 Mc, B = 5,173.77 Mc, C = 3,721.13 Mc (NO_2Cl^{35}); A = 13,250 Mc, B = 5,018.97 Mc, C = 3,640.35 Mc (NO_2Cl^{37}). These constants predict accurately the frequencies of all transitions observed in this investigation and elsewhere; small residual differences are attributable to centrifugal distortion.

Moments of inertia given by the rigid-rotor rotational constants correspond to a Y-shaped molecular structure with a central nitrogen nucleus; d(N-Cl) = 1.830 ± 0.01 A, d(N-O) = 1.207 ± 0.01 A, ONO angle = 129.5° ± 1°. A diamond (or "kite") configuration with the same moments of inertia is rejected; it leads to absurdities in the bond structure.

The hyperfine structures of all observed transitions are predicted accurately by the first-order theory of nuclear quadrupole interaction.

Coupling constants obtained through statistical fitting of the J: $2 \rightarrow 3$ transitions are the following: $\chi_{aa} = -94.7\underline{0}$ Mc, $\chi_{bb} = 52.\underline{4}$ Mc, $\chi_{cc} = 42.\underline{3}$ Mc (NO_2Cl^{35}); and $\chi_{aa} = -74.5\underline{8}$ Mc, $\chi_{bb} = 41.\underline{3}$ Mc, $\chi_{cc} = 33.\underline{3}$ Mc (NO_2Cl^{37}).

Analysis of the Stark effect of the J_τ: $2_1 \rightarrow 3_0$ transition of NO_2Cl^{35} discloses a large interaction between the nearly-degenerate 2_1 and 2_2 rotational states; second-order theory and the method of Mizushima are inaccurate. The displacement of the $M_F = 7/2$ component, however, shows no detectable deviation from that predicted by the near-degeneracy theory of Golden and Wilson, and indicates a dipole moment of 0.533 ± 0.01 debye for NO_2Cl^{35}. The absence of higher-order effects of quadrupole interaction is attributed to fortunate properties of the matrix elements of the quadrupole perturbation: the elements $(2_1|H_q|2_2)$ vanish in nitryl chloride because the molecular electronic distribution is symmetrical to π-rotation about the chlorine-bond axis, and the elements $(2_2|H_q|2_2)$ are nearly equal to the elements $(2_1|H_q|2_1)$. In such situations the use of correct degenerate-case Stark energies in the diagonal elements of the Mizushima secular determinant should provide an adequate correction to the theory; this expectation is confirmed by the displacements of the $M_F = 5/2$ components.

The ONO group in nitryl chloride has the same configuration as in other compounds. The N-Cl distance, however, is somewhat longer than expected, the quadrupole coupling constants are unusually close to those of atomic chlorine, and the molecular dipole moment is much smaller than is ordinarily associated with the nitro-group. These

features can be accounted for by the rather crude concept of quantum-mechanical resonance among the following bond structures in the proportions indicated:

48.4 %

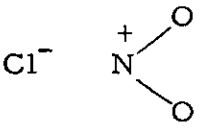

31.1 %

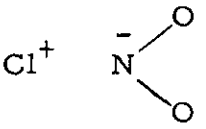

15.2 %

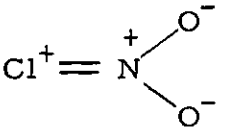

5.3 % .

The molecule may be of interest for tests of modern bond theories because its large quadrupole coupling and small dipole moment restrict the latitude of adjustment of bond parameters to a greater degree than in most other molecules considered.

APPENDICES

APPENDIX A

THEORY OF THE RIGID ASYMMETRIC ROTOR

An outline of the development of the quantum-mechanical theory of the rigid asymmetric rotor has been given in Chapter I. In this appendix the fundamentals of the theory are derived and other applicable results are collected in summary.

The asymmetric rotor has been treated very extensively in the literature. The original papers are reviewed and supplemented in recent articles by Nielsen (59) and Van Winter (60), and practical results of the theory are discussed in several texts (61, 62, 63). These results are well known and have found widespread application in the analysis of molecular spectra. However, the theory itself is generally regarded as quite difficult. Van Winter notes that "the original literature is no easy reading, ... which may explain the fact that a discussion of the subject is wanting in the textbooks." For this reason the derivation of the elements of the asymmetric rotor energy matrix is presented in detail here. It is shown to be a simple problem (although lengthy) which can be handled with only the most elementary wave mechanics.

The energy matrix elements are obtained by manipulation of the rotor Schrödinger equation. A similar approach was taken by Witmer (64) in 1927 and was followed through to a general solution by Wang (1) in 1929. (Van Winter's comment is particularly appropriate to these papers, largely because of their cryptic brevity and complicated

notation.) This procedure is admittedly crude compared to the more common one, used for example by King,Hainer, and Cross (3), based upon the quantum-mechanical theory of angular momentum. There the energy matrix elements are obtained almost immediately from the commutation relationships among the angular momentum operators. This powerful and compact treatment is undoubtedly the one best suited for earnest theoretical work. However, it provides little direct insight into the asymmetric rotor problem because in it all of the physics is concentrated in the angular momentum theory and the application to the rotor is almost trivial.

The wave equation.--The orientation of the inertia ellipsoid of a rigid body can be specified as indicated in Figure 10, by the Euler angles θ, χ, φ relating a body-fixed coordinate system xyz to the space-fixed axes XYZ (65). Let x, y, z lie along the principal axes of the inertia ellipsoid, setting aside for the moment the notation a, b, c which has been used previously to identify specifically the axes of least, intermediate, and greatest moments of inertia respectively. The kinetic energy of the classical rotor is then

$$T = \frac{1}{2}(I_x\omega_x^2 + I_y\omega_y^2 + I_z\omega_z^2) \ . \qquad (A-1)$$

The components of angular velocity ω_x, ω_y, ω_z, expressed in terms of the Euler angles, are (66):

$$\omega_x = \dot{\chi} \sin\theta \sin\varphi + \dot{\theta} \cos\varphi \qquad (A-2)$$

$$\omega_y = \dot{\chi} \sin\theta \cos\varphi - \dot{\theta} \sin\varphi$$

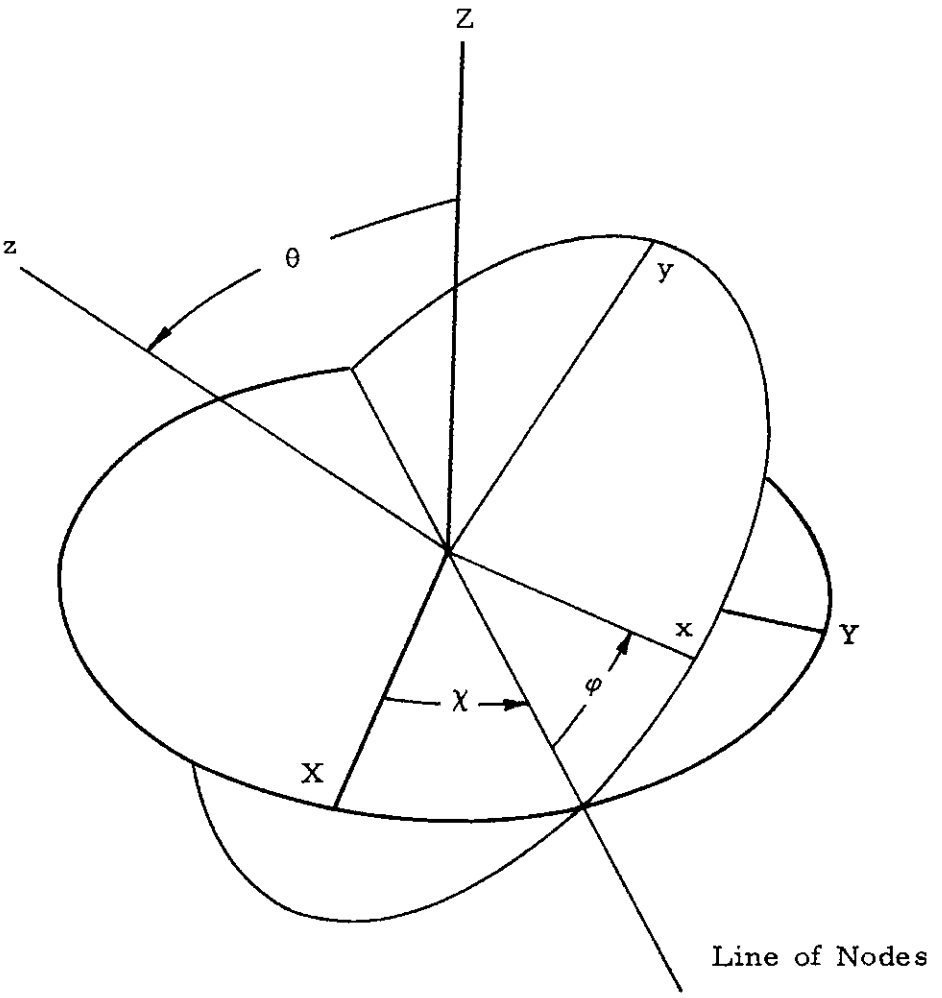

Conventions:

θ is measured from positive Z axis to positive z axis, counterclockwise about line of nodes. The sense of rotation thus defines the positive terminus of the line of nodes.

χ is measured from positive X axis to positive terminus of line of nodes, counterclockwise about Z axis.

φ is measured from positive terminus of line of nodes to positive x axis, counterclockwise about z axis.

Figure 10. Euler Angles Relating a Body-Fixed Coordinate System to Space-Fixed Axes.

$$\omega_z = \dot{\chi} \cos\theta + \dot{\varphi} \quad .$$

Substituion of these expressions in (A-1) gives the kinetic energy in terms of the generalized coordinates and velocities:

$$T(q, \dot{q}) = \frac{1}{2}\Big\{(I_x \cos^2\varphi + I_y \sin^2\varphi)\,\dot{\theta}^2 + (I_x - I_y)\sin\theta \sin 2\varphi\,\dot{\theta}\dot{\chi} + [(I_x \sin^2\varphi + I_y \cos^2\varphi)\sin^2\theta + I_z \cos^2\theta]\,\dot{\chi}^2 + 2I_z \cos\theta\,\dot{\chi}\dot{\varphi} + I_z\,\dot{\varphi}^2\Big\} \quad . \tag{A-3}$$

Let $I_s = \frac{1}{2}(I_y + I_x)$; $I_d = \frac{1}{2}(I_y - I_x)$. (A-4)

Then $$T(q, \dot{q}) = \frac{1}{2}\Big\{(I_s - I_d \cos 2\varphi)\,\dot{\theta}^2 - 2I_d \sin 2\varphi \sin\theta\,\dot{\theta}\dot{\chi} + [(I_s + I_d \cos 2\varphi)\sin^2\theta + I_z \cos^2\theta]\,\dot{\chi}^2 + 2I_z \cos\theta\,\dot{\chi}\dot{\varphi} + I_z\,\dot{\varphi}^2\Big\} \quad . \tag{A-5}$$

For translation to quantum mechanics, however, the kinetic energy must be expressed not in terms of the generalized coordinates and velocities but in terms of the coordinates and the generalized momenta:

$$p_\theta = \frac{\partial T}{\partial \dot{\theta}} = (I_s - I_d \cos 2\varphi)\,\dot{\theta} - I_d \sin 2\varphi \sin\theta\,\dot{\chi} \tag{A-6}$$

$$p_\varphi = \frac{\partial T}{\partial \dot{\varphi}} = I_z\,\dot{\varphi} + I_z \cos\theta\,\dot{\chi}$$

$$p_\chi = \frac{\partial T}{\partial \dot{\chi}} = -I_d \sin 2\varphi \sin\theta\,\dot{\theta} + I_z \cos\theta\,\dot{\varphi} + [(I_s + I_d \cos 2\varphi)\sin^2\theta + I_z \cos^2\theta]\,\dot{\chi} \quad .$$

By application of Cramer's rule, this set may be inverted for the velocities in terms of the momenta:

$$\dot{\theta} = \frac{1}{(I_s^2 - I_d^2)\sin^2\theta}\left\{(I_s + I_d\cos 2\varphi)\sin^2\theta\, p_\theta + (I_d \sin 2\varphi \sin\theta)(-\cos\theta\, p_\varphi + p_\chi)\right\} , \tag{A-7}$$

$$\dot{\varphi} = \frac{1}{(I_s^2 - I_d^2)\sin^2\theta}\left\{I_d \sin 2\varphi \sin\theta\cos\theta\, p_\theta + (I_s - I_d\cos 2\varphi)(\cos^2\theta\, p_\varphi - \cos\theta\, p_\chi)\right\} + \frac{1}{I_z} p_\varphi ,$$

$$\dot{\chi} = \frac{1}{(I_s^2 - I_d^2)\sin^2\theta}\left\{I_d \sin 2\varphi \sin\theta\, p_\theta - (I_s - I_d\cos 2\varphi)(\cos\theta\, p_\varphi - p_\chi)\right\} .$$

Noting that $T = \frac{1}{2}(p_\theta\,\dot{\theta} + p_\varphi\,\dot{\varphi} + p_\chi\,\dot{\chi})$ and substituting, one obtains:

$$T(p,q) = \frac{1}{2(I_s^2 - I_d^2)\sin^2\theta}\left\{(I_s + I_d\cos 2\varphi)\sin^2\theta\, p_\theta^2 - 2I_d \sin 2\varphi\,(\sin\theta\cos\theta\, p_\theta\, p_\varphi - \sin\theta\, p_\theta\, p_\chi) + (I_s - I_d\cos 2\varphi)(\cos^2\theta\, p_\varphi^2 - 2\cos\theta\, p_\varphi\, p_\chi + p_\chi^2)\right\} + \frac{1}{2I_z} p_\varphi^2 . \tag{A-8}$$

This expression is a quadratic form in the generalized momenta, and it can be abbreviated:

$$T(p, q) = \frac{1}{2} \sum_{ij} a_{ij} p_i p_j \quad . \tag{A-9}$$

It will be recognized that the procedure through which the matrix $[a_{ij}] = \underline{a}$ has been obtained is precisely that of determining the inverse of the similar matrix associated with $T(q, \dot{q})$; that is, if

$$T(q, \dot{q}) = \frac{1}{2} \sum_{ij} b_{ij} \dot{q}_i \dot{q}_j \quad , \tag{A-10}$$

then

$$p_i = \frac{\partial T}{\partial \dot{q}_i} = \sum_j b_{ij} \dot{q}_j \quad . \tag{A-11}$$

If the p_i and $\dot{q}_j$ are regarded as the elements of vectors $\underline{p}$ and $\underline{\dot{q}}$, then

$$\underline{p} = \underline{b}\, \underline{\dot{q}} \quad . \tag{A-12}$$

Premultiplication by the inverse matrix $\underline{b}^{-1}$ gives

$$\underline{\dot{q}} = \underline{b}^{-1} \underline{p} \quad , \tag{A-13}$$

or

$$\dot{q}_i = \sum_j (\underline{b}^{-1})_{ij} p_j \quad . \tag{A-14}$$

Substitution of (A-11) in (A-10) gives

$$T = \frac{1}{2} \sum_i p_i \dot{q}_i \quad , \tag{A-15}$$

and further substitution of (A-14) gives finally

$$T(p, q) = \frac{1}{2} \sum_{ij} (\underline{b}^{-1})_{ij} p_i p_j \quad . \tag{A-16}$$

Comparison of (A-16) with (A-9) confirms that $\underline{a} = \underline{b}^{-1}$.

The form of the wave equation appropriate to a non-cartesian coordinate system, given by Schrödinger in the third of his original papers (67, 68) and used by Reiche and Rademacher (69) in their treatment of the symmetric rotor, is the following:

$$\frac{\hbar^2}{2}\,\Delta_p^{\frac{1}{2}} \sum_k \frac{\partial}{\partial q_k}\left\{\Delta_p^{-\frac{1}{2}} \frac{\partial T}{\partial p_k}\right\} - V(q_k)\,\psi + E\psi = 0 \quad , \tag{A-17}$$

where the quantity Δ_p is the discriminant of the quadratic form $T(p, q)$; that is, the determinant $\left|\frac{1}{2}\,\underline{a}\right| = \left(\frac{1}{2}\right)^3 \left|\underline{a}\right|$. In the derivatives $\frac{\partial T}{\partial p_k}$, the momenta p_k are to be replaced by $\frac{\partial \psi}{\partial q_k}$ wherever they appear in the classical expressions for the derivatives.

Evaluation of the discriminant gives

$$\left(\frac{1}{2}\right)^3 \left|\underline{a}\right| = \frac{1}{8\, I_z (I_s^2 - I_d^2)\sin^2\theta} = \frac{1}{8\, I_x\, I_y\, I_z \sin^2\theta} \quad . \tag{A-18}$$

For the operators $\frac{\partial T}{\partial p_k}$ one obtains:

$$\frac{\partial T}{\partial p_\theta} = \frac{1}{(I_s^2 - I_d^2)\sin^2\theta}\left\{(I_s + I_d \cos 2\varphi)\sin^2\theta \frac{\partial \psi}{\partial \theta}\right. \tag{A-19}$$

$$\left. - I_d \sin 2\varphi\,(\sin\theta\cos\theta \frac{\partial \psi}{\partial \varphi} - \sin\theta \frac{\partial \psi}{\partial \chi})\right\} \quad ,$$

$$\frac{\partial T}{\partial p_\varphi} = \frac{1}{(I_s^2 - I_d^2)\sin^2\theta}\left\{- I_d \sin 2\varphi \sin\theta\cos\theta \frac{\partial \psi}{\partial \theta}\right.$$

$$\left. + (I_s - I_d \cos 2\varphi)(\cos^2\theta \frac{\partial \psi}{\partial \varphi} - \cos\theta \frac{\partial \psi}{\partial \chi})\right\} + \frac{1}{I_z} \frac{\partial \psi}{\partial \varphi} \quad ,$$

$$\frac{\partial T}{\partial p_\chi} = \frac{1}{(I_s^2 - I_d^2)\sin^2\theta}\left\{ I_d \sin 2\varphi \sin\theta \frac{\partial\psi}{\partial\theta} \right. \qquad \text{(A-19) cont'd.}$$

$$\left. + (I_s - I_d \cos 2\varphi)(-\cos\theta \frac{\partial\psi}{\partial\varphi} + \frac{\partial\psi}{\partial\chi}) \right\} \quad .$$

With these substitutions, and with V = 0 for the field-free case, the wave equation becomes:

$$\frac{\hbar^2}{2} \frac{1}{(I_s^2 - I_d^2)\sin\theta} \left[\frac{\partial}{\partial\theta} \left\{ (I_s + I_d \cos 2\varphi)\sin\theta \frac{\partial\psi}{\partial\theta} \right. \right. \qquad \text{(A-20)}$$

$$\left. - I_d \sin 2\varphi \,(\cos\theta \frac{\partial\psi}{\partial\varphi} - \frac{\partial\psi}{\partial\chi}) \right\} + \frac{\partial}{\partial\varphi} \left\{ - I_d \sin 2\varphi \cos\theta \frac{\partial\psi}{\partial\theta} \right.$$

$$+ (I_s - I_d \cos 2\varphi)(\frac{\cos^2\theta}{\sin\theta} \frac{\partial\psi}{\partial\varphi} - \frac{\cos\theta}{\sin\theta} \frac{\partial\psi}{\partial\chi})$$

$$\left. + \frac{I_s^2 - I_d^2}{I_z} \sin\theta \frac{\partial\psi}{\partial\varphi} \right\} + \frac{\partial}{\partial\chi} \left\{ I_d \sin 2\varphi \frac{\partial\psi}{\partial\theta} \right.$$

$$\left. \left. + (I_s - I_d \cos 2\varphi)(-\frac{\cos\theta}{\sin\theta} \frac{\partial\psi}{\partial\varphi} + \frac{1}{\sin\theta} \frac{\partial\psi}{\partial\chi}) \right\} \right] + E\psi = 0.$$

By carrying out the indicated derivatives and grouping terms in various ways one can arrive at a number of equivalent expressions for the wave equation, including the one used by Witmer (64) and by Wang (1). However, the following form is more easily interpreted:

$$\frac{\hbar^2}{2[I_s - (I_d^2/I_s)]}\left[\frac{1}{\sin\theta}\frac{\partial}{\partial\theta}(\sin\theta\frac{\partial\psi}{\partial\theta}) + \left[\frac{I_s - (I_d^2/I_s)}{I_z}\right.\right. \qquad \text{(A-21)}$$

$$\left.+ \frac{\cos^2\theta}{\sin^2\theta}\right]\frac{\partial^2\psi}{\partial\varphi^2} + \frac{1}{\sin^2\theta}\frac{\partial^2\psi}{\partial\chi^2} - 2\frac{\cos\theta}{\sin^2\theta}\frac{\partial^2\psi}{\partial\varphi\partial\chi}$$

$$+\frac{I_d}{I_s}\left\{-\cos 2\varphi\left[\frac{1}{\sin\theta}\frac{\partial}{\partial\theta}(\sin\theta\frac{\partial\psi}{\partial\theta}) + \frac{\cos^2\theta}{\sin^2\theta}\frac{\partial^2\psi}{\partial\varphi^2}\right.\right.$$

$$\left.+\frac{1}{\sin^2\theta}\frac{\partial^2\psi}{\partial\chi^2} - 2\frac{\cos\theta}{\sin^2\theta}\frac{\partial^2\psi}{\partial\varphi\partial\chi} - 2\frac{\partial^2\psi}{\partial\theta^2}\right]$$

$$+ 2\sin 2\varphi\left[-\frac{\cos\theta}{\sin\theta}\frac{\partial^2\psi}{\partial\theta\partial\varphi} + \frac{1}{\sin\theta}\frac{\partial^2\psi}{\partial\theta\partial\chi}\right.$$

$$\left.\left.\left.\left.+ (\frac{1}{2} + \frac{\cos^2\theta}{\sin^2\theta})\frac{\partial\psi}{\partial\varphi} - \frac{\cos\theta}{\sin^2\theta}\frac{\partial\psi}{\partial\chi}\right]\right\}\right] + E\psi = 0.$$

For $I_d = 0$, all of the bracketed expression beyond the second line vanishes. The remaining expression will be recognized as the wave equation for the symmetric rotor (69, 70, 71, 72) with $I_s = I_x = I_y$. In this case φ and χ are cyclic coordinates, and the equation separates with the substitution

$$\psi_{sym} = U = \Theta(\theta)\, e^{iK\varphi}\, e^{iM\chi} \quad , \qquad \text{(A-22)}$$

where K and M must be integers or zero to satisfy the requirement that the wavefunction be single-valued. The substitution yields the following differential equation for $\Theta(\theta)$:

$$\frac{1}{\sin\theta}\frac{d}{d\theta}\left(\sin\theta\frac{d\Theta}{d\theta}\right) \tag{A-23}$$

$$-\left[\frac{(M - K\cos\theta)^2}{\sin^2\theta} + \frac{I_s}{I_z}K^2 - \frac{2I_s}{\hbar^2}E_s\right]\Theta = 0.$$

Solutions of this equation are expressible in terms of hypergeometric series. The series must terminate if Θ is to remain finite at all values of θ, and this requires (69, 70, 72) that

$$E_s = \frac{\hbar^2}{2}\left[\frac{1}{I_s}J(J+1) + \left(\frac{1}{I_z} - \frac{1}{I_s}\right)K^2\right] \quad , \tag{A-24}$$

where $\begin{cases} J = 0, 1, 2, \ldots \\ J \geq |K| \\ J \geq |M| \end{cases}$

For the general case $I_d \neq 0$ the coordinate χ is still cyclic in (A-21), so that ψ can be written

$$\psi = F(\theta, \varphi)\, e^{iM\chi} \quad . \tag{A-25}$$

No simple further separation of variables is possible. Wang's method of solution consists in expanding ψ in a linear combination of symmetric rotor eigenfunctions U_{JKM}, constructing the Hamiltonian matrix in the U representation, and solving the corresponding set of simultaneous linear equations for the energy eigenvalues and the expansion coefficients. The success of this method in giving an exact solution lies in the fact that each ψ is expressible in terms of a finite number of U functions having the same J and M.

Technique of solution.--The approach just outlined lies wholly within the framework of basic wave mechanics, although in conformity with convention certain matrix terminology has been used. The method, developed by P. S. Epstein in 1926, is described quite simply by Pauling and Wilson (73).

Assume that ψ can be represented by a finite expansion of the form

$$\psi_{JM} = \sum_{K} a_{JK} U_{JKM} . \qquad (A-26)$$

The set of U_{JKM} restricted to particular values of J and M is not a complete basis for the representation of an arbitrary function of the Euler angles,* but it will prove sufficient for exact representation of the ψ function of the same J and M.

Write the orthonormal U_{JKM} functions in the form

$$U_{JKM} = \frac{1}{2\pi} \Theta_{JKM} e^{iK\varphi} e^{iM\chi} \quad . \qquad (A-27)$$

The factor $1/(2\pi)$ makes Θ_{JKM} separately normalized; that is, if

$$\int_{v} U^{*}_{J'K'M'} U_{JKM} \, dv = \delta_{J'K'M',\, JKM} \quad , \qquad (A-28)$$

where $dv = \sin\theta \, d\theta \, d\varphi \, d\chi$

θ: $0 \rightarrow \pi$

φ: $0 \rightarrow 2\pi$

χ: $0 \rightarrow 2\pi$,

---

*The unrestricted set with J, $|K|$, $|M|$ ranging from zero to infinity is complete.

then

$$\int_0^{\pi} \Theta_{JKM}^2 \sin\theta \, d\theta = 1 \quad . \tag{A-29}$$

The weighting function sin θ warrants comment. In the Schrödinger formulation (74) of the equation (A-17), the eigenfunctions are required to satisfy a normalization integral in which the "volume element" of the configuration space is $\Delta_p^{-\frac{1}{2}} \, dq_1 \ldots dq_n$. In the present problem, from (A-18),

$$dv = 8(I_x I_y I_z)^{\frac{1}{2}} \sin\theta \, d\theta \, d\varphi \, d\chi \quad . \tag{A-30}$$

The constant factor is immaterial since it is removed in the normalization process. One can also observe that in a Sturm-Liouville problem with equation

$$\frac{d}{dx}\left(p(x)\frac{dy}{dx}\right) - q(x)\, y + \lambda\rho(x)\, y = 0 \tag{A-31}$$

the characteristic-function solutions are orthogonal <u>only</u> with respect to the weighting function ρ(x). (75) If (A-23) is put in the form of (A-31), then ρ(θ) = sin θ. Thus the inclusion of sin θ in the volume element is an automatic consequence of the requirement that the symmetric rotor eigenfunctions be suitably orthonormal.

If the wave equation is now written

$$H\psi_{JM} - E\psi_{JM} = 0 \quad , \tag{A-32}$$

where H is the negative of the bracketed operator in (A-21), the substitution of (A-26) gives

$$\sum_K a_{JK} (H - E) U_{JKM} = 0 \quad . \tag{A-33}$$

Multiplication by $U^*_{JK'M} dv$ and integration over the configuration space gives

$$\sum_K a_{JK} \left[(JK'M|H|JKM) - E\delta_{K'K} \right] = 0 \quad , \tag{A-34}$$

where the "matrix element" $(JK'M|H|JKM)$ is the integral

$$(JK'M|H|JKM) = \int_v U^*_{JK'M} H U_{JKM} \sin\theta \, d\theta \, d\varphi \, d\chi \quad . \tag{A-35}$$

Since K ranges from -J to +J, including zero, the linear combination (A-34) has 2J+1 terms (some of which, however, will vanish). Furthermore, there will be 2J+1 different linear combinations corresponding to the possible choices of K'. Consequently (A-34) amounts to 2J+1 simultaneous linear equations in 2J+1 unknown a_{JK}'s.

If one can evaluate all the integrals of the form (A-35) to obtain simply a number for each $(JK'M|H|JKM)$, solution for the unknown a_{JK}'s becomes just a problem in algebra. It is well known that such a set of linear equations has a simultaneous solution only if the determinant of the coefficients of the unknowns vanishes. Here, expanding the determinant and equating the result to zero gives a secular equation of order 2J+1. This equation has 2J+1 real roots, the eigenvalues of E for which the determinant does indeed vanish. Often these allowed

asymmetric-rotor energies are all that one wants to know. However, the wave function $\psi_{J\tau M}$ corresponding to a particular eigenvalue $E_{J\tau}$ can be obtained by inserting $E_{J\tau}$ explicitly in the simultaneous equations and solving for the $a_{J\tau K}$'s. The index τ, used here to distinguish among the $2J+1$ E_J's and ψ_{JM}'s, is not a quantum number and has no physical significance. By convention the states are numbered from $\tau = -J$ to $\tau = +J$ in the order of increasing energy.

Because of the factorization (A-25) the matrix elements $(JK'M|H|JKM)$ are the same for all M, and the energy eigenvalues are therefore independent of M in the field-free case.

Evaluation of the Hamiltonian matrix elements.--To evaluate the integrals of the form (A-35), first examine the effect of allowing H to operate on U_{JKM}. HU_{JKM} is the negative of the expression (A-21), excluding the E term, with ψ replaced by U_{JKM}. Note that HU_{JKM} can be written in two parts: $H_s U_{JKM} + (I_d/I_s)H_a U_{JKM}$, corresponding to the first two lines and last four lines of (A-21) respectively. Now H_s is the Hamiltonian for a symmetric rotor with I_s replaced by $I_s - (I_d^2/I_s)$; therefore $H_s U_{JKM}$ is just U_{JKM} multiplied by a quantity obtained by making the same replacement in (A-24):

$$H_s U_{JKM} = \frac{\hbar^2}{2\,[I_s - (I_d^2/I_s)]} \times \left[J(J+1) + \left(\frac{I_s - (I_d^2/I_s)}{I_z} - 1 \right) K^2 \right] U_{JKM} \quad . \tag{A-36}$$

Furthermore, the first two lines of H_a reduce to

$$-\cos 2\varphi \left[H_s + \frac{\hbar^2}{2I_z} \frac{\partial^2}{\partial \varphi^2} + \frac{\hbar^2}{I_s - (I_d^2/I_s)} \frac{\partial^2}{\partial \theta^2} \right] \quad , \tag{A-37}$$

which simplifies the substitution. If now U_{JKM} is factored in the form (A-27) and $\sin 2\varphi$, $\cos 2\varphi$ are replaced by their equivalent exponential expressions, one obtains upon carrying out the differentiations and regrouping terms:

$$HU_{JKM} = \frac{\hbar^2}{2[I_s - (I_d^2/I_s)]} \times \tag{A-38}$$

$$\left\{ \left[J(J+1) + \left(\frac{I_s - (I_d^2/I_s)}{I_z} - 1 \right) K^2 \right] U_{JKM} \right.$$

$$\left. - \frac{I_d}{I_s} \left[f(\theta) \frac{1}{2\pi} e^{i(K+2)\varphi} e^{iM\chi} + g(\theta) \frac{1}{2\pi} e^{i(K-2)\varphi} e^{iM\chi} \right] \right\} \quad ,$$

where

$$f(\theta) = \frac{d}{d\theta} \left[\frac{d}{d\theta} \Theta_{JKM} + \frac{M - K\cos\theta}{\sin\theta} \Theta_{JKM} \right] \tag{A-39}$$

$$- \frac{1}{2} \left[-J(J+1) + K(K+1) \right] \Theta_{JKM} \quad ,$$

$$g(\theta) = \frac{d}{d\theta} \left[\frac{d}{d\theta} \Theta_{JKM} - \frac{M - K\cos\theta}{\sin\theta} \Theta_{JKM} \right] \tag{A-40}$$

$$- \frac{1}{2} \left[-J(J+1) + K(K-1) \right] \Theta_{JKM} \quad .$$

The crux of Wang's solution is the proof that the functions $f(\theta)$ and $g(\theta)$ are just the Θ functions for K+2 and K-2 respectively, multiplied by constants:

$$f(\theta) = \frac{1}{2}\left[(J-K-1)(J-K)(J+K+1)(J+K+2)\right]^{\frac{1}{2}} \Theta_{J,\,K+2,\,M} \quad , \qquad (A-41)$$

$$g(\theta) = \frac{1}{2}\left[(J+K-1)(J+K)(J-K+1)(J-K+2)\right]^{\frac{1}{2}} \Theta_{J,\,K-2,\,M} \quad . \qquad (A-42)$$

Wang establishes this identification by working with the hypergeometric functions in terms of which explicit solutions of (A-23) can be expressed. The reduction follows from certain relations, developed by Gauss, among hypergeometric functions and their derivatives. This approach, however, involves an intricate chain of substitutions and requires consideration of nine separate cases of the relative magnitudes of K and M. A more attractive procedure is to derive (A-41, 42) directly from the Θ wave equation (A-23), which with substitution of E_s from (A-24) takes the following form:

$$\frac{1}{\sin\theta}\frac{d}{d\theta}(\sin\theta\,\Theta') = \Theta'' + \frac{\cos\theta}{\sin\theta}\Theta' \qquad (A-43)$$

$$= \left[\frac{(M - K\cos\theta)^2}{\sin^2\theta} - J(J+1) + K^2\right] \Theta \quad ,$$

where (') means $\frac{d}{d\theta}$, and $\Theta = \Theta_{JKM}$.

It will first be shown that $f(\theta)$ satisfies an equation of the type (A-43) with K replaced by K+2. In addition to the form of $f(\theta)$ expressed

by (A-39), it will be convenient to use an alternate form obtained by carrying out the differentiation indicated in (A-39) and substituting for Θ'' from (A-43).

$$f(\theta) = \frac{M - (K+1)\cos\theta}{\sin\theta}\left[\Theta' + \frac{M - K\cos\theta}{\sin\theta}\Theta\right] \qquad \text{(A-44)}$$

$$+\frac{1}{2}\left[-J(J+1) + K(K+1)\right]\Theta \quad .$$

Differentiate (A-44) to obtain $f' = \frac{d}{d\theta}[f(\theta)]$:

$$f' = \frac{M - (K+1)\cos\theta}{\sin\theta}\frac{d}{d\theta}\left[\Theta' + \frac{M - K\cos\theta}{\sin\theta}\Theta\right] \qquad \text{(A-45)}$$

$$+\frac{(K+1) - M\cos\theta}{\sin^2\theta}\left[\Theta' + \frac{M - K\cos\theta}{\sin\theta}\Theta\right]$$

$$+\frac{1}{2}\left[-J(J+1) + K(K+1)\right]\Theta \quad .$$

Now note that

$$\frac{(K+1) - M\cos\theta}{\sin^2\theta} = (K+1) - \frac{\cos\theta}{\sin\theta}\left[\frac{M - (K+1)\cos\theta}{\sin\theta}\right] \qquad \text{(A-46)}$$

and make the substitutions, from (A-39) and (A-44) respectively,

$$\frac{d}{d\theta}\left[\Theta' - \frac{M - K\cos\theta}{\sin\theta}\Theta\right] = f + \frac{1}{2}\left[-J(J+1) + K(K+1)\right]\Theta; \qquad \text{(A-47)}$$

$$\frac{M - (K+1)\cos\theta}{\sin\theta}\left[\Theta' + \frac{M - K\cos\theta}{\sin\theta}\Theta\right] \qquad \text{(A-48)}$$

$$= f - \frac{1}{2}\left[-J(J+1) + K(K+1)\right]\Theta \quad .$$

With regrouping of terms, the result is

$$f' = \frac{M - (K+2)\cos\theta}{\sin\theta} f \qquad \text{(A-49)}$$

$$+ \frac{1}{2}\left[-J(J+1) + (K+2)(K+1)\right]\left[\Theta' + \frac{M - K\cos\theta}{\sin\theta}\Theta\right] \quad .$$

A further differentiation of $(\sin\theta)f'$ gives:

$$\frac{1}{\sin\theta}\frac{d}{d\theta}(\sin\theta\, f') = \frac{M - (K+2)\cos\theta}{\sin\theta} f' + (K+2)\, f \qquad \text{(A-50)}$$

$$+ \frac{1}{2}\left[-J(J+1) + (K+2)(K+1)\right]\left\{\frac{d}{d\theta}\left[\Theta' + \frac{M - K\cos\theta}{\sin\theta}\Theta\right]\right.$$

$$\left. + \frac{\cos\theta}{\sin\theta}\left[\Theta' + \frac{M - K\cos\theta}{\sin\theta}\Theta\right]\right\} \quad .$$

Replace f' by the expression in (A-49).

$$\frac{1}{\sin\theta}\frac{d}{d\theta}(\sin\theta\, f') = \frac{\left[M - (K+2)\cos\theta\right]^2}{\sin^2\theta} f + (K+2)\, f \qquad \text{(A-51)}$$

$$+ \frac{1}{2}\left[-J(J+1) + (K+2)(K+1)\right]\left\{\frac{d}{d\theta}\left[\Theta' + \frac{M - K\cos\theta}{\sin\theta}\Theta\right]\right.$$

$$\left. + \frac{M - (K+1)\cos\theta}{\sin\theta}\left[\Theta' + \frac{M - K\cos\theta}{\sin\theta}\Theta\right]\right\} \quad .$$

From (A-47) and (A-48), the quantity in braces is just $2f$. Therefore,

$$\frac{1}{\sin\theta}\frac{d}{d\theta}(\sin\theta\, f') = \left[\frac{[M-(K+2)\cos\theta]^2}{\sin^2\theta} - J(J+1) + (K+2)^2\right] f \quad . \tag{A-52}$$

Comparison of this expression with (A-43) shows that it is identical to the symmetric rotor wave equation for $\Theta_{J,\,K+2,\,M}$; therefore

$$f(\theta) = N\,\Theta_{J,\,K+2,\,M} \quad , \tag{A-53}$$

where N is a constant. Because the Θ functions have been taken as normalized in accordance with (A-29), the value of N can be determined by evaluating the integral

$$\int_0^\pi f^2 \sin\theta\, d\theta = N^2 \int_0^\pi \Theta^2_{J,\,K+2,\,M} \sin\theta\, d\theta = N^2 \quad . \tag{A-54}$$

The integration of f^2 is best approached with the aid of the identity

$$\int (f + n\Theta)(f - n\Theta) \sin\theta\, d\theta \equiv \tag{A-55}$$

$$\int f^2 \sin\theta\, d\theta - n^2 \int \Theta^2 \sin\theta\, d\theta \quad ,$$

where n is an arbitrary constant and $\Theta = \Theta_{JKM}$. Let

$$n = \frac{1}{2}[-J(J+1) + K(K+1)] \quad . \tag{A-56}$$

Obtain $f + n\Theta$ from (A-47) and $f - n\Theta$ from (A-48). Use of (A-55) then gives

$$\int_0^{\pi} f^2 \sin\theta \, d\theta = N^2 = n^2 \int_0^{\pi} \Theta^2 \sin\theta \, d\theta \qquad \text{(A-57)}$$

$$+ \int_0^{\pi} [\, M - (K+1)\cos\theta] \left[\Theta' + \frac{M - K\cos\theta}{\sin\theta}\,\Theta\right] \times$$

$$\frac{d}{d\theta}\left[\,\Theta' + \frac{M - K\cos\theta}{\sin\theta}\,\Theta\right] d\theta \ .$$

The first integral is unity, since Θ is normalized in accordance with (A-29). The second integral can be evaluated by a succession of integrations by parts; the first step in this process yields:

$$N^2 = n^2 - \tfrac{1}{2}(K+1) \int_0^{\pi} \left[\Theta' + \frac{M - K\cos\theta}{\sin\theta}\,\Theta\right]^2 \sin\theta \, d\theta \qquad \text{(A-58)}$$

$$+ \tfrac{1}{2}\left[[\, M - (K+1)\cos\theta] \left[\Theta' + \frac{M - K\cos\theta}{\sin\theta}\,\Theta\right]^2\right]_0^{\pi} \ .$$

The integral term, with the square expanded, is

$$- \tfrac{1}{2}(K+1) \int_0^{\pi} \left[(\Theta')^2 + 2\,\frac{M - K\cos\theta}{\sin\theta}\,\Theta\Theta' \right. \qquad \text{(A-59)}$$

$$\left. + \frac{(M - K\cos\theta)^2}{\sin^2\theta}\,\Theta^2\right] \sin\theta \, d\theta \ .$$

But again by parts,

$$\int (\Theta')^2 \sin\theta \, d\theta = \Theta\Theta' \sin\theta - \int \Theta \frac{d}{d\theta}(\sin\theta\,\Theta') \, d\theta \ . \qquad \text{(A-60)}$$

With substitution from (A-43) for $\frac{d}{d\theta}(\sin\theta\Theta')$ and insertion of the result in (A-59), the latter becomes:

$$-\tfrac{1}{2}(K+1)\left\{-[-J(J+1)+K^2]\int_0^{\pi}\Theta^2\sin\theta\,d\theta\right. \tag{A-61}$$

$$\left.+2\int_0^{\pi}(M-K\cos\theta)\Theta\Theta'\,d\theta+[\Theta\Theta'\sin\theta]_0^{\pi}\right\}.$$

Again by parts,

$$2\int_0^{\pi}(M-K\cos\theta)\Theta\Theta'\,d\theta=-K\int_0^{\pi}\Theta^2\sin\theta\,d\theta \tag{A-62}$$

$$+[(M-K\cos\theta)\Theta^2]_0^{\pi}.$$

With this substitution in (A-61), and with replacement of the Θ normalization integral by unity as before, the integral term of (A-58) becomes finally

$$-\tfrac{1}{2}(K+1)\left\{-n+\Theta\Theta'\sin\theta+[(M-K\cos\theta)\Theta^2]_0^{\pi}\right\}, \tag{A-63}$$

and the whole expression becomes

$$N^2=n^2+\tfrac{1}{2}(K+1)n+\tfrac{1}{2}\left[\sin\theta\left\{\left[\Theta'+\frac{M-K\cos\theta}{\sin\theta}\Theta\right]\times\right.\right. \tag{A-64}$$

$$\left.\left.\left[\frac{M-(K+1)\cos\theta}{\sin\theta}\left(\Theta'+\frac{M-K\cos\theta}{\sin\theta}\Theta\right)-(K+1)\Theta\right]\right\}\right]_0^{\pi}.$$

It is now necessary to examine the behavior of the expression involving Θ and its derivative at the end points 0 and π. Compare the expression in braces with the expression for $f(\theta)$ in (A-44). Although the expression above contains $\sin\theta$ in the denominator, it does so to lesser degree than does $f^2(\theta)$. Now $f(\theta)$ has been proved to be a symmetric rotor theta eigenfunction, and all such functions are known to remain finite for all θ, including the end points. (It was this requirement that necessitated termination of the hypergeometric series by specification of E_s as in (A-24).) Therefore the expression in braces must also remain finite, and the appearance of the factor $\sin\theta$ outside the braces is sufficient to make the whole quantity vanish at 0 and π. Thus

$$N^2 = n^2 + \tfrac{1}{2}(K+1)n \qquad \text{(A-65)}$$

$$= \tfrac{1}{4}\left\{\left[-J(J+1) + K(K+1)\right]^2 + 2(K+1)\left[-J(J+1) + K(K+1)\right]\right\} \quad .$$

Factoring the expression in braces and taking the square root, one obtains finally,

$$N = \tfrac{1}{2}\left[(J-K-1)(J-K)(J+K+1)(J+K+2)\right]^{\frac{1}{2}} \quad , \qquad \text{(A-66)}$$

which when inserted in (A-53) agrees[†] with (A-41). The manipulation of $g(\theta)$ to obtain (A-42) is identical to that of $f(\theta)$ except that M and K are replaced by their negatives wherever they appear.

[†] Wang found an irregularity of the sign of N whenever $M - K = 1$. To avoid it he redefined the symmetric rotor eigenfunctions, taking them to be the so-called "Van Vleck" functions. The latter are the ordinary eigenfunctions multiplied by $(-1)^x$, where x is the larger of M or K. This

Insertion of (A-41) and (A-42) in (A-38) now gives:

$$HU_{JKM} = \frac{\hbar^2}{2[I_s - (I_d^2/I_s)]} \times \tag{A-67}$$

$$\left\{ \left[J(J+1) + \left(\frac{I_s - (I_d^2/I_s)}{I_z} - 1 \right) K^2 \right] U_{JKM} \right.$$

$$- \frac{I_d}{I_s} \frac{1}{2} [(J-K-1)(J-K)(J+K+1)(J+K+2)]^{\frac{1}{2}} U_{J,K+2,M}$$

$$\left. - \frac{I_d}{I_s} \frac{1}{2} [(J+K-1)(J+K)(J-K+1)(J-K+2)]^{\frac{1}{2}} U_{J,K-2,M} \right\} .$$

If this expression is multiplied on the left by $U^*_{J'K'M'}$ and integrated in the manner of (A-35), it is clear because of the orthonormality condition (A-28) that all such integrals vanish except when $J' = J$, $M' = M$, and K' is either K, $K-2$, or $K+2$. It is this circumstance which permits exact expansion of an asymmetric rotor eigenfunction in terms of a restricted set of symmetric rotor eigenfunctions as in (A-26), and which confirms that J and M are legitimate quantum numbers for characterization of asymmetric rotor states.

---

irregularity has not appeared in the present approach, which has given only the magnitude of N; the positive sign of the square root in (A-66) was chosen arbitrarily. Various treatments differ in the choice of this sign, which is of consequence only in the determination of certain symmetry properties of the eigenfunctions; care must be taken to maintain self-consistency in the assumptions of these and other sign behaviors.

The non-vanishing integrals are the following:

$$(J, K-2, M|\,H\,|\,JKM) = \tag{A-68}$$

$$-\frac{\hbar^2}{4}\left[\frac{I_d}{I_s^2 - I_d^2}\right][(J+K-1)(J+K)(J-K+1)(J-K+2)]^{\frac{1}{2}}$$

$$(JKM|\,H\,|\,JKM) = \tag{A-69}$$

$$\frac{\hbar^2}{2}\left[\frac{I_s}{I_s^2 - I_d^2}\right]\left[J(J+1) + \left(\frac{I_s^2 - I_d^2}{I_s I_z} - 1\right)K^2\right]$$

$$(J, K+2, M|\,H\,|\,JKM) = \tag{A-70}$$

$$-\frac{\hbar^2}{4}\left[\frac{I_d}{I_s^2 - I_d^2}\right][(J-K-1)(J-K)(J+K+1)(J+K+2)]^{\frac{1}{2}} \quad .$$

With reintroduction of I_x and I_y from (A-4),

$$(J, K-2, M|\,H\,|\,JKM) = \tag{A-71}$$

$$-\frac{\hbar^2}{4}\left[\frac{1}{2}\left(\frac{1}{I_x} - \frac{1}{I_y}\right)\right][(J+K-1)(J+K)(J-K+1)(J-K+2)]^{\frac{1}{2}}$$

$$(JKM|\,H\,|\,JKM) = \tag{A-72}$$

$$\frac{\hbar^2}{2}\left[\frac{1}{2}\left(\frac{1}{I_x} + \frac{1}{I_y}\right)\right]J(J+1) + \frac{\hbar^2}{2}\left[\frac{1}{I_z} - \frac{1}{2}\left(\frac{1}{I_x} + \frac{1}{I_y}\right)\right]K^2$$

$$(J, K+2, M|\,H\,|\,JKM) = \qquad (A-73)$$

$$-\frac{\hbar^2}{4}\left[\frac{1}{2}\left(\frac{1}{I_x}-\frac{1}{I_y}\right)\right]\left[(J-K-1)(J-K)(J+K+1)(J+K+2)\right]^{\frac{1}{2}} \quad .$$

In some treatments the "off-diagonal" matrix elements (A-71) and (A-73) appear with positive instead of negative sign, the result of the freedom of choice of the sign of the square root in (A-66) or of interchange of the x and y axis assignments in the definitions of the Euler angles (Figure 10). The negative sign agrees with Wang (1), Van Winter (76) and others. This ambiguity does not affect the energy solutions, but it complicates correlation of various treatments when one attempts to examine symmetry properties of the eigenfunctions. This point is discussed in detail by King, Hainer, and Cross (77).

Calculation of energy levels.--The matrix elements (A-71, 72, 73) for a particular value of J now can be inserted in the set of linear equations (A-34), and those equations can be solved for the allowed energy levels in the manner described previously. One finds in the literature a number of techniques, involving the introduction of various "asymmetry parameters," for rearranging the equations to simplify the mathematical mechanics of the solution. The most valuable of these is that of Ray (2) and King, Hainer, and Cross (3), because it is the basis of several digital-computer tabulations of "asymmetric rotor eigenvalues."

Let a "reduced energy" $E(\kappa)$ be defined in relation to the rotor energy E by the expression

$$E = \frac{\hbar^2}{2}\left[\frac{1}{2}\left(\frac{1}{I_x} - \frac{1}{I_y}\right)E(\kappa) + \frac{1}{2}\left(\frac{1}{I_x} + \frac{1}{I_y}\right)J(J+1)\right] \quad . \tag{A-74}$$

If this substitution is made for E in the equations (A-34), the "diagonal" terms (K = K') become:

$$a_{JK}\left[(JKM|H|JKM) - E\right] = \tag{A-75}$$

$$a_{JK}\frac{\hbar^2}{2}\left\{\left[\frac{1}{I_z} - \frac{1}{2}\left(\frac{1}{I_x} + \frac{1}{I_y}\right)\right]K^2 - \frac{1}{2}\left(\frac{1}{I_x} - \frac{1}{I_y}\right)E(\kappa)\right\} ,$$

where $(JKM|H|JKM)$ has been obtained from (A-72). The "off-diagonal" terms in which (A-71) and (A-73) appear remain unchanged. Now divide every term of each equation by

$$\frac{\hbar^2}{2}\left[\frac{1}{2}\left(\frac{1}{I_x} - \frac{1}{I_y}\right)\right] \quad ,$$

and let

$$\kappa = \frac{\frac{1}{I_z} - \frac{1}{2}\left(\frac{1}{I_x} + \frac{1}{I_y}\right)}{\frac{1}{2}\left(\frac{1}{I_x} - \frac{1}{I_y}\right)} \quad . \tag{A-76}$$

The result is a modified set of simultaneous linear equations of the form

$$\sum_K a_{JK}\left[(JK'M|H_\kappa|JKM) - E(\kappa)\delta_{K'K}\right] = 0 \quad , \tag{A-77}$$

whose non-vanishing $(JK'M|H_\kappa|JKM)$ are:

$$(J, K-2, M|\, H_\kappa \,|\, JKM) = -\frac{1}{2}[(J+K-1)(J+K)(J-K+1)(J-K+2)]^{\frac{1}{2}} \quad (A-78)$$

$$(JKM|\, H_\kappa \,|\, JKM) = \kappa K^2 \quad (A-79)$$

$$(J, K+2, M|\, H_\kappa \,|\, JKM) = -\frac{1}{2}[(J-K-1)(J-K)(J+K+1)(J+K+2)]^{\frac{1}{2}} \,. \quad (A-80)$$

All terms of this new set of equations are dimensionless numbers, and the rotor moments of inertia appear only in the determination of the "asymmetry parameter" κ. All rotors with the same degree of asymmetry therefore have the same reduced energy eigenvalues $E(\kappa)$. It is thus possible to prepare a universal table of these eigenvalues, for incremental steps of the parameter κ, from which the rotational energy levels of any asymmetric rotor can be determined. The original paper of King, Hainer, and Cross (3) included such a table for J = 0 through J = 10. A very useful digital-computer tabulation for J = 0 through J = 12, with finer κ resolution, has been prepared by Turner, Hicks, and Reitwiesner (36). Nielsen (59) mentions an extended tabulation to J = 40 by Erlandsson in Sweden. The compilation and use of these tables is simplified by the fact that when the states are numbered in order of increasing energy by the τ index introduced previously,

$$E_{J\tau}(\kappa) = -E_{J,-\tau}(-\kappa) \,. \quad (A-81)$$

It is customary in microwave spectroscopy to express (A-74) and (A-76) in terms of the "rotational constants" introduced in Chapter I:

$$A = \frac{h}{8\pi^2 I_a} \quad ; \quad B = \frac{h}{8\pi^2 I_b} \quad ; \quad C = \frac{h}{8\pi^2 I_c} \tag{A-82}$$

where $I_a \leq I_b \leq I_c$.

Let the magnitude-ordered moments of inertia be identified with I_x, I_y, I_z in the following manner:*

$$I_x = I_a \quad ; \quad I_y = I_c \quad ; \quad I_z = I_b \quad . \tag{A-83}$$

The substitution of (A-82) in (A-74) and (A-76) then gives

$$\frac{E}{h} = \frac{1}{2}[(A-C)E(\kappa) + (A+C)J(J+1)] \quad , \tag{A-84}$$

and

$$\kappa = \frac{2B - A - C}{A - C} \quad . \tag{A-85}$$

The quantities E/h, A, B, and C have dimensions t^{-1} and are commonly expressed in megacycles per second (Mc). If the moments of inertia are expressed in (atomic mass units)×(Angstroms)^2, the rotational constants are most conveniently obtained by expressing $h/8\pi^2$ as

$$\frac{h}{8\pi^2} = (5.0553 \pm 0.0003) \times 10^5 \text{ Mc amu } A^2 \quad . \tag{A-86}$$

---

*There are six ways in which right-handed and left-handed abc axes can be identified with the xyz axes. The correspondence used here is the one called "Type II^l" by King, Hainer, and Cross (77).

An important characteristic of the determinant associated with the equations (A-77) permits expression of the rotational energy for low J values in closed algebraic form. The determinant has such symmetry that the secular equation obtained by equating it to zero always factors into a product of expressions (four, for $J \geq 2$) of lower degree in $E(\kappa)$. The equations obtained by equating these expressions separately to zero are of second degree at most for $J \leq 3$. Solution of these equations gives the rotor energies listed by Gordy, Smith, and Trambarulo (33). Certain roots for $J = 4, 5$ also are obtained from quadratic factors of the secular equations.

Symmetry properties of the eigenfunctions.--Regardless of a rotor's physical structure, its rotational motion is described in terms of the motion of an inertia ellipsoid which is symmetrical with respect to a 180-degree rotation about any principal axis. This fact gives rise to symmetry properties of the rotational eigenfunctions which are of importance in establishing transition selection rules.

It is customary to indicate a 180-degree rotation about an axis i by the operator symbol C_2^i. By inspection of Figure 10 one can determine the effect upon the angular coordinates θ, φ, χ of C_2^i operations with respect to the body-fixed axes xyz. The rotations are equivalent to the following substitutions:

$$
\begin{aligned}
C_2^x &: \quad \theta \rightarrow \pi - \theta \; ; \quad \varphi \rightarrow \pi - \varphi \; ; \quad \chi \rightarrow \pi + \chi \\
C_2^y &: \quad \theta \rightarrow \pi - \theta \; ; \quad \varphi \rightarrow -\varphi \; ; \quad \chi \rightarrow \pi + \chi \\
C_2^z &: \quad \theta \rightarrow \theta \; ; \quad \varphi \rightarrow \pi + \varphi \; ; \quad \chi \rightarrow \chi \; .
\end{aligned}
\tag{A-87}
$$

Note that any two of these substitutions performed in succession produce the remaining one, and that all three performed in succession restore the original configuration.

The behavior of a symmetric rotor eigenfunction U_{JKM} with respect to these substitutions is readily determined. Replacements of the φ and χ coordinates can be made directly in the exponential factors of (A-27); the effect on Θ_{JKM} can be established by making the substitution for θ in equation (A-43). Both C_2^x and C_2^y produce the substitution $\theta \rightarrow (\pi - \theta)$, which when made in (A-43) simply changes the sign of $(K \cos \theta)$ to positive. The new equation is satisfied by $\Theta_{J,-K,M}$. With inclusion of the exponential factors one therefore concludes:

$$C_2^x : \; U_{JKM} \rightarrow (-1)^{K+M+\alpha} U_{J,-K,M} \qquad \text{(A-88)}$$

$$C_2^y : \; U_{JKM} \rightarrow (-1)^{M+\alpha} U_{J,-K,M}$$

$$C_2^z : \; U_{JKM} \rightarrow (-1)^{K} U_{JKM} \quad .$$

(The integer α allows specification of the sign behavior assumed for $\Theta_{JKM} \rightarrow (-1)^{\alpha} \Theta_{J,-K,M}$; it depends upon the formalism used to define the "positive" Θ_{JKM}'s.)

Evidently a π-rotation about the z-axis either leaves U_{JKM} unchanged or at most changes its sign; but C_2^x and C_2^y transform U_{JKM} into $\pm U_{J,-K,M}$, with which it is degenerate. This reversal of the sign of K is consistent with the identification, made in the various treatments of the symmetric rotor, of $\hbar K$ as an eigenvalue of the component

of angular momentum along the z-axis. Both C_2^x and C_2^y reverse the spatial orientation of the z-axis and hence reverse the sign of an angular momentum component referred to it.

For the asymmetric rotor there is no such fixed component of angular momentum whose direction can resolve spatial reversals of the z-axis. Any operation C_2^i about a principal axis therefore brings the inertia ellipsoid to an orientation that is indistinguishable from the initial one. The probability densities $\psi^*\psi$ of the two orientations must consequently be the same; this implies that $\psi_{J\tau M}$ either is unchanged by the rotation or is changed only in sign. This condition is satisfied automatically when the equations

$$\sum_K a_{J\tau K} \left[(JK'M|H|JKM) - E_{J\tau}\delta_{K'K} \right] = 0 \qquad \text{(A-89)}$$

are solved simultaneously for the $a_{J\tau K}$'s. It is found that in the expansion

$$\psi_{J\tau M} = \sum_K a_{J\tau K} U_{JKM} , \qquad \text{(A-90)}$$

the coefficients of U_{JKM} and $U_{J,-K,M}$ always have the same absolute magnitude, and the resulting combinations

$$a_{J\tau K} (U_{JKM} \pm U_{J,-K,M})$$

are clearly symmetrical or antisymmetrical with respect to C_2^x and C_2^y as well as to C_2^z. Furthermore, it is found that all such combinations

appearing in the expansion of a particular $\psi_{J\tau M}$ have the same behavior with respect to rotation, so that $\psi_{J\tau M}$ is symmetrical or antisymmetrical in the same manner.

A ψ-function can either be symmetrical with respect to C_2^i about all three principal axes, or it can be symmetrical with respect to one axis and antisymmetrical with respect to the other two. (Any other combination would contradict the observation that the three substitutions (A-87) performed in succession restore the original configuration.) There are consequently four possible combinations of behaviors. These "symmetry species" are enumerated in Table 12, together with the species designations assigned to them by Mulliken (78) following group theory convention.

Table 12. Symmetry Classification of Asymmetric Rotor Eigenfunctions

Species Designation	Behavior		
	C_2^c	C_2^b	C_2^a
A	+	+	+
B_c	+	-	-
B_b	-	+	-
B_a	-	-	+

Eigenfunctions of all four types exist for every $J \geq 2$; each of the four factors of the secular equation yields solutions of a particular species. Specification of symmetry with respect to the ordered principal axes

abc results in a unique correspondence between the symmetries of eigenstates and the magnitudes of their energy eigenvalues. Dennison (79) has shown that for a given J, the C_2^c behavior of the state of highest energy is always +, and the C_2^c behaviors of the remaining states alternate in pairs in order of descending energy: −, −, +, +, −, −, etc. Similarly, the C_2^a behavior of the state of lowest energy is always +, and the C_2^a behaviors of the remaining states alternate in pairs in order of ascending energy: −, −, +, +, etc. Dennison denotes species by juxtaposing the behavior symbols for C_2^c, C_2^a. Thus ++ corresponds to species A; +− to B_c; −− to B_b; −+ to B_a.

Transition probabilities and selection rules.--If a rotor having an electric dipole moment μ is subjected to an external electric field of strength $\mathcal{E}$, the rotor Hamiltonian operator includes the interaction energy term

$$H' = -\mu\mathcal{E}\cos\alpha \quad , \tag{A-91}$$

where α is the angle of orientation of μ with respect to $\mathcal{E}$. When the field is that of a plane-polarized electromagnetic wave of frequency ν, the instantaneous field strength is

$$\mathcal{E}(t) = \mathcal{E}\cos 2\pi\nu t = \frac{1}{2}\mathcal{E}\left(e^{i2\pi\nu t} + e^{-i2\pi\nu t}\right) \quad . \tag{A-92}$$

According to time-dependent perturbation theory (80), if an unperturbed system with stationary-state wave functions $\Psi_j^o(q, t)$ is subjected to a

time-varying perturbation H'(t), then the wave functions of the perturbed system can be written as

$$\Psi(q, t) = \sum_j a_j(t)\, \Psi_j^o(q, t) \quad , \tag{A-93}$$

where the expansion coefficients $a_j(t)$ are found from the set of simultaneous differential equations

$$\frac{da_m(t)}{dt} = -\frac{i}{\hbar} \sum_j a_j(t) \int \Psi_m^o(q, t)^* \; H' \; \Psi_j^o(q, t)\, dv \tag{A-94}$$

$$m = 0,\ 1,\ 2,\ \ldots \quad .$$

If the system is in state n at time zero, solution of these equations with the boundary condition $a_m(0) = 0$; $a_n(0) = 1$ gives an expansion of the wave function at any subsequent time t. The quantity $a_m^*(\Delta t)a_m(\Delta t)$ then represents the probability that the system is in state m after a time interval Δt. If the perturbation is small and the time interval is short all expansion coefficients remain small compared to $a_n(t)$, which remains nearly unity. Therefore, to first-order approximation,

$$\frac{da_m(t)}{dt} = -\frac{i}{\hbar} \int \Psi_m^o(q, t)^* H' \; \Psi_n^o(q, t)\, dv \quad . \tag{A-95}$$

Now the wave function $\Psi_j^o(q, t)$ can be factored as

$$\Psi_j^o(q, t) = \psi_j^o \; e^{-iE_j/\hbar} \quad , \tag{A-96}$$

where $\psi_j^o = \psi_j^o(q)$ is an amplitude eigenfunction and E_j is the corresponding energy eigenvalue. Substitution of (A-96) and (A-91) in (A-95) gives

$$\frac{da_m(t)}{dt} = \frac{1}{2}\mu\mathcal{E}(m|\cos\alpha|n)\frac{i}{\hbar}\left[e^{\frac{i}{\hbar}(E_m-E_n+h\nu)t} + e^{\frac{i}{\hbar}(E_m-E_n-h\nu)t}\right], \tag{A-97}$$

where

$$(m|\cos\alpha|n) = \int \psi_m^{o*}\cos\alpha\,\psi_n^o\,dv \quad . \tag{A-98}$$

Equation (A-97) integrates immediately. With integration constants chosen to make $a_m(0) = 0$,

$$a_m(t) = -\frac{1}{2}\mu\mathcal{E}(m|\cos\alpha|n)\left[\frac{1-e^{\frac{i}{\hbar}(E_m-E_n+h\nu)t}}{E_m-E_n+h\nu} + \frac{1-e^{\frac{i}{\hbar}(E_m-E_n-h\nu)t}}{E_m-E_n-h\nu}\right] . \tag{A-99}$$

This expression has significant magnitude only if $E_m-E_n \approx \pm h\nu$, when one or the other of the "resonance denominators" approaches zero. In either case, retaining the significant term only, one obtains for the transition probability:

$$a_m^*(t)a_m(t) = \mu^2\mathcal{E}^2(m|\cos\alpha|n)^2 \times \left[\frac{\sin^2\frac{\pi}{h}(|E_m-E_n| - h\nu)t}{(|E_m-E_n| - h\nu)^2}\right] , \tag{A-100}$$

where

$$(m|\cos\alpha|n)^2 = (m|\cos\alpha|n)^*(m|\cos\alpha|n) \quad . \tag{A-101}$$

For monochromatic radiation with $h\nu$ precisely equal to $(E_m - E_n|$, the quantity in brackets becomes $(\pi t/h)^2$. If the matrix element (A-98) does not vanish, the probability of a radiation-induced transition from state n to state m is finite and increases as t^2. If $E_m > E_n$, energy $h\nu$ is absorbed from the radiation field in transition; if $E_n > E_m$, the energy is emitted.

When a macroscopic molecular gas is represented by an ensemble of rotors, the condition of precise frequency equality is not realizable. Even if the radiation is purely monochromatic, the frequency seen by an individual rotor is shifted by the Doppler effect of translational motion of the rotor relative to the source. Furthermore, collision effects tend to "smear" the energy levels E_n. For prediction of absorption by a macroscopic ensemble, the bracketed quantity in (A-100) therefore must be averaged over a range of the argument $(|E_m - E_n| - h\nu)$. Let $S(\nu)$ be a statistical distribution function such that $S(\nu)d\nu$ is the fraction of the total number of rotors in the state n for which $(|E_m - E_n| - h\nu)$ lies between $(|E_m - E_n|_o - h\nu)$ and $(|E_m - E_n|_o - h[\nu + d\nu])$. Then the average value of the bracketed quantity is

$$\int_\nu S(\nu) \, \frac{\sin^2 \frac{\pi}{h}(|E_m - E_n| - h\nu)t}{(|E_m - E_n| - h\nu)^2} \, d\nu \quad . \tag{A-102}$$

Now the factor of the form $(\sin^2 x)/x^2$ has negligibly small amplitude except in the central peak and adjacent lobes about x = 0, and the integral

$$\int \frac{\sin^2 x}{x^2}\, dx$$

over the central region is very nearly π. If the distribution $S(\nu)$ is assumed to have a broad maximum so that it remains near its maximum value S_o over the central region of the integral, then (A-102) can be approximated

$$S_o \frac{\pi t}{h^2} \int_x \frac{\sin^2 x}{x^2}\, dx \approx S_o \frac{\pi^2}{h^2} t \quad .$$

Consequently,

$$a_m^*(t) a_m(t) \approx \frac{\pi^2}{h^2} \mu^2 \mathcal{E}^2 (m|\cos \alpha|n)^2 S_o t \qquad \text{(A-103)}$$

for radiation of frequency $\nu_o = (|E_m - E_n|_o)/h$. The averaging process has produced a linear time dependence.

Consider a plane wave of frequency ν_o incident normally upon a wafer-like section of gas of surface area A and thickness dX. The rate at which energy is transported through A is[†]

$$P = \frac{c}{8\pi} \mathcal{E}^2 A. \qquad \text{(A-104)}$$

c = velocity of light

[†] The permittivity of the gas is assumed to be essentially that of free space. Electrostatic cgs units are used.

If $E_m > E_n$, each transition $n \rightarrow m$ induced by the radiation as it traverses the volume of gas is accompanied by loss of energy $h\nu_o$. The probable number of such transitions in unit time is, from (A-103),

$$\frac{\pi^2}{h^2} \mu^2 \mathcal{E}^2 (m|\cos \alpha|n)^2 S_o N_n A \, dX \quad ,$$

where $N_n A \, dX$ is the number of molecules initially in state n. The probable number of induced reverse transitions $m \rightarrow n$, which augment the radiation, is given by the same expression with N_n replaced by N_m. The net rate of energy absorption is therefore

$$-dP = \frac{1}{h} \pi^2 \nu_o (N_n - N_m) \mu^2 \mathcal{E}^2 (m|\cos \alpha|n)^2 S_o A \, dX \quad . \qquad \text{(A-105)}$$

A convenient measure of net absorption is the "absorption coefficient" γ, defined as

$$\gamma = -\frac{1}{P} \frac{dP}{dX} \quad .$$

For frequency ν_o, substitution of (A-104) and (A-105) gives

$$\gamma_o = \frac{8\pi^3 \nu_o (N_n - N_m)}{hc} \mu^2 (m|\cos \alpha|n)^2 S_o \quad . \qquad \text{(A-106)}$$

If the radiation density is low and does not disturb significantly the thermal equilibrium of the gas, the Boltzman distribution law gives (81):

$$N_n - N_m \approx N_n \frac{h\nu_o}{kT} \quad ,$$

so that

$$\gamma_o = \frac{8\pi^3 \nu_o^2 N_n}{ckT} \mu^2 (m|\cos \alpha|n)^2 S_o \quad . \tag{A-107}$$

Selection rules for allowed transitions and relative absorption line intensities (apart from the dependence upon the statistical population of states and the frequency) are obtained from determination of the non-vanishing matrix elements (A-98). It is convenient to resolve the dipole moment into components along the rotor principal axes. Then if the radiation is polarized along a space-fixed axis F,

$$\mu^2 (m|\cos \alpha|n)^2 = \left[\sum_g \mu_g (m|\cos \alpha_{Fg}|n)\right]^2 \quad , \tag{A-108}$$

where g represents each of the principal axes and α_{Fg} is the angle between g and F. The "direction cosines" are usually abbreviated

$$\cos \alpha_{Fg} = \Phi_{Fg} \quad .$$

Selection rules based on the symmetries of ψ_m^o and ψ_n^o can be deduced without actually evaluating the matrix element integrals

$$(m|\Phi_{Fg}|n) = \int_v \psi_m^{o*} \cos \alpha_{Fg} \psi_n^o \, dv \quad . \tag{A-109}$$

In the course of integration over $dv = \sin\theta \, d\theta \, d\varphi \, d\chi$ the inertia ellipsoid is carried through all possible orientations. Each contribution to the integral for a particular orientation is accompanied by a contribution for an orientation which differs by a π-rotation about a principal

axis. Now cos α_{Fg} is unchanged by such rotation about g, but it changes sign for π-rotation about either of the other two principal axes; in the notation of Table 12, it is of species B_g. The eigenfunctions are similarly symmetric or antisymmetric; therefore the integrand of (A-109) is symmetric or antisymmetric with respect to C_2^a, C_2^b, and C_2^c. If it is antisymmetric with respect to any of the three operations, each positive contribution to the integral is cancelled by an equal negative contribution and the integral vanishes. Combinations of symmetries which give totally symmetric integrals are easily determined with the aid of Table 12; the resulting "symmetry selection rules" are listed in Table 13.

Table 13. Symmetry Selection Rules

A Dipole Moment Component	Can Produce Transitions Only Between States of Symmetry Species		
μ_a		$A \rightleftharpoons B_a$	$(++ \rightleftharpoons -+)$
	or	$B_b \rightleftharpoons B_c$	$(-- \rightleftharpoons +-)$
μ_b		$A \rightleftharpoons B_b$	$(++ \rightleftharpoons --)$
	or	$B_a \rightleftharpoons B_c$	$(-+ \rightleftharpoons +-)$
μ_c		$A \rightleftharpoons B_c$	$(++ \rightleftharpoons +-)$
	or	$B_a \rightleftharpoons B_b$	$(-+ \rightleftharpoons --)$

The matrix elements (A-109) have been evaluated by Cross, Hainer, and King (82). They first show that the elements for symmetric

rotor eigenfunctions can be written as the product of three factors, each a simple algebraic function of the integers J, K, or M which appear in its subscript:

$$(JKM|\Phi_{Fg}|J'K'M') = \qquad \text{(A-110)}$$

$$(\Phi_{Fg})_{J;J'}\ (\Phi_{Fg})_{JK;J'K'}\ (\Phi_{Fg})_{JM;J'M'} \quad .$$

All elements vanish except those for

$$J' - J = 0, \pm 1 \quad , \qquad \text{(A-111)}$$

the familiar selection rule for dipole transitions. The factor involving M also vanishes except for $M' - M = 0, \pm 1$; but when there is no fixed external field this fact imposes no meaningful restriction because all states are degenerate in M.

Matrix elements of Φ_{Fg} for asymmetric rotor eigenfunctions can be found as linear combinations of those for the symmetric rotor once the expansion coefficients in (A-90) are known.* Since all the U_{JKM}'s in the expansion of a particular $\psi_{J\tau M}$ have the same J and M, the factors of (A-110) which do not contain K remain factors of $(J\tau M|\Phi_{Fg}|J'\tau'M')$:

$$(J\tau M|\Phi_{Fg}|J'\tau'M') = \qquad \text{(A-112)}$$

$$(\Phi_{Fg})_{J;J'}\ (\Phi_{Fg})_{J\tau;J'\tau'}\ (\Phi_{Fg})_{JM;J'M'} \quad .$$

---

*This of course amounts to applying to the matrix of Φ_{Fg} the same transformation that diagonalizes the asymmetric rotor Hamiltonian matrix.

The selection rule (A-111) therefore still applies.

The squares of these matrix elements (in the sense of (A-101)) are needed in (A-108). For plane-polarized radiation in the absence of a fixed external field, F may be taken to be the space-fixed Z axis; the third factor in (A-112) then vanishes except when M' = M. The total transition probability between states $J\tau$, $J'\tau'$ is obtained by summing the squared direction cosine matrix elements over the degenerate M states. The appropriate elements for use in (A-108) and (A-107) are then

$$(J\tau\,|\,\Phi_{Zg}\,|\,J'\tau')^2 = \sum_M (J\tau M\,|\,\Phi_{Zg}\,|\,J'\tau' M)^2 \quad . \qquad \text{(A-113)}$$

Cross, Hainer, and King (82) have calculated and tabulated quantities called "line strengths" which are these elements multiplied by 3;

$$(J\tau\,|\,\Phi_{Zg}\,|\,J'\tau')^2 = \frac{1}{3}\lambda_g\,(J\tau;J'\tau') \quad . \qquad \text{(A-113')}$$

Their tables, which have been reprinted in the text by Townes and Schawlow (35), list $\lambda_g \times 10^4$ for K = -1, - 0.5, 0, 0.5, 1; J = 0 to 12. Direct inspection of the tables is the most reliable method of determining the allowed transitions for a rotor of specific asymmetry.

Restrictions imposed by identical nuclei.--The presence of identical nuclei in a molecule imposes restrictions on the extent to which stationary states predicted by rotor theory are actually populated. Identical nuclei are those which if interchanged render a molecular configuration indistinguishable from the original one; e.g., two O^{16} nuclei

in nitryl chloride. Since the probability densities of the indistinguishable configurations must be the same, the wavefunctions describing the configuration of the molecule as a whole must be either symmetric or antisymmetric with respect to any sequence of operations whose only effect is to interchange the nuclei.

It has been found experimentally that without exception systems having identical nuclei of half-integral spin populate only their antisymmetric states; such nuclei are said to obey Fermi-Dirac statistics. Similarly, only the symmetric states of systems having identical nuclei of zero or integral spin are populated; such nuclei are said to obey Bose-Einstein statistics.

To the degree of approximation appropriate here, the total molecular wavefunction can be regarded as the product of separate rotational, vibrational, electronic, and nuclear spin wavefunctions:

$$\psi_t = \psi_r \psi_v \psi_e \psi_s \quad . \qquad \text{(A-114)}$$

The coordinates appearing in ψ_r are the Euler angles of Figure 10. Those in ψ_v can be taken to be the cartesian coordinates of individual nuclei in the rotating xyz system; those in ψ_e the coordinates of individual electrons in the same system. The spin function ψ_s specifies the projections of the nuclear spins on some fixed direction (83). The interchange symmetry of ψ_t can be determined by examining the behaviors of the individual factors under a sequence of operations whose end effect is only an exchange of nuclei. The relative extents to which states having antisymmetric and symmetric configuration functions

$\psi_r\psi_v\psi_e$ are populated (i.e., their "statistical weights") are established by the number of available antisymmetric or symmetric spin functions with which the configuration functions can be associated to produce the requisite symmetry of ψ_t.

In the theory of molecular vibrations it is convenient to effect a transformation from the set of cartesian coordinates $x_i y_i z_i$ of individual nuclei to so-called "normal coordinates" Q_k corresponding to the normal modes of oscillation of a classical system of intercoupled particles (84, 85). When such a system oscillates in a normal mode, all particles execute simple harmonic motions of the same frequency in phase unison. The instantaneous cartesian-coordinate displacements of all particles from their equilibrium positions remain in fixed ratios to one another throughout the vibration. The motion of the entire assembly is then described by the single normal coordinate

$$Q_k = Q_k^o \cos (2\pi\nu_k t + \beta_k) \quad , \qquad \text{(A-115)}$$

where ν_k is the frequency characteristic of the mode, together with a specification of the fixed amplitude ratios. Any arbitrary motion of the system can be described by a superposition of such normal modes with appropriate amplitudes and phases. A system of N non-colinear particles has (3N-6) independent normal modes of vibration; a linear configuration has (3N-5).

The quantum mechanical treatment of normal vibrations (86, 87) shows that a vibrational wavefunction can be expressed as a product

$$\psi_v = \psi(Q_1)\,\psi(Q_2)\ldots\psi(Q_{3N-6}) \quad , \qquad \text{(A-116)}$$

where each $\psi(Q_k)$ is a Hermite orthogonal function of a single normal coordinate. Each such function is characterized by a frequency ν_k and a quantum number $v_k = 0, 1, 2, \ldots$; the total vibrational energy is the sum

$$E_v = \sum_{k=1}^{3N-6} (v_k + \tfrac{1}{2})h\nu_k \quad . \qquad \text{(A-117)}$$

The state for which all v_k's are zero is called the "ground" vibrational state. A state for which a single v_k is unity and all others are zero is called a "fundamental" vibrational state; if the single non-zero v_k is greater than unity the state is an "overtone." States characterized by more than one non-zero v_k are "combinations." The $\psi(Q_k)$ are even functions of the Q_k for even v_k and odd functions of the Q_k for odd v_k; that is, if Q_k is replaced by $-Q_k$, the function $\psi(Q_k)$ remains unchanged or changes sign for even or odd v_k respectively (88).

Consider now the sequence of operations necessary to effect an interchange of identical nuclei in a planar, Y-shaped molecule like nitryl chloride. The six normal modes of vibration for such molecules are shown in the left-hand column of Figure 11. (89) The small vectors indicate the instantaneous amplitude-ratio relationships among the displacements of the nuclei. An operation C_2^x upon the Euler-angle coordinates produces the configurations in the right-hand column. For the ground vibrational state and for the normal modes ν_1, ν_2, ν_3 the resulting vibrational configuration is indistinguishable from the original one. To complete the exchange it is then only necessary to return all

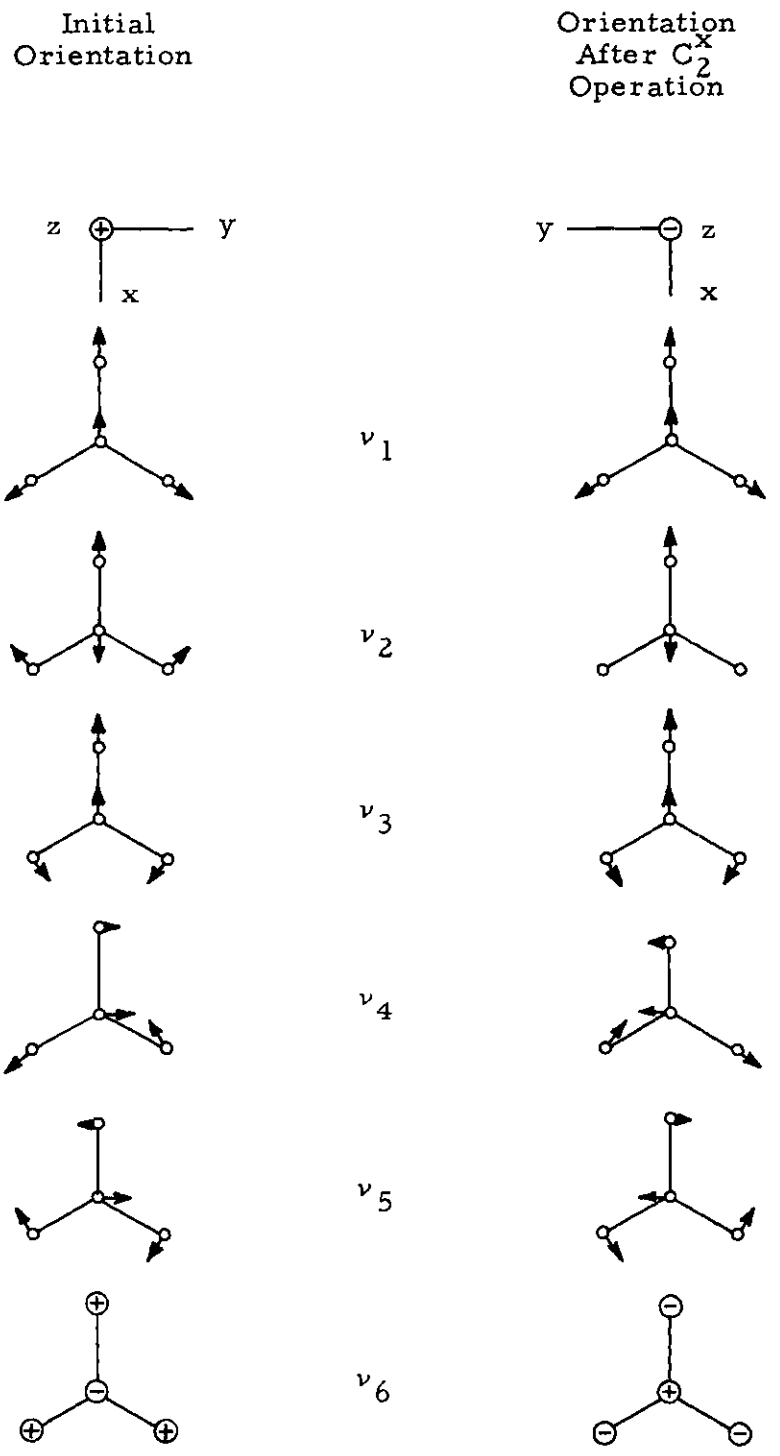

Figure 11. Normal Modes of Vibration of Nitryl Chloride

electrons to their original spatial positions by replacing the coordinates y_i and z_i in ψ_e by their negatives. For modes ν_4, ν_5, ν_6, however, the vibrational configuration is antisymmetric with respect to C_2^x. To restore the original configuration it is further necessary to replace the coordinates Q_4, Q_5, Q_6 by their negatives, which reverses the directions of all displacement vectors. The effect of this operation upon ψ_v is determined by the rule given in the preceding paragraph.

Since O^{16} has zero spin, ψ_t must be interchange-symmetric for the abundant oxygen-isotope species of nitryl chloride; moreover, since no antisymmetric ψ_s exists, the configuration function $\psi_r\psi_v\psi_e$ must itself be symmetric. Nearly all molecules have totally symmetric ground electronic states, and the spectrum of nitryl chloride is consistent with the assumption that it is no exception. Consequently, for the ground vibrational state and for any degree of excitation of vibrational modes ν_1, ν_2, ν_3 only those ψ_r states are populated that are symmetric with respect to π-rotation about the x axis of Figure 11, which for nitryl chloride is the axis a of least moment of inertia. In the Dennison notation, these are the states of symmetry species ++ and -+. The same rotational states are populated if the sum of the vibrational quantum numbers $v_4+v_5+v_6$ is an even number. However, ψ_v for the fundamentals ν_4, ν_5, ν_6 (and for $v_4+v_5+v_6$ odd) is antisymmetric with respect to interchange; in such vibrational states only the antisymmetric ψ_r states +- and -- can be populated.

APPENDIX B

THEORY OF NUCLEAR QUADRUPOLE INTERACTIONS IN ASYMMETRIC-ROTOR MOLECULES

The nature of nuclear quadrupole hyperfine splitting has been discussed briefly in Chapter I. In this appendix the applicable results of the theory are presented in a form that has proved convenient in the application of the theory to analysis of spectra.

Origin of the interaction; classical viewpoint.--The positive electrical charge of a nucleus can be visualized as distributed in a spheroidal cloud, with rotational symmetry about the axis $\underline{s}$ of nuclear spin and reflectional symmetry with respect to a plane perpendicular to $\underline{s}$ through the center of the nucleus. If such a cloud is not perfectly spherical it has an electric quadrupole moment, and it will experience an orientation-dependent torque when placed in a non-uniform external electric field.

An electric quadrupole is in general a tensor quantity, defined by six components of the form

$$Q_{ij} = \int_v \rho(x_i, x_j, x_k) \left[3x_i x_j - r^2 \delta_{ij} \right] dx_i\, dx_j\, dx_k \qquad \text{(B-1)}$$

where $\rho(x_i, x_j, x_k)$ is the charge density of the distribution, v is the volume over which it extends, the x_i's are a set of three cartesian coordinates, and $r^2 = x_i^2 + x_j^2 + x_k^2$. (90) However, the symmetry of the spheroidal charge distribution assumed for the nucleus is such that the

quadrupole moment tensor is diagonal in the nuclear coordinate system s, u, v; where u and v are cartesian coordinates in the plane perpendicular to s. Moreover, the diagonal terms are simply related (91):

$$Q_{uu} = Q_{vv} = -\frac{1}{2} Q_{ss} \quad . \tag{B-2}$$

Therefore it is possible to describe the quadrupolar tensor by a single quantity; this "nuclear quadrupole moment" is defined as

$$Q = \frac{1}{e} Q_{ss} \tag{B-3}$$

where e is the charge of one proton. Q is positive for a prolate nuclear charge spheroid, negative for an oblate spheroid, and zero for a perfect sphere.

The potential energy of a quadrupole in an external electric field described by the potential function V is

$$E_q = \frac{1}{6} \sum_i \sum_j Q_{ij} \frac{\partial^2 V}{\partial x_i \partial x_j} \quad , \tag{B-4}$$

or for the diagonal nuclear quadrupole moment,

$$E_q = \frac{1}{6} Q_{ss} \left[\frac{\partial^2 V}{\partial s^2} - \frac{1}{2} \frac{\partial^2 V}{\partial u^2} - \frac{1}{2} \frac{\partial^2 V}{\partial v^2} \right] \tag{B-5}$$

$$= \frac{1}{6} Q_{ss} \left[\frac{3}{2} \frac{\partial^2 V}{\partial s^2} - \frac{1}{2} \left(\frac{\partial^2 V}{\partial s^2} + \frac{\partial^2 V}{\partial u^2} + \frac{\partial^2 V}{\partial v^2} \right) \right] \quad .$$

Since V is assumed to be due entirely to charges external to the nucleus,

the quantity in parentheses vanishes by Laplace's equation. Thus, with (B-3),

$$E_q = \frac{eQ}{4} \frac{\partial^2 V}{\partial s^2} \quad . \tag{B-6}$$

Quantum-mechanical treatment.--In a molecule the potential V which gives rise to a non-uniform field at the quadrupolar nucleus is due principally to valence-orbital electrons, whose average distribution is constant relative to the molecular principal axes. From (B-4) the quadrupole-interaction Hamiltonian for a single quadrupolar nucleus is

$$H_q = \frac{1}{6} \sum_i \sum_j Q_{ij} \frac{\partial^2 V}{\partial x_i \partial x_j} \tag{B-7}$$

where the x_i are the nuclear coordinates s, u, v. Interrelation of the molecular and the nuclear coordinate systems can be accomplished by transformations which express both the nuclear quadrupole tensor and the molecular field gradient tensor in the space-fixed coordinate system XYZ.

The most general way to determine the allowed energy levels of a rotor with quadrupole interaction is to construct the matrix $(n|H_r + H_q|n')$ in a convenient representation and solve its secular equation (or "diagonalize" the matrix). One suitable representation is that of the rotational-nuclear wavefunctions,

$$\psi^{rn}_{J\tau MIm} = \psi^{r}_{J\tau M} \psi^{n}_{Im} \tag{B-8}$$

where $\psi^{r}_{J\tau M}$ is an asymmetric-rotor eigenfunction (Appendix A), and ψ^{n}_{Im} is a nuclear spin eigenfunction characterized by the spin quantum number I and the quantum number m of the projection of the spin on the space-fixed Z axis. Another representation, particularly appropriate for the field-free rotation of the molecule, is that of the wavefunctions

$$\psi^{rn}_{J\tau IFM_F} = \sum_i C_i \psi^{rn}_{J\tau M_i Im_i} \quad ; \quad M_i + m_i = M_F \quad . \tag{B-9}$$

Here F is the quantum number of the vector resultant of $\vec{J}$ and $\vec{I}$. It can take the values

$$F = I + J,\ I + J - 1,\ I + J - 2, \ldots |I - J| \quad . \tag{B-10}$$

M_F is the quantum number of the projection of $\vec{F}$ on the space-fixed Z axis. Each eigenfunction in the $J\tau IFM_F$ representation is a linear combination of those eigenfunctions in the $J\tau MIm$ representation for which $M + m = M_F$. The expansion coefficients are the "Clebsch-Gordan" or "vector-addition" coefficients (92).

The forms of the matrix elements of H_q in the $J\tau IFM_F$ representation have been given by Bragg (93). The matrix is independent of M_F; the non-vanishing elements are those for $F' = F$; $J' = J,\ J \pm 1,\ J \pm 2$.

First-order theory.--If the quadrupole interaction energy is small compared to the difference between the rotational energy of the state J_τ and that of any other state, the perturbation will cause negligible modification of the J_τ eigenfunctions by mixing with those of other states. In this case the interaction can be handled by conventional first-order perturbation theory. The first-order quadrupole interaction energy E_q,

which is to be added algebraically to the rotational energy $E_{J\tau}$, is given by the value of the single matrix element

$$E_q = (J\tau IFM_F | H_q | J\tau IFM_F) \quad . \tag{B-11}$$

With Bragg's expression for this element one can write

$$E_q = eQq_{J\tau}g(I, J, F) \quad , \tag{B-12}$$

where

$$Q = \frac{1}{e}(Im | Q_{ZZ} | Im)_{m=I} \quad , \tag{B-13}$$

$$q_{J\tau} = (J\tau M \left| \frac{\partial^2 V}{\partial Z^2} \right| J\tau M)_{M=J} \quad , \tag{B-14}$$

$$g(I, J, F) = \frac{(3/4)C(C + 1) - I(I + 1)J(J + 1)}{2I(2I - 1)J(2J - 1)} \quad ; \tag{B-15}$$

$$C = F(F + 1) - I(I + 1) - J(J + 1) \quad . \tag{B-15'}$$

Equation (B-13) is the quantum-mechanical definition of the nuclear quadrupole moment; it corresponds to the classical definition (B-3). Q_{ZZ} is a tensor component of the form (B-1); here the coordinates x_i, x_j, x_k, have their origin at the centroid of the nucleus but have fixed orientation parallel to the space-fixed XYZ axes. Q_{ZZ} is averaged over the spin motion of the nucleus in the state m = I, for which the nuclear symmetry axis s most nearly coincides with Z.

In the factor $q_{J\tau}$ the second derivative of V is taken with respect to the axis x_k parallel to the space-fixed Z axis; it is averaged over the rotational motion of the molecule in the state M = J, for which $\vec{J}$

most nearly coincides with Z. The evaluation of $q_{J\tau}$ is the only feature of the problem that differs for asymmetric, symmetric, and linear rotor molecules.

With the notation $(\partial^2 V/\partial x\, \partial y) = V_{xy}$, etc., one can express V_{ZZ} in terms of the derivatives of V with respect to the rotor principal axes by

$$V_{ZZ} = \Phi_{Za}^2 V_{aa} + \Phi_{Zb}^2 V_{bb} + \Phi_{Zc}^2 V_{cc} \qquad \text{(B-16)}$$

$$+ 2\Phi_{Za}\Phi_{Zb} V_{ab} + 2\Phi_{Za}\Phi_{Zc} V_{ac}$$

$$+ 2\Phi_{Zb}\Phi_{Zc} V_{bc} \quad ,$$

where the Φ's are the direction cosines introduced in Appendix A. Bragg shows (5), that the "cross product" matrix elements

$$(J\tau M|\, \Phi_{Za}\Phi_{Zb}\,|J'\tau' M) \quad , \text{ etc.}, \qquad \text{(B-17)}$$

vanish for $J', \tau' = J, \tau$, so that only the matrix elements of the squared direction cosines appear in (B-14). Bragg and Golden (6) express the Φ_{Zg}^2's in terms of the squared angular momentum operators P_g^2, which also appear in the rotational Hamiltonian. In this manner they are able to derive $q_{J\tau}$ for the state J_τ in terms of the rotor reduced energy $E(\kappa)$ for that state:

$$q_{J\tau} = \frac{1}{(J+1)(2J+3)} \left\{ V_{aa} \left[J(J+1) + E(\kappa) - (\kappa+1)\frac{\partial E(\kappa)}{\partial \kappa} \right] \right. \qquad \text{(B-18)}$$

$$\left. + 2V_{bb}\frac{\partial E(\kappa)}{\partial \kappa} + V_{cc}\left[J(J+1) - E(\kappa) + (\kappa-1)\frac{\partial E(\kappa)}{\partial \kappa} \right] \right\} .$$

In substituting this expression in (B-12), one obtains as factors the "quadrupole coupling constants,"

$$\chi_{aa} = eQV_{aa} \quad ; \quad \chi_{bb} = eQV_{bb} \quad ; \quad \chi_{cc} = eQV_{cc} \quad . \tag{B-19}$$

Since V obeys Laplace's equation, the relation

$$\chi_{aa} + \chi_{bb} + \chi_{cc} = 0 \tag{B-20}$$

can be used to effect a simplification. Appropriate factoring yields the expression

$$E_q = G(J, \tau)\, f(I, J, F) \quad , \tag{B-21}$$

where $G(J, \tau) = A(J, \tau)\, \chi_+ + B(J, \tau)\, \chi_-$, (B-22)

$$A(J, \tau) = 1 - \frac{3}{J(J+1)} \frac{\partial E(\kappa)}{\partial \kappa} \tag{B-23}$$

$$B(J, \tau) = \frac{1}{J(J+1)} \left[E(\kappa) - \kappa \frac{\partial E(\kappa)}{\partial \kappa} \right] \quad , \tag{B-24}$$

$$\chi_+ = \chi_{aa} + \chi_{cc} \quad ; \quad \chi_- = \chi_{aa} - \chi_{cc} \quad , \tag{B-25}$$

$$f(I, J, F) = \frac{J}{2J+3}\, g(I, J, F) \quad . \tag{B-26}$$

The factor f(I, J, F) is known as Casimir's function; it is tabulated in the books by Townes and Schawlow (94) and by Gordy, Smith, and Trambarulo (95).

Table 14. Coefficients for Evaluation of Quadrupole Interaction Energies in Asymmetric-Rotor Molecules

$J\tau$	$A(J,\tau)$	$B(J,\tau)$
0_0	0	0
1_1	$-1/2$	$1/2$
1_0	1	0
1_{-1}	$-1/2$	$-1/2$
2_2	$\frac{-\kappa}{\sqrt{\kappa^2+3}}$	$\frac{1}{\sqrt{\kappa^2+3}}$
2_1	$1/2$	$1/2$
2_0	-1	0
2_{-1}	$1/2$	$-1/2$
2_{-2}	$\frac{\kappa}{\sqrt{\kappa^2+3}}$	$\frac{-1}{\sqrt{\kappa^2+3}}$

(Continued)

Table 14. (Continued)

$J\tau$	$A(J,\tau)$	$B(J,\tau)$
$^3_3$	$-\frac{1}{4}\left[1+\frac{8\kappa-6}{\sqrt{4\kappa^2-6\kappa+6}}\right]$	$\frac{1}{4}\left[1-\frac{2\kappa-4}{\sqrt{4\kappa^2-6\kappa+6}}\right]$
$^3_2$	$\frac{1}{2}\left[1-\frac{\kappa}{\sqrt{\kappa^2+15}}\right]$	$\frac{1}{2}\left[\frac{5}{\sqrt{\kappa^2+15}}\right]$
$^3_1$	$-\frac{1}{4}\left[1+\frac{8\kappa+6}{\sqrt{4\kappa^2+6\kappa+6}}\right]$	$-\frac{1}{4}\left[1-\frac{2\kappa+4}{\sqrt{4\kappa^2+6\kappa+6}}\right]$
$^3_0$	0	0
$^3_{-1}$	$-\frac{1}{4}\left[1-\frac{8\kappa-6}{\sqrt{4\kappa^2-6\kappa+6}}\right]$	$\frac{1}{4}\left[1+\frac{2\kappa-4}{\sqrt{4\kappa^2-6\kappa+6}}\right]$
$^3_{-2}$	$\frac{1}{2}\left[1+\frac{\kappa}{\sqrt{\kappa^2+15}}\right]$	$-\frac{1}{2}\left[\frac{5}{\sqrt{\kappa^2+15}}\right]$
$^3_{-3}$	$-\frac{1}{4}\left[1-\frac{8\kappa+6}{\sqrt{4\kappa^2+6\kappa+6}}\right]$	$-\frac{1}{4}\left[1+\frac{2\kappa+4}{\sqrt{4\kappa^2+6\kappa+6}}\right]$

It is sometimes convenient to write explicitly

$$G(J,\tau) = C(J,\tau)\,\chi_{aa} + D(J,\tau)\,\chi_{cc} \quad , \tag{B-27}$$

where

$$C(J,\tau) = A(J,\tau) + B(J,\tau) \quad , \tag{B-28}$$

$$D(J,\tau) = A(J,\tau) - B(J,\tau) \quad . \tag{B-28}$$

For calculation of the coefficients $A(J,\tau)$ and $B(J,\tau)$, $E(\kappa)$ and its derivative can be found by interpolation in reduced energy tables (36). However, for low-J energy levels $A(J,\tau)$ and $B(J,\tau)$ can be expressed as explicit functions of κ; these expressions are given in Table 14 for the levels through $J = 3$.

It is customary to express the quadrupole coupling constants in megacycles; in this usage Planck's constant is an implicit divisor of eQV_{gg} in the definitions (B-19). Equation (B-21) then gives E_q/h in megacycles.

The Mizushima treatment of the combined Stark and quadrupole perturbations (Appendix C) uses the $J'\tau' = J\tau$ matrix elements of H_q in the $J\tau MIm$ representation (B-8). These elements have been evaluated by Kellogg et al. (96); they can be written:

$$(J\tau MIm|H_q|J\tau M'Im') = Z(J,\tau)\,(Mm|T|M'm') \quad , \tag{B-29}$$

where

$$Z(J,\tau) = \frac{G(J,\tau)}{2I(2I-1)(2J-1)(2J+3)} \quad , \tag{B-30}$$

$$(Mm|T|Mm) = \tfrac{1}{2}[3m^2 - I(I+1)]\,[3M^2 - J(J+1)] \quad , \tag{B-31}$$

$$(Mm|T|M-1, m+1) = \frac{3}{4}(2M-1)(2m+1)[(J+M)(J-M+1)(I-m)(I+m+1)]^{\frac{1}{2}} , \quad \text{(B-32)}$$

$$(Mm|T|M+1, m-1) = \frac{3}{4}(2M+1)(2m-1)[(J-M)(J+M+1)(I+m)(I-m+1)]^{\frac{1}{2}} , \quad \text{(B-33)}$$

$$(Mm|T|M-2, m+2) = \frac{3}{4}[(J+M)(J+M-1)(J-M+1)(J-M+2) \times (I-m)(I-m-1)(I+m+1)(I+m+2)]^{\frac{1}{2}} , \quad \text{(B-34)}$$

$$(Mm|T|M+2, m-2) = \frac{3}{4}[(J-M)(J-M-1)(J+M+1)(J+M+2) \times (I+m)(I+m-1)(I-m+1)(I-m+2)]^{\frac{1}{2}} . \quad \text{(B-35)}$$

Limitations of first-order theory.--In an asymmetric rotor one often finds pairs of rotational levels for which the energy separation is not many times greater than the quadrupole interaction energy. If H_q has a non-vanishing matrix element connecting a pair of such states, the perturbation will cause intermixing of their wavefunctions. The first-order treatment, in which the average value of the interaction energy is evaluated with the eigenfunction of one state only, then becomes inaccurate. The correct allowed rotational-plus-interaction energies for the two near-degenerate states can be determined, however, by solving the quadratic secular equation of the 2×2 matrix $(n|H_r + H_q|n')$:

$$\begin{vmatrix} E_{J\tau}(1) + (1|H_q|1) - E & (1|H_q|2) \\ (2|H_q|1) & E_{J\tau}(2) + (2|H_q|2) - E \end{vmatrix} = 0 , \qquad (B-36)$$

where $n, n' = 1, 2$ represent the quantum-number labels of the two states.

While Bragg (93) has given the forms of the off-diagonal elements of H_q, the factors

$$(J\tau M|V_{ZZ}|J'\tau' M)_{M=J} \qquad (B-37)$$

which appear in them (analogous to $q_{J\tau}$) have not yet been evaluated for $J'\tau' \neq J\tau$.

The most frequently occurring pairs of near-degenerate states are those adjacent levels of the same J which would be completely degenerate in the symmetric-rotor limit. From a symmetry argument Bragg shows that for these levels the only contribution to (B-37) comes from one of the direction-cosine cross products (B-17). The matrix element connecting the states therefore contains a cross-derivative of V as a factor. Fortunately, in nitryl chloride and in numerous other molecules the structural configuration is such that the inertial principal axes are also principal axes of the field gradient tensor. All cross-derivatives of V then vanish and no degeneracy effects are observed.

Characteristics of hyperfine structure.--The selection rule for hyperfine structure is

$$\Delta F = 0, \pm 1 , \qquad (B-38)$$

which is to be used in conjunction with the selection rules for pure

rotational transitions discussed in Appendix A. Relative intensities of the hyperfine components are strongly dependent upon ΔF; they can be found from published tables (94, 95).

If the quadrupole interaction energy is written in the form (B-21), with χ's expressed in megacycles, the frequency of the hyperfine component $J\tau F \rightarrow J'\tau'F'$ is

$$\nu = \nu_o + G(J',\tau')\, f(IJ'F') - G(J,\tau)\, f(IJF) \quad , \tag{B-39}$$

where ν_o is the unperturbed "group-center" frequency for the transition $J_\tau \rightarrow J'_{\tau'}$. The frequency separation between two such hyperfine components of the same transition is therefore

$$\nu_1 - \nu_2 = \left[f(IJ'F'_1) - f(IJ'F'_2)\right]\, G(J',\tau') - \left[f(IJF_1) - f(IJF_2)\right]\, G(J,\tau) \quad . \tag{B-40}$$

As a preliminary step in the analysis of spectra, it is helpful to prepare a table of the numerical values of the bracketed coefficients of the G's for the spacings between all pairs of hyperfine components of each transition of interest. This can be done quite readily by reference to tables of Casimir's function, and it will generally be found that certain pairs of spacings are either equal or otherwise simply related in magnitude regardless of the values of the molecular parameters $G(J,\tau)$ and $G(J',\tau')$. This result, a consequence of the simple rational-fraction form of f(IJF), is useful in the identification of components. Furthermore, certain spacings can often be found from which numerical values of the G's can be determined immediately, thus leading quickly to first

estimates of the quadrupole coupling constants. Because the spacing relations determined in this manner depend only upon I, J, and J', and are independent of τ and the G's, one table suffices for several transitions and applies to any molecule with the same I.

Maximum likelihood calculation of quadrupole couplings.--The process of calculating quadrupole couplings is one of successive refinement, closely connected with the determination of group-center frequencies and the calculation of rotational constants. A first estimate of group-center frequencies from intensity-weighted averages of hyperfine component frequencies will generally permit calculation of the rotational constants and κ with sufficient accuracy for making first estimates of the quadrupole coupling constants. These couplings in turn permit a more accurate determination of group-center frequencies, from which κ can be obtained with sufficient accuracy for use in calculation of precise quadrupole couplings. Finally, the rotational constants can be revised if necessary, using precise group-center frequencies.

If appropriate transitions can be observed, various spacings may be found such that each depends strongly upon a different coupling constant; in this case a quick solution from the expressions for $G(J, \tau)$ is likely to be accurate. However, when spacings are small or when the experimental data are limited (as for nitryl chloride, where many energy levels are not populated), the quadrupole coupling determination becomes quite sensitive to frequency-measurement errors. It is then important to make efficient use of all available data.

Numerous equations of the form (B-40) can be written for the spacings among various hyperfine components of observed transitions.

These equations represent an overdetermined set in χ_{aa} and χ_{cc}; they will be slightly inconsistent because of frequency measurement errors. This situation suggests application of the "method of least squares" (97), whereby values of χ_{aa} and χ_{cc} can be chosen to minimize the sum of the squares of the differences between the measured and the calculated line spacings. However, the merit of this procedure depends upon certain discretion in its use; it is necessary to consider in what sense a least-squares fitting of experimental data may be considered a "best" fit (98).

Let X_i represent the measured value of a physical quantity for which the calculated or theoretical value is $X_i^o(\alpha, \beta, \ldots)$; where $\alpha, \beta, \ldots$ are parameters in the theoretical expression. If the hypothesis is made that X_i^o is the actual exact value of the quantity, the difference

$$x_i = (X_i - X_i^o) \tag{B-41}$$

must be attributed to experimental measurement error. If such errors are random and are characterized by the "normal" or "Gaussian" distribution law with standard deviation σ, the amplitude of the probability density function at $x = x_i$ is

$$w(x_i) = \frac{1}{\sigma\sqrt{2\pi}} e^{-\frac{1}{2\sigma^2} x_i^2} \tag{B-42}$$

Suppose that a number of different quantities $X_1, X_2, \ldots$ have been measured, to which there correspond theoretical values $X_1^o, X_2^o, \ldots$, all functions of the same parameters $\alpha, \beta, \ldots$. If (and only if) the measurement errors are independent of each other and are characterized by the same standard deviation, the over-all probability density for the set of

errors $x_1, x_2, \ldots$ is given by the product

$$w(x_1, x_2, \ldots) = \prod_{i=1}^{n} w(x_i) = \left(\frac{1}{\sigma\sqrt{2\pi}}\right)^n e^{-\frac{1}{2\sigma^2}\sum_i x_i^2} \quad . \qquad \text{(B-43)}$$

A logical objective of data-fitting is the adjustment of the parameters $\alpha, \beta, \ldots$ to maximize the likelihood that the residual differences x_i are due to random measurement errors. This condition requires that the exponent factor

$$\sum_i x_i^2$$

be minimized, the "principle of least squares." The validity of this principle rests upon the assumptions that the measurement errors are independent of each other and have the same standard deviation.

In general the errors in an indiscriminately selected set of hyperfine component spacings will not be independent, and a least-squares reduction of such data will not give "maximum likelihood" values of the quadrupole couplings. The independent errors are those in the individual line-frequency measurements. It is possible to select spacings and combinations of spacings which represent a complete set of independent, equally weighted "statistical degrees of freedom;" but it is more straightforward to express the χ's directly in terms of individual line frequencies.

Let ν_i be the measured frequency of one of the n hyperfine components of the transition $J\tau \rightarrow J'\tau'$. The frequency ν_i^o calculated from

the first-order theory is given by the right-hand side of (B-39); it may be written

$$\nu_i^o = \nu_o + c_i\chi_{aa} + d_i\chi_{cc} \quad , \tag{B-44}$$

where

$$c_i = C(J'\tau')\, f(IJ'F_i') - C(J\tau)\, f(IJF_i) \quad ,$$

$$d_i = D(J'\tau')\, f(IJ'F_i') - D(J\tau)\, f(IJF_i) \quad .$$

Here c_i and d_i are numerical coefficients obtained by inserting f's from published tables and C, D's from equations (B-28, 23, 24). The expressions of the form (B-44) for i = 1, 2, . . . n constitute an overdetermined set in the unknowns ν_o, χ_{aa}, χ_{cc}, which are to be chosen to minimize the sum

$$\sum_i (\nu_i - \nu_i^o)^2 = \sum_i (\nu_i - \nu_o - c_i\chi_{aa} - d_i\chi_{cc})^2 \quad . \tag{B-45}$$

Minimization of this quantity is accomplished by requiring that its derivatives with respect to ν_o, χ_{aa}, and χ_{cc} each vanish. These conditions give the following three linear equations to be solved simultaneously for the three unknowns:

$$\sum_i \nu_i = \sum_i (\nu_o + c_i\chi_{aa} + d_i\chi_{cc}) \quad , \tag{B-46}$$

$$\sum_i c_i\nu_i = \sum_i (c_i\nu_o + c_i^2\chi_{aa} + c_i d_i\chi_{cc}) \quad , \tag{B-47}$$

$$\sum_i d_i\nu_i = \sum_i (d_i\nu_o + c_i d_i\chi_{aa} + d_i^2\chi_{cc}) \quad . \tag{B-48}$$

The first of these equations can be written

$$\nu_o = \frac{1}{n} \sum_i (\nu_i - c_i\chi_{aa} - d_i\chi_{cc}) \quad . \tag{B-49}$$

As might have been expected, it states that the maximum-likelihood value of the group-center frequency is the arithmetic mean of the individual line frequencies minus their quadrupole-interaction shifts as calculated with maximum-likelihood χ's.

Substitution of (B-49) in (B-47) and (B-48) gives the following two equations, from which χ_{aa} and χ_{cc} can be obtained readily.

$$\sum_i c_i S_i = \sum_i [\, c_i(c_i - \bar{c})\, \chi_{aa} + c_i(d_i - \bar{d})\, \chi_{cc} \,] \quad , \tag{B-50}$$

$$\sum_i d_i S_i = \sum_i [\, d_i(c_i - \bar{c})\, \chi_{aa} + d_i(d_i - \bar{d})\, \chi_{cc} \,] \quad , \tag{B-51}$$

where

$$S_i = (\nu_i - \bar{\nu}) \quad , \tag{B-52}$$

$$\bar{\nu} = \frac{1}{n} \sum_i \nu_i \quad , \tag{B-53}$$

$$\bar{c} = \frac{1}{n} \sum_i c_i \quad , \tag{B-54}$$

$$\bar{d} = \frac{1}{n} \sum_i d_i \quad . \tag{B-55}$$

The summations should include all well-resolved lines of the transition; it is reasonable to assume that all such lines are measured with equal probable error. Lines not well-resolved can be excluded

from consideration; n then becomes the number of lines included in the determination. For a strong determination of the quadrupole couplings, it is desirable to perform a maximum-likelihood fitting of the hyperfine structures of several transitions simultaneously. Values of $\overline{\nu}$, $\overline{c}$, and $\overline{d}$ must of course be calculated for each transition separately, but once this is done the lines of all transitions can be included in the single pair of summations (B-50) and (B-51).

Illustration of maximum-likelihood data reduction.--Consider, for example, the J_τ: $^2_{-2} \rightarrow {}^3_{-3}$ transition of NO_2Cl^{37}. Appendix D lists the measured frequencies of seven hyperfine components, all well-resolved:

$F = 3/2 \rightarrow F' = 3/2$; $\nu_1 = 25,369.52$ Mc

$F = 5/2$, $F' = 5/2$; $\nu_2 = 25,364.68$

$F = 5/2$, $F' = 7/2$; $\nu_3 = 25,356.38$

$F = 7/2$, $F' = 9/2$; $\nu_4 = 25,355.97$

$F = 3/2$, $F' = 5/2$; $\nu_5 = 25,351.64$

$F = 1/2$, $F' = 3/2$; $\nu_6 = 25,351.20$

$F = 7/2$, $F' = 7/2$; $\nu_7 = 25,338.08$.

The arithmetic mean of the measured frequencies is $\overline{\nu} = 25,355.353$ Mc, and the spacings from the mean are:

$S_1 = 14.167$ Mc $\qquad S_5 = -3.713$

$S_2 = 9.327 \qquad S_6 = -4.153$

$S_3 = 1.027 \qquad S_7 = -17.273$.

$S_4 = 0.617$

The tables of Townes and Schawlow (94) give the following values of Casimir's function, f(IJF), for I = 3/2; they are rational fractions which could have been obtained from (B-26) and (B-15).

J	F	f(IJF)
2	7/2	0.071429
	5/2	-0.178571
	3/2	0
	1/2	0.250000
3	9/2	0.083333
	7/2	-0.166667
	5/2	-0.050000
	3/2	0.200000

The final values of the NO_2Cl^{37} rotational constants, listed in Table 2, Chapter IV, give $\kappa = (2B-A-C)/(A-C) = -0.71308$. From equations (B-28) and Table 14, one finds

$$C(2,-2) = -0.914572 \qquad D(2,-2) = 0.153180$$
$$C(3,-3) = -0.793937 \qquad D(3,-3) = 0.370143 \quad .$$

The coefficients c_i and d_i in equation (B-44) are therefore:

$$c_1 = -0.1587874 \qquad d_1 = 0.0740286$$
$$c_2 = -0.1236192 \qquad d_2 = 0.0088464$$
$$c_3 = -0.0309932 \qquad d_3 = -0.0343370$$
$$c_4 = -0.0008345 \qquad d_4 = 0.0199038$$
$$c_5 = 0.0396968 \qquad d_5 = -0.0185072$$
$$c_6 = 0.0698556 \qquad d_6 = 0.0357336$$
$$c_7 = 0.1976498 \qquad d_7 = -0.0726320 \quad .$$

The arithmetic means of the coefficients are $\overline{c} = -0.0010046$; $\overline{d} = 0.0018623$. Consequently,

$$
\begin{aligned}
c_1 - \overline{c} &= -0.1577828 & d_1 - \overline{d} &= 0.0721663 \\
c_2 - \overline{c} &= -0.1226146 & d_2 - \overline{d} &= 0.0069841 \\
c_3 - \overline{c} &= -0.0299886 & d_3 - \overline{d} &= -0.0361993 \\
c_4 - \overline{c} &= 0.0001701 & d_4 - \overline{d} &= 0.0180415 \\
c_5 - \overline{c} &= 0.0407014 & d_5 - \overline{d} &= -0.0203695 \\
c_6 - \overline{c} &= 0.0708602 & d_6 - \overline{d} &= 0.0338713 \\
c_7 - \overline{c} &= 0.1986544 & d_7 - \overline{d} &= -0.0744943 \quad .
\end{aligned}
$$

The summed coefficients appearing in equations (B-50) and (B-51) are now found to be:

$$\sum_i c_i(c_i - \overline{c}) = 0.08697044$$

$$\sum_i d_i(d_i - \overline{d}) = 0.01400421$$

$$\sum_i c_i(d_i - \overline{d}) = \sum_i d_i(c_i - \overline{c}) = -0.02438188$$

$$\sum_i c_i S_i = -7.28639 \text{ Mc}$$

$$\sum_i d_i S_i = 2.28318 \text{ Mc}.$$

The two equations thus become:

$$-7.28639 \text{ Mc} = 0.08697044\, \chi_{aa} - 0.02438188\, \chi_{cc}$$

$$2.28318 \text{ Mc} = -0.02438188\, \chi_{aa} + 0.01400421\, \chi_{cc} \quad .$$

These equations are readily solved, e. g. by Cramer's rule, for the χ's:

$$\chi_{aa} = -74.38 \text{ Mc}$$
$$\chi_{cc} = 33.54 \text{ Mc}.$$

Use of the final rotational constants has changed χ_{cc} by 0.17 Mc from the value found in the preliminary fitting (Table 6, Chapter IV); χ_{aa} is unchanged. The refinement in the determination that results from including lines of all J: $2 \rightarrow 3$ transitions has been discussed in Chapter IV.

APPENDIX C

THEORY OF THE STARK EFFECT IN ASYMMETRIC-ROTOR MOLECULES

The theory of the Stark effect for the asymmetric rotor has been summarized in Chapter I. In this appendix the applicable results of the theory are presented and discussed in greater detail.

Stark effect in the absence of quadrupole interaction.--If a rotor having an electric dipole moment μ is subjected to an external electric field of strength $\mathcal{E}$, the rotor Hamiltonian operator includes the Stark-effect interaction energy term

$$H_s = -\mu \mathcal{E} \cos \alpha \quad , \tag{C-1}$$

where α is the angle of orientation of μ with respect to $\mathcal{E}$. This perturbation has the same form as the one considered in the discussion of transition probabilities and selection rules in Appendix A, where $\mathcal{E}$ was the oscillating field of an electromagnetic wave. The Stark-effect problem differs only in that the applied field is to be regarded as fixed.* Several properties of H_s therefore can be established immediately from the radiation-interaction discussion.

---

*This assumption does not exclude fields that are switched at a slow rate in the time scale of molecular processes, as in a Stark-modulated spectrograph. Stark effects for more rapidly varying fields are discussed by Townes and Schawlow (99).

The matrix elements of cos α (and consequently of H_s) for asymmetric-rotor states $J\tau M$ and $J'\tau'M'$ vanish except for $J - J' = 0, \pm 1$ and $M - M' = 0, \pm 1$. It is convenient to let the direction of the fixed field define the space-fixed Z axis, and to resolve the dipole moment into components along the rotor principal axes; then

$$H_s = -\mathcal{E} \sum_g \mu_g \Phi_{Zg} \quad , \tag{C-2}$$

where as before g represents each of the principal axes and Φ_{Zg} is the cosine of the angle between Z and g. Letting the field define Z results in no loss of generality and it simplifies the problem; one will recall that the matrix elements of Φ_{Zg} vanish except for $M' = M$.

The direction cosine matrix elements further vanish except for states whose symmetries with respect to π-rotation about an inertial principal axis are paired as in Table 13. In every case they vanish for states of the same symmetry, so that in particular

$$(J\tau M | H_s | J\tau M) = 0 \quad . \tag{C-3}$$

In perturbation theory this matrix element, the quantum-mechanical "average" of the interaction energy for the state $J\tau M$, gives the first-order perturbation energy; the fact that it vanishes here shows that the asymmetric rotor exhibits no first-order Stark effect. One could proceed directly to the conventional second-order perturbation energy expression, but the importance of near-degeneracy effects makes it desirable to take a different approach.

The nature of the complication that arises in the case of near-degeneracy has been pointed out in Chapter I. The problem has been worked out completely in an elegant manner by Golden and Wilson (7). For the usual situation where the energy of the level of interest is close to that of only one other state, their result can be obtained by an elementary method which shows more clearly how the transition occurs from the non-degenerate to the degenerate case.

A quite general way to determine the allowed energy levels of a rotor in an external electric field is to construct the matrix $(J\tau M|H_r+H_q|J'\tau'M')$ and solve its secular equation (or "diagonalize the matrix). Since the matrix is diagonal in M, one can treat the submatrices for the various M's separately. The submatrices have diagonal elements $E_r(J_\tau)$ and off-diagonal elements of H_s connecting various states for which $J-J' = 0, \pm 1$. Now conventional non-degenerate perturbation theory provides a technique for finding approximate values of those roots of the secular equation that lie near a given unperturbed level, say $E_r(n)$. Margenau and Murphy (100) show that the second-order perturbation approximation corresponds to retaining only those off-diagonal elements of the secular determinant that involve the state n, and replacing all other off-diagonal elements by zero. In the present treatment it is desired to admit the possibility of degeneracy between a pair of states, say "1" and "2". It is necessary therefore to retain off-diagonal elements involving both states, and the secular determinant takes the form:

$$\begin{vmatrix} E_r(1)-E & (1|H_s|2) & (1|H_s|3) & (1|H_s|4) & (1|H_s|5) & \longrightarrow \\ (2|H_s|1) & E_r(2)-E & (2|H_s|3) & (2|H_s|4) & (2|H_s|5) & \longrightarrow \\ (3|H_s|1) & (3|H_s|2) & E_r(3)-E & 0 & 0 & 0 \\ (4|H_s|1) & (4|H_s|2) & 0 & E_r(4)-E & 0 & 0 \\ (5|H_s|1) & (5|H_s|2) & 0 & 0 & E_r(5)-E & 0 \\ \downarrow & \downarrow & 0 & 0 & 0 & \searrow \end{vmatrix}$$

The off-diagonal elements in the third through $n^{\underline{th}}$ rows can be eliminated by subtracting multiples of the third through $n^{\underline{th}}$ columns from the first two columns. Multiply the third column by $(3|H_s|1)/[E_r(3) - E]$ and subtract the result from the first column; multiply the third column by $(3|H_s|2)/[E_r(3) - E]$ and subtract the result from the second column. This operation eliminates off-diagonal elements from the third row. Continuing in this fashion for the remaining fourth through $n^{\underline{th}}$ rows, one obtains:

$$\begin{vmatrix} A_{11} & A_{12} & (1|H_s|3) & (1|H_s|4) & (1|H_s|5) & \longrightarrow \\ A_{21} & A_{22} & (2|H_s|3) & (2|H_s|4) & (2|H_s|5) & \longrightarrow \\ 0 & 0 & E_r(3)-E & 0 & 0 & 0 \\ 0 & 0 & 0 & E_r(4)-E & 0 & 0 \\ 0 & 0 & 0 & 0 & E_r(5)-E & 0 \\ 0 & 0 & 0 & 0 & 0 & \searrow \end{vmatrix}$$

where $$A_{11} = [E_r(1) - E] - \sum_{n\neq 1,2} \frac{(1|H_s|n)(n|H_s|1)}{E_r(n) - E} \quad ,$$

$$A_{22} = [\, E_r(2) - E] - \sum_{n\neq 1,2} \frac{(2|H_s|n)(n|H_s|2)}{E_r(n) - E} \quad ,$$

$$A_{12} = (1|H_s|2) - \sum_{n\neq 1,2} \frac{(1|H_s|n)(n|H_s|2)}{E_r(n) - E} \quad ,$$

$$A_{21} = (2|H_s|1) - \sum_{n\neq 1,2} \frac{(2|H_s|n)(n|H_s|1)}{E_r(n) - E} \quad .$$

The secular equation for roots near $E_r(1)$ or $E_r(2)$ is therefore

$$A_{11}A_{22} - A_{21}A_{12} = 0 \quad ,$$

or

$$[\, E-E_r(1)][\, E-E_r(2)] - [\, E-E_r(2)] \sum_{n\neq 1,2} \frac{(1|H_s|n)^2}{E-E_r(n)} \qquad \text{(C-4)}$$

$$- [\, E-E_r(1)] \sum_{n\neq 1,2} \frac{(2|H_s|n)^2}{E-E_r(n)}$$

$$+ \sum_{n\neq 1,2} \frac{(1|H_s|n)^2}{E-E_r(n)} \sum_{n\neq 1,2} \frac{(2|H_s|n)^2}{E-E_r(n)}$$

$$- (1|H_s|2)^2 + (1|H_s|2) \sum_{n\neq 1,2} \frac{(2|H_s|n)(n|H_s|1)}{E-E_r(n)}$$

$$+(2|H_s|1) \sum_{n\neq 1,2} \frac{(1|H_s|n)(n|H_s|2)}{E-E_r(n)}$$

$$+ \sum_{n\neq 1,2} \frac{(1|H_s|n)(n|H_s|2)}{E-E_r(n)} \sum_{n\neq 1,2} \frac{(2|H_s|n)(n|H_s|1)}{E-E_r(n)} = 0.$$

The squares of matrix elements are taken in the sense

$$(m|H_s|n)^2 = (m|H_s|n)^* (m|H_s|n) = (m|H_s|n)(n|H_s|m) \quad ,$$

where use has been made of the Hermitian character of H_s. Terms of the form $[E_r(n) - E]$ have been written as $-[E - E_r(n)]$.

In the non-degenerate situation one seeks solutions for E near $E_r(1)$, with the assumption that the difference between E and $E_r(1)$ is very small compared to the difference $E - E_r(n)$, $n \neq 1$. Terms of the form $[E - E_r(n)]$ in (C-4) then can be replaced by $[E_r(1) - E_r(n)]$, $n \neq 1$. Upon making this substitution, dropping terms of higher than second order,† and dividing through by $[E_r(1) - E_r(2)]$, one obtains:

$$E - E_r(1) = \frac{(1|H_s|2)^2}{E_r(1) - E_r(2)} + \frac{E - E_r(1)}{E_r(1) - E_r(2)} \sum_{n \neq 1,2} \frac{(2|H_s|n)^2}{E_r(1) - E_r(2)}$$

$$+ \sum_{n \neq 1,2} \frac{(1|H_s|n)^2}{E_r(1) - E_r(n)} \quad .$$

---

†The third order terms vanish anyway, as can be shown through a symmetry argument indicated by Golden and Wilson (7). Clearly the terms vanish individually except when states 1, 2, and n are of three different symmetries. In this situation, inspection of Table 12 will show that the three elements of H_s in each product involve three different components of μ. Table I of Cross, Hainer, and King (82) shows that of the three direction-cosine matrix elements involved, two are real and one is imaginary. But because of the Hermitian character of H_s, the two third-order terms in (C-4) are mutually complex conjugate; therefore they cancel.

Since the assumption has been made that the ratio multiplying the middle term is very small, the term can be dropped. The term in $(1|H_s|2)$ can be included in the third-term summation. The result is the expression for the conventional second-order perturbation energy:

$$E - E_r(1) = \sum_{n\neq 1,2} \frac{(1|H_s|n)^2}{E_r(1)-E_r(n)} \quad . \tag{C-5}$$

In the case of near-degeneracy between $E_r(1)$ and $E_r(2)$, the difference $[E - E_r(1)]$ is no longer very small compared to $[E - E_r(2)]$. It then is appropriate to obtain solutions near $E_r(1)$ by retaining E as an unknown in $[E - E_r(2)]$, while replacing it by $E_r(1)$ as before in $[E - E_r(n)]$, $n\neq 1, 2$. Equation (C-4) becomes a quadratic in E, easily solved. Actually, if $[E_r(1) - E_r(2)]$ is small compared to $[E - E_r(n)]$, $n\neq 1, 2$, it makes little difference whether E in the latter expression is replaced by $E_r(1)$ or by $E_r(2)$. By replacing it by $E_r(2)$ in the denominators of terms involving $(2|H_s|n)$ and by $E_r(1)$ in the denominators of terms involving $(1|H_s|n)$, one can put the secular equation (C-4) in a symmetrical form from which the Stark energies associated with both levels can be obtained simultaneously. Dropping the last three higher-order terms,† one obtains from the quadratic-solution formula:

---

†See preceding footnote.

$$E = \frac{1}{2}\left[E_r(1) + \sum_{n\neq 1,2} \frac{(1|H_s|n)^2}{E_r(1)-E_r(n)}\right] \qquad \text{(C-6)}$$

$$+\frac{1}{2}\left[E_r(2) + \sum_{n\neq 1,2} \frac{(2|H_s|n)^2}{E_r(2)-E_r(n)}\right]$$

$$\pm\frac{1}{2}\left[\left\{\left[E_r(1) + \sum_{n\neq 1,2} \frac{(1|H_s|n)^2}{E_r(1)-E_r(n)}\right]\right.\right.$$

$$\left.\left. -\left[E_r(2) + \sum_{n\neq 1,2} \frac{(2|H_s|n)^2}{E_r(2)-E_r(n)}\right]\right\}^2 + 4(1|H_s|2)^2\right]^{1/2} .$$

This is Golden and Wilson's result for the case of two near-degenerate levels. Energies near the larger E_r are obtained with the positive square root; those near the smaller E_r with the negative square root. For the nearly degenerate levels of a "slightly asymmetric" rotor, $4(1|H_s|2)^2$ becomes the dominant term of the radicand and a predominantly first-order Stark effect results. The summation terms then represent a second-order correction, probably ignorable. For the same type of near-degeneracy in a more asymmetric rotor like nitryl chloride the entire expression should be used.

With substitution from (C-2) the squared matrix elements of H_s in equations (C-5) or (C-6) take the form

$$(J\tau M|H_s|J'\tau' M)^2 = \mu_g^2 \mathcal{E}^2 (J\tau M|\Phi_{Zg}|J'\tau' M)^2 \quad , \qquad \text{(C-7)}$$

where g is the one axis for which the direction-cosine matrix element does not vanish for the particular symmetries of states $J\tau$ and $J'\tau'$. It will be recalled from equations (A-113) and (A-113') that

$$\sum_{M} (J\tau M|\Phi_{Zg}|J'\tau' M)^2 = \frac{1}{3}\lambda_g(J\tau;J'\tau') \quad ,$$

where $\lambda_g(J\tau;J'\tau')$ is the "line strength" tabulated by Cross, Hainer, and King (82, 35). The summation over M involves only the factor $(\Phi_{Zg})_{JM;J'M}$ in equation (A-112). Consequently,

$$(J\tau M|\Phi_{Zg}|J'\tau' M)^2 = \frac{\left[(\Phi_{Zg})_{JM;J'M}\right]^2}{\sum_{J} 3\sum_{M=-J}\left[(\Phi_{Zg})_{JM;J'M}\right]^2}\lambda_g(J\tau;J'\tau') \quad ,$$

where (82)

$$\left[(\Phi_{Zg})_{JM;JM}\right]^2 = 4M^2$$

$$\left[(\Phi_{Zg})_{JM;J-1,M}\right]^2 = 4\left[J^2 - M^2\right]$$

$$\left[(\Phi_{Zg})_{JM;J+1,M}\right]^2 = 4\left[(J+1)^2 - M^2\right] \quad .$$

The sum over M in each case can be put in closed form with use of the fact that the sum of the squares of the first N integers is $(1/6)N(N+1)(2N+1)$. One obtains

$$(J\tau M|\Phi_{Zg}|J\tau' M)^2 = \frac{M^2}{J(J+1)(2J+1)}\lambda_g(J\tau;J\tau') \quad , \qquad (C-8)$$

$$(J\tau M|\Phi_{Zg}|J-1,\tau'M)^2 = \frac{J^2 - M^2}{J(2J+1)(2J-1)}\,\lambda_g(J\tau;J-1,\tau') \quad , \qquad (C-9)$$

$$(J\tau M|\Phi_{Zg}|J+1,\tau'M)^2 = \frac{(J+1)^2 - M^2}{(J+1)(2J+1)(2J+3)}\,\lambda_g(J\tau;J+1,\tau'). \qquad (C-10)$$

In the non-degenerate situation, insertion of (C-7) in (C-5) gives a "quadratic" Stark effect in which the energy-level shift is proportional to the square of the field strength. For complete or almost complete degeneracy, (C-6) gives a "linear" Stark effect in which the shift is directly proportional to the field strength. "Near" degeneracy results in a "transitional" Stark effect, intermediate between the limiting cases.

In the foregoing equations, energies are expressed in ergs when μ and $\mathcal{E}$ are expressed in electrostatic cgs units. All energies E_i can be replaced by E_i/h in megacycles per second if $\mu_g\mathcal{E}$ in (C-7) is replaced by $(\mu_g\mathcal{E})/h$ in megacycles per second:

$$\frac{\mu\mathcal{E}}{h}\,(\text{in Mc}) = 0.5035\,\mu(\text{in debye})\;\mathcal{E}\,(\text{in volts/cm}) \quad ;$$

$$1 \text{ debye} = 10^{-18} \text{ esu}.$$

Stark-effect selection rules depend upon the orientation of the radiation electric field with respect to the static field, which defines the space-fixed Z axis. In the conventional microwave spectrograph the fields are essentially parallel. The squared direction-cosine matrix element in the absorption-coefficient expressions (A-107, 108) then becomes $(J\tau M|\Phi_{Zg}|J'\tau'M')^2$, which vanishes except for M=M'. "Line

strengths" of Stark components for various M's are given by the applicable expression (C-8), (C-9), or (C-10). For $M \neq 0$ the expression must be doubled to sum the transition probabilities for the degenerate +M and -M states. If the radiation electric field has a component perpendicular to the static field, the matrix elements $(J\tau M|\Phi_{Xg}|J'\tau'M')^2$ and $(J\tau M|\Phi_{Yg}|J'\tau'M')^2$ will give rise to transitions $M' = M \pm 1$. Transitions of this type due to imperfect field parallelism in the conventional spectrograph are ordinarily quite weak (101).

Stark effect in the presence of quadrupole interaction.--The combined Stark and quadrupole-interaction effects can be handled by simple perturbation theory only when one perturbation is much weaker than the other one. In the case of general interest, however, the two effects are of the same order of magnitude. The problem could be handled in a straightforward but very laborious manner by constructing the entire matrix $(m|H_r+H_s+H_q|n)$ in a convenient representation and solving its secular equation.

Mizushima (8) has proposed a much simpler secular determinant, constructed from the elements

$$E_{rs}(J\tau M) + (J\tau MIm|H_q|J\tau MIm) - E \qquad \text{(on-diagonal)}, \quad \text{(C-11)}$$

$$(J\tau MIm|H_q|J\tau M'Im') \qquad \text{(off-diagonal)}.$$

Here $E_{rs}(J\tau M)$ is the combined rotational and Stark-effect energy for the state $J\tau M$, calculated by second-order perturbation theory for the rotor without quadrupole interaction; i.e., the energy "E" of equation (C-5). The H_q matrix elements are those in the $J\tau MIm$ representation,

given by equations (B-29) through (B-35). The determinant is diagonal in $J\tau$, and also (as inspection of the aforementioned equations will show) in the sum $M_F = M + m$.

It is evident that Mizushima's method amounts to evaluating the matrix elements $(m|H_r+H_s+H_q|n)$ with eigenfunctions of H_r+H_s and assuming that the elements of H_q thus obtained are negligibly different from those obtained with eigenfunctions of H_r only. The propriety of this assumption has been discussed by Eagle (9), who shows that if the Stark and quadrupole perturbations are of the same general magnitude, the neglected corrections to the energies are of about the same magnitude as the neglected higher-order Stark energy terms. This argument holds for the situation in which the $J\tau$ off-diagonal elements of H_q due to cross-derivatives of the potential function V vanish or are negligibly small. (See Appendix B.)

The highest order of the M_F subfactors of Mizushima's secular determinant is 2J+1 or 2I+1, whichever is smaller. In general, numerical solutions for the allowed E's are best obtained with the aid of a digital-computer matrix diagonalization routine. However, the energy of the component for which M+m = J+I can be obtained immediately from a first-degree secular equation:

$$E = E_{rs} + (J\tau JII|H_q|J\tau JII) \quad .$$

That is, the energy for $M_F = J+I$ is equal to the sum of the rotational energy, the zero-field quadrupole-interaction energy for F = J+I, and the Stark energy of the rotor without quadrupole interaction.

The Stark-effect selection rule $\Delta M = 0$ still holds for the strong-field case in the presence of quadrupole interaction, and tends to predominate in the intermediate-field case also. In the latter situation the quadrupole interaction intermixes the rotational wavefunctions for various M's to a degree which decreases with increasing field. It is usually easy to identify the dominant M character of a Stark component by the magnitude of its displacement. For weak fields the intermixing is more complete, and the selection rule is more adequately represented by $\Delta M_F = 0$.

Mizushima does not consider degeneracy effects, and his method is inaccurate in the near-degenerate case. Obviously a substantial improvement in accuracy can be accomplished simply by obtaining E_{rs} from (C-6) instead of from (C-5) for insertion in the Mizushima secular determinant. However, the effect of ignoring the relatively large intermixing of the wavefunctions of the closely-spaced states in calculating the matrix elements of H_q is then of real concern. A fortunate situation occurs for the near-degenerate states 2_1 and 2_2 of nitryl chloride; the elements $(2_1|H_q|2_2)$ vanish because of the symmetry of the potential function V, and the elements $(2_2|H_q|2_2)$ are nearly equal to the elements $(2_1|H_q|2_1)$. One therefore would expect the use of the correct E_{rs} in the Mizushima determinant to give an accurate description of the combined interactions, and this is confirmed by the calculations discussed in Chapter IV.

The significance of the degeneracy problem, correctly assessed by Golden and Wilson, has not been universally appreciated. Mizushima

comments (8), "Golden and Wilson discussed the case of accidental degeneracy of rotational levels, but since such a case was never found actually, the second-order formula will be enough in discussing experimental results." Elsewhere (102) one reads, "It should be pointed out, however, that, although such degeneracies are possible, coincidences to within, say, 50 Mc are rare. Quadratic Stark effects as large as this are seldom observed because of the large fields necessary." Actually even for coincidences within a few hundred megacycles one has not a quadratic but a transitional Stark effect, and large Stark shifts result. It is important to be able to handle these cases correctly; it seems evident that often, as in nitryl chloride, only the transitional Stark effects will produce shifts large enough for accurate measurement in dipole moment determinations. A further investigation of this problem is being carried out by Eagle (10).

APPENDIX D

SPECTRUM OF NITRYL CHLORIDE; 25,000 - 40,600 MC

Table 15 lists the measured absorption line frequencies for molecules in the ground vibration state. Where frequencies are listed to 0.01 Mc, it is estimated that measurement errors seldom exceed 0.05 Mc and are more often around 0.02 Mc. Where difficulty was encountered in resolving weak lines from noise or from adjacent strong lines, frequencies are listed to 0.1 Mc.

Measured and calculated group-center frequencies (the frequencies of the rotational transitions without quadrupole splitting) are listed for each transition. The measured group-center frequency ν_o^m was determined by taking the measured line frequencies of the group, subtracting the calculated quadrupole-splitting displacements $\Delta\nu_q$, and averaging. The group-center frequency ν_o^c was calculated from the rotational constants listed in Table 2, Chapter IV. The column headed "$\nu_o^m + \Delta\nu_q$" gives the sum of the measured group-center frequency and the calculated quadrupole interaction shift for each line. Frequencies in the column headed "Calculated Frequency ($\nu_o^c + \Delta\nu_q$)" were determined entirely by calculation.

Table 15. Spectrum of Nitryl Chloride; 25,000 - 40,600 Mc.

Transition $J_\tau \rightarrow J'_{\tau'}$	Transition F→F'	Theoretical Relative Intensity	NO_2Cl^{35} Measured Frequency	NO_2Cl^{35} $\nu_o^m+\Delta\nu_q$	NO_2Cl^{35} Calculated Frequency $(\nu_o^c+\Delta\nu_q)$	NO_2Cl^{37} Measured Frequency	NO_2Cl^{37} $\nu_o^m+\Delta\nu_q$	NO_2Cl^{37} Calculated Frequency $(\nu_o^c+\Delta\nu_q)$
$2_{-2}\rightarrow 3_{-3}$			25 986.49=ν_o^m		ν_o^c= 25 986.48	25 355.22=ν_o^m		ν_o^c= 25 355.19
	3/2-3/2	4.00	26 004.59	26 004.60	26 004.59	25 369.52	25 369.53	25 369.51
	5/2-5/2	5.22	25 998.57	25 998.56	25 998.55	25 364.68	25 364.73	25 364.71
	5/2-7/2	24.5	25 988.01	25 988.00	25 987.99	25 356.38	25 356.38	25 356.35
	7/2-9/2	35.7	25 987.43	25 987.40	25 987.39	25 355.97	25 355.94	25 355.92
	3/2-5/2	16.0	25 981.95	25 981.95	25 981.95	25 351.64	25 351.64	25 351.61
	1/2-3/2	10.0	25 981.33	25 981.36	25 981.35	25 351.20	25 351.20	25 351.18
	7/2-7/2	4.08	obscured*	25 964.76	25 964.75	25 338.08	25 338.05	25 338.02
$2_1 \rightarrow 3_0$			26 684.67=ν_o^m		ν_o^c= 26 684.70	25 977.93=ν_o^m		ν_o^c= 25 977.96
	1/2 **	10	26 708.33	26 708.35	26 708.38	25 996.61	25 996.57	25 996.61
	7/2 **	40	26 691.44	26 691.44	26 691.46	25 983.23	25 983.25	25 983.29
	3/2 **	20	26 684.68	26 684.67	26 684.70	25 977.92	25 977.93	25 977.96
	5/2 **	30	26 667.77	26 667.76	26 667.79	25 964.60	25 964.61	25 964.64

*Obscured by NO_2Cl^{37} line, $2_1 \rightarrow 3_0$; F_2 = 5/2.

**3_0 level degenerate in F.

Table 15. Spectrum of Nitryl Chloride; 25,000 - 40,600 Mc. (Continued)

Transition $J_\tau \rightarrow J'_{\tau'}$	$F \rightarrow F'$	Theoretical Relative Intensity	NO_2Cl^{35} Measured Frequency	NO_2Cl^{35} $\nu_o^m + \Delta_q$	NO_2Cl^{35} Calculated Frequency $(\nu_o^c + \Delta\nu_q)$	NO_2Cl^{37} Measured Frequency	NO_2Cl^{37} $\nu_o^m + \Delta\nu_q$	NO_2Cl^{37} Calculated Frequency $(\nu_o^c + \Delta\nu_q)$
$2_2 \rightarrow 3_1$			*27 382.92 = ν_o^m		ν_o^c = 27 382.92	*26 600.74 = ν_o^m		ν_o^c = 26 600.73
	1/2-3/2	10.0	27 407.00	27 406.99	27 406.99	26 619.69	26 619.68	26 619.66
	7/2-9/2	35.7	27 389.88	27 389.90	27 389.91	26 606.22	26 606.23	26 606.22
	7/2-7/2	4.08	27 388.8	27 388.86	27 388.87	not reslvd.	26 605.48	26 605.47
	3/2-3/2	4.00	27 383.8	27 383.75	27 383.75	26 601.4	26 601.34	26 601.33
	3/2-5/2	16.0	27 382.73	27 382.71	27 382.71	26 600.60	26 600.59	26 600.58
	5/2-5/2	5.22	27 366.1	27 366.11	27 366.11	26 587.5	26 587.50	26 587.49
	5/2-7/2	24.5	27 365.61	27 365.63	27 365.63	26 587.14	26 587.15	26 587.14
$3_{-3} \rightarrow 4_{-4}$			*33 932.71 = ν_o^m		ν_o^c = 33 933.30	33 158.89 = ν_o^m		ν_o^c = 33 159.47
	5/2-5/2	2.30	33 953.0	33 952.94	33 953.53	not meas.	33 174.91	33 175.49
	7/2-7/2	3.02	33 941.4	33 941.52	33 942.11	not meas.	33 165.84	33 166.43
	7/2-9/2	25.5	33 933.83	33 933.81	33 934.40	33 159.75	33 159.74	33 160.32
	9/2-11/2	33.3	33 933.17	33 933.16	33 933.75	33 159.29	33 159.26	33 159.84
	5/2-7/2	19.1	33 930.97	33 930.96	33 931.55	33 157.49	33 157.49	33 158.07
	3/2-5/2	14.3	33 930.27	33 930.31	33 930.90	33 156.97	33 157.01	33 157.60
	9/2-9/2	2.31	33 911.19	33 911.18	33 911.77	not meas.	33 141.84	33 142.42

*Obtained from the four principal lines only.

Table 15. Spectrum of Nitryl Chloride; 25,000 - 40,600 Mc. (Continued)

Transition $J_\tau \rightarrow J'_{\tau'}$	$F \rightarrow F'$	Theoretical Relative Intensity	NO_2Cl^{35} Measured Frequency	NO_2Cl^{35} $\nu_o^m + \Delta\nu_q$	NO_2Cl^{35} Calculated Frequency $(\nu_o^c + \Delta\nu_q)$	NO_2Cl^{37} Measured Frequency	NO_2Cl^{37} $\nu_o^m + \Delta_q$	NO_2Cl^{37} Calculated Frequency $(\nu_o^c + \Delta\nu_q)$
$3_0 \rightarrow 4_{-1}$			35 439.63 $= \nu_o^m$		$\nu_o^c = 35\,439.95$	34 512.83 $= \nu_o^m$		$\nu_o^c = 34\,513.14$
	* 5/2	16.7	35 446.36	35 446.32	35 446.64	34 518.11	34 518.11	34 518.42
	* 11/2	33.3	35 443.08	35 443.04	35 443.36	34 515.53	34 515.52	34 515.83
	* 7/2	22.2	35 436.91	35 436.95	35 437.27	34 510.72	34 510.72	34 511.03
	* 9/2	27.8	35 433.63	35 433.67	35 433.99	34 508.11	34 508.13	34 508.44
$3_1 \rightarrow 4_0$			37 085.46 $= \nu_o^m$		$\nu_o^c = 37\,085.36$	35 990.35 $= \nu_o^m$		$\nu_o^c = 35\,990.25$
	5/2-5/2	2.30	not reslvd.	37 093.56	37 093.46	not reslvd.	35 996.65	35 996.55
	3/2-5/2	14.3	37 092.52	37 092.52	37 092.42	35 995.90	35 995.91	35 995.80
	9/2-11/2	33.3	37 089.15	37 089.13	37 089.03	35 993.27	35 993.24	35 993.13
	7/2-7/2	3.02	not reslvd.	37 082.99	37 082.89	not reslvd.	35 988.39	35 988.29
	5/2-7/2	19.1	37 082.50	37 082.51	37 082.41	35 988.03	35 988.04	35 987.94
	7/2-9/2	25.5	37 079.11	37 079.12	37 079.02	35 985.36	35 985.37	35 985.27
	9/2-9/2	2.31	not reslvd.	37 078.08	37 077.98	not reslvd.	35 984.63	35 984.52

*3_0 level degenerate in F.

Table 15. Spectrum of Nitryl Chloride; 25,000 - 40,600 Mc. (Continued)

Transition J J' , F F'	Theoretical Relative Intensity	Measured Frequency	NO_2Cl^{37} $\nu_o^m + \nu_q$	Calculated Frequency $(\nu_o^c + \nu_q)$
$4_{-4}\ 5_{-5}$		40 600.57 = ν_o^m		ν_o^c = 40 602.78
7/2-7/2	1.48	not meas.	40 616.88	40 619.09
9/2-9/2	1.96	not meas.	40 605.99	40 608.20
9/2-11/2	25.8	40 601.22	40 601.19	40 603.41
11/2-13/2	31.8	40 600.75	40 600.77	40 602.98
7/2-9/2	20.7	40 599.89	40 599.88	40 602.09
5/2-7/2	16.7	40 599.43	40 599.46	40 601.67
11/2-11/2	1.49	not meas.	40 583.77	40 585.99

APPENDIX E

EXCITED VIBRATION SPECTRUM

In addition to the strong absorption lines of the primary spectrum (Appendix D), a careful search with the chart recorder disclosed the eight groups of weaker lines listed in the accompanying table. A weak group is found a few hundred megacycles below each of the primary transitions $2_1 \rightarrow 3_0$, $2_2 \rightarrow 3_1$, $3_0 \rightarrow 4_1$, and $3_1 \rightarrow 4_0$. Each group exhibits four lines in a pattern which appears identical to that of the principal lines of the corresponding primary transition. Associated weak groups were not observed for the $2_{-2} \rightarrow 3_{-3}$ and the $3_{-3} \rightarrow 4_{-4}$ transitions. These transitions require very high Stark voltages for detection, and the intensities of their weaker counterparts might well be below the sensitivity limit of the spectrograph.

Calculations show that these lines do not result from isotopic forms of nitryl chloride containing N^{15} or O^{18}. They are believed to arise from molecules in an excited vibration state. The normal modes of vibration of nitryl chloride have been indicated in Figure 11, Appendix A. Ryason and Wilson (19) report the following assignments of fundamental frequencies for these modes:

$\nu_1 = 1,293 \text{ cm}^{-1}$ $\qquad$ $\nu_4 = 1,685 \text{ cm}^{-1}$

$\nu_2 = 794 \text{ cm}^{-1}$ $\qquad$ $\nu_5 = 367 \text{ cm}^{-1}$

$\nu_3 = 651 \text{ cm}^{-1}$ $\qquad$ $\nu_6 = 411 \text{ cm}^{-1}$

Lines Attributed to Molecules in an Excited Vibration State

J_τ	NO_2Cl^{35} (Mc)	NO_2Cl^{37} (Mc)
$3_1 \rightarrow 4_0$		35,689.5
	36,740†	35,686.9
	(4 lines)	35,681.7
		35,679.0
$3_0 \rightarrow 4_{-1}$	35,129.4	
	35,126.2	34,210†
	35,120.0	(4 Lines)
	35,116.8	
$2_2 \rightarrow 3_1$	27,165.3	
	27,148.3	26,375†
	27,141.3	*
	27,124.3	26,350†
$2_1 \rightarrow 3_0$	26,450†	25,750†
	*	*
	26,425†	25,730†

† Measurements made with absorption wavemeter.

* The two larger of the four lines are given here.

As is pointed out in Appendix A, restrictions placed on the total molecular wavefunction by the presence of identical oxygen nuclei require that if the transitions observed here are for molecules in a singly excited normal mode, the mode must be either ν_1, ν_2, or ν_3. Of these, the last would be the most highly populated on the basis of Ryason and Wilson's assignments. However, the populations should not be greatly different for any of the following vibrational states, all of which allow transitions of the type observed: ν_2, ν_3, doubly excited ν_5 or ν_6, or $\nu_5 + \nu_6$ combination. Only a single weak group was found associated with each ground-state transition. The more highly populated singly excited ν_5 and ν_6 modes should permit the transitions $^2_0 \rightarrow {}^3_{-1}$ and $^2_{-1} \rightarrow {}^3_{-2}$, which are forbidden in the ground state. A search was made for the $^2_{-1} \rightarrow {}^3_{-2}$ transition, but none was found. These results may indicate that a lower fundamental frequency should be assigned to one of the symmetrical normal modes.

BIBLIOGRAPHY

1. S. C. Wang, "On the Asymmetrical Top in Quantum Mechanics," The Physical Review 34, 243 (1929).

2. B. S. Ray, "Uber die Eigenwerte des asymmetrischen Kreisels," Zeitschrift für Physik 78, 74 (1932).

3. G. W. King, R. M. Hainer, and P. C. Cross, "The Asymmetric Rotor: I. Calculation and Symmetry Classification of Energy Levels," The Journal of Chemical Physics 11, 27 (1943).

4. H. B. G. Casimir, On the Interaction between Atomic Nuclei and Electrons. From Archives due Musée Teyler, Série III, Vol. VIII, Fascicule 3, p. 201. La Haye: Martinus Nijhoff, 1936.

5. J. K. Bragg, "The Interaction of Nuclear Electric Quadrupole Moments with Molecular Rotation in Asymmetric-Top Molecules, I.," The Physical Review 74, 533 (1948).

6. J. K. Bragg and S. Golden, "The Interaction of Nuclear Electric Quadrupole Moments with Molecular Rotation in Asymmetric Top Molecules. II. Approximate Methods for First-Order Coupling," The Physical Review 75, 735 (1949).

7. S. Golden and E. B. Wilson, Jr., "The Stark Effect for a Rigid Asymmetric Rotor," The Journal of Chemical Physics 16, 669 (1948).

8. M. Mizushima, "Theory of the Stark Effect of Asymmetric Rotator with Hyperfine Structure," The Journal of Chemical Physics 21, 539 (1953).

9. D. F. Eagle, Stark Effect and Nuclear Quadrupole Splitting in the Rotation Spectrum of Nitrosyl Bromide. M. S. Thesis, Georgia Institute of Technology, 1956.

10. D. F. Eagle, Ph. D. Thesis, Georgia Institute of Technology, to be published.

11. W. A. Noyes, "Rediscovery of Nitryl Chloride," The Journal of the American Chemical Society 54, 3615 (1932).

12. R. Müller, "Beitrag zur Kenntnifs der Untersalpetersäure," Annalen der Chemie und Pharmacie 122, 1 (1862).

13. K. Dachlauer, Deutch Reich Patent 509405 (1929).

14. H. J. Schumacher and G. Sprenger, "Die Darstellung und Eigenschaften des Nitrylchlorides," Zeitschrift für anorganische und allgemeine Chemie 182, 139 (1929).

15. M. Schmeisser and E. Gregor-Haschke, "Uber das Nitrylchlorid NO_2Cl," Zeitschrift für anorganische Chemie 255, 33 (1948).

16. H. H. Batey and H. H. Sisler, "Some Inorganic Reactions of Nitryl Chloride," The Journal of the American Chemical Society 74, 3408 (1952).

17. R. J. Athey, The Absorption Spectrum of Nitryl Chloride. M. S. Thesis, Georgia Institute of Technology, 1950.

18. W. H. Eberhardt, private communication to M. K. Wilson, June 25, 1953.

19. R. Ryason and M. K. Wilson, "Vibrational Spectrum and Structure of Nitr yl Chloride," The Journal of Chemical Physics 22, 2000 (1954).

20. D. J. Millen and K. M. Sinnott, "The Microwave Spectrum and Structure of Nitryl Chloride," Chemistry and Industry, May 7, 1955, p. 538.

21. L. Cla yton, Q. Williams, and T. L. Weatherly, "Quadrupole Coupling Constants of Nitryl Chloride," Bulletin of the American Physical Soc iety II, 1, 341 (1956).

22. T. L. Weatherly, Q. Williams, and L. Clayton, Determination of Molecular Constants by Microwave and Radio-Frequency Spectroscopy. Final Report, Contract No. DA-01-009ORD-465 (Project A-265). Atlanta: Engineering Experiment Station of the Georgia Institute of Technology, 1957.

23. D. J. Millen and K. M. Sinnott, "The Microwave Spectrum, Structure, and Dipole Moment of Nitryl Chloride," Journal of the Chemical Society (London) 1958, 350 (1958).

24. L. Clayton, Q. Williams, and T. L. W eatherly, "Nitryl Ch loride Molecular Constants from Microwave Spectrum Analysis," Journal of Chemical Physics 30, 1328 (1959); 31, 554 (1959).

25. R. H. Hughes and E. B. Wilson, Jr., "A Microwave Spectrograph," The Physical Review 71, 562 (1947).

26. W. E. Good, New Techniques in Microwave Spectroscopy. Westinghouse Scientific Paper No. 1538. East Pittsburgh: Westinghouse Research Laboratories, 1950.

27. W. Gordy, W. V. Smith, and R. F. Trambarulo, Microwave Spectroscopy. New York: Wiley and Sons, 1953, p. 60.

28. R. R. Unterberger and W. V. Smith, "A Microwave Secondary Frequency Standard," The Review of Scientific Instruments 19, 580 (1948).

29. J. H. Mauldin, A High Voltage Square Wave Generator for Stark Modulation. M.S. Thesis, Georgia Institute of Technology, 1955.

30. Gordy et al., op. cit., p. 57.

31. H. Shechter, F. Conrad, A. L. Daulton, and R. B. Kaplan, "Orientation in Reactions of Nitryl Chloride and Acrylic Systems," The Journal of the American Chemical Society 74, 3052 (1952).

32. L. Pauling, The Nature of the Chemical Bond, 2nd ed. Ithaca: Cornell University Press, 1940, p. 202.

33. Gordy et al., op. cit., p. 111.

34. C. H. Townes and A. L. Schawlow, Microwave Spectroscopy, New York: McGraw-Hill, 1955, p. 105.

35. Ibid., Appendix V.

36. T. E. Turner, B. L. Hicks, and G. Reitwiesner, Asymmetric Rotor Eigenvalue Table. Ballistic Research Laboratories Report No. 878. Aberdeen: Aberdeen Proving Ground, 1953.

37. Gordy, et al., op. cit., p. 308.

38. G. Herzberg, Infrared and Raman Spectra of Polyatomic Molecules. New York: Van Nostrand, 1945, p. 461.

39. Townes and Schawlow, op. cit., p. 644.

40. Gordy, et al., op. cit., p. 338.

41. Townes and Schawlow, op. cit., pp. 236, 237.

42. Y. K. Syrkin and M. E. Dyatkina, Structure of Molecules and the Chemical Bond. New York: Interscience Publishers, Inc., 1950, p. 184.

43. Ibid., p. 225.

44. Ibid., p. 191; Pauling, op. cit., p. 249.

45. Townes and Schawlow, op. cit., pp. 225-244.

46. Syrkin and Dyatkina, op. cit., p. 26.

47. Townes and Schawlow, op. cit., p. 243, 239.

48. Ibid., p. 237.

49. Gordy, et al., op. cit., p. 315.

50. W. G. Palmer, Valency. Cambridge: University Press, 1959, p. 120.

51. J. H. Goldstein, "Quadrupole Coupling and Bond Character in the Vinyl Halides," The Journal of Chemical Physics 24, 106 (1956).

52. Pauling, op. cit., p. 185.

53. Palmer, op. cit., p. 136, p. 127

54. C. A. Coulson and J. Duchesne, "La Molecule N_2O_4 et un Nouveau Type de Liason Chimique," Bulletin de la Classe des Sciences, Academie Royale de Belgique 5-XLIII, 522 (1957).

55. L. Burnelle and J. Duchesne, "Molecular Orbitals and Vibrational Potential Function of Nitryl Fluoride," Nature 182, 653 (1958).

56. Syrkin and Dyatkina, op. cit., pp. 474-478.

57. Pauling, op. cit., p. 46.

58. W. H. Eberhardt, private communication.

59. H. H. Nielsen, "The Vibration-rotation Energies of Molecules and their Spectra in the Infra-red," Handbuch der Physik XXXVII/1, 173 (1959).

60. C. Van Winter, "The Asymmetric Rotator in Quantum Mechanics," Physica 20, 274 (1954).

61. Townes and Schawlow, op. cit., pp. 83 ff.

62. Herzberg, op. cit., pp. 42 ff.

63. Gordy et al., op. cit., pp. 108 ff.

44. Ibid., p. 191; Pauling, op. cit., p. 249.

45. Townes and Schawlow, op. cit., pp. 225-244.

46. Syrkin and Dyatkina, op. cit., p. 26.

47. Townes and Schawlow, op. cit., p. 243, 239.

48. Ibid., p. 237.

49. Gordy, et al., op. cit., p. 315.

50. W. G. Palmer, Valency. Cambridge: University Press, 1959, p. 120.

51. J. H. Goldstein, "Quadrupole Coupling and Bond Character in the Vinyl Halides," The Journal of Chemical Physics 24, 106 (1956).

52. Pauling, op. cit., p. 185.

53. Palmer, op. cit., p. 136, p. 127

54. C. A. Coulson and J. Duchesne, "La Molecule N_2O_4 et un Nouveau Type de Liason Chimique," Bulletin de la Classe des Sciences, Academie Royale de Belgique 5-XLIII, 522 (1957).

55. L. Burnelle and J. Duchesne, "Molecular Orbitals and Vibrational Potential Function of Nitryl Fluoride," Nature 182, 653 (1958).

56. Syrkin and Dyatkina, op. cit., pp. 474-478.

57. Pauling, op. cit., p. 46.

58. W. H. Eberhardt, private communication.

59. H. H. Nielsen, "The Vibration-rotation Energies of Molecules and their Spectra in the Infra-red," Handbuch der Physik XXXVII/1, 173 (1959).

60. C. Van Winter, "The Asymmetric Rotator in Quantum Mechanics," Physica 20, 274 (1954).

61. Townes and Schawlow, op. cit., pp. 83 ff.

62. Herzberg, op. cit., pp. 42 ff.

63. Gordy et al., op. cit., pp. 108 ff.

64. E. E. Witmer, "The Quantization of the Rotational Motion of the Polyatomic Molecule by the New Wave Mechanics," Proceedings of the National Academy of Sciences of the United States of America 13, 60 (1927).

65. Herbert Goldstein, Classical Mechanics. Cambridge: Addison-Wesley Press, Inc., 1951, p. 107.

66. Ibid., p. 134.

67. E. Schrödinger, "Uber das Verhältnis der Heisenberg-Born-Jordanschen Quanten Mechanik zu der Meinen," Annalen der Physik 79, 734 (1926). Equation 31.

68. E. Schrödinger, Collected Papers on Wave Mechanics. London and Glasgow: Blackie and Son Limited, 1928, p. 56.

69. F. Reiche and H. Rademacher, "Die Quantelung des symmetrichen Kreisels nach Schrödingers Undulationsmechanik," Zeitschrift für Physik 39, 444 (1927).

70. R. de L. Kronig and I. I. Rabi, "The Symmetrical Top in the Undulatory Mechanics," The Physical Review 29, 262 (1927).

71. Gordy, et al., op. cit., p. 98.

72. L. Pauling and E. B. Wilson, Introduction to Quantum Mechanics. New York: McGraw-Hill Book Company, Inc., 1935, p. 275.

73. Pauling and Wilson, op. cit., p. 191, p. 280.

74. Schrodinger, Collected Papers, p. 11, p. 55.

75. F. B. Hildebrand, Advanced Calculus for Engineers. New York: Prentice-Hall, Inc., 1949, p. 227.

76. Van Winter, op. cit., p. 282.

77. King, Hainer, and Cross, op. cit., pp. 30, 31.

78. R. S. Mulliken, "Species Classification and Rotational Energy Level Patterns of Non-Linear Triatomic Molecules," The Physical Review 59, 873 (1941).

79. D. M. Dennison, "The Infrared Spectra of Polyatomic Molecules," Reviews of Modern Physics 3, 280 (1931).

80. Pauling and Wilson, op. cit., pp. 294 ff.

81. Gordy et al., op. cit., p. 186.

82. P. C. Cross, R. M. Hainer, and G. W. King, "The Asymmetric Rotor: II. Calculation of Dipole Intensities and Line Classification," The Journal of Chemical Physics 12, 210 (1944).

83. Townes and Schawlow, op. cit., p. 70.

84. Herzberg, op. cit., pp. 61 ff.

85. E. B. Wilson, J. C. Decius, and P. C. Cross, Molecular Vibrations. New York: McGraw-Hill, 1955, pp. 17 ff.

86. Ibid., pp. 34 ff.

87. Herzberg, op. cit., pp. 76 ff.

88. Ibid., p. 80.

89. Ibid., p. 65.

90. M. W. P. Strandberg, Microwave Spectroscopy, New York: John Wiley and Sons, Inc., 1954, p. 31.

91. Townes and Schawlow, op. cit., p. 134.

92. M. E. Rose, Elementary Theory of Angular Momentum. New York: John Wiley and Sons, Inc., 1957, pp. 32 ff.

93. Bragg, Quadrupole Interaction I, p. 537.

94. Townes and Schawlow, op. cit., Appendix I.

95. Gordy et al., op. cit., pp. 374 ff.

96. J. M. B. Kellogg, I. I. Rabi, N. F. Ramsey, and J. R. Zacharias, "An Electrical Quadrupole Moment of the Deuteron," The Physical Review 57, 677 (1940).

97. H. Margenau and G. M. Murphy, The Mathematics of Physics and Chemistry. New York: D. Van Nostrand Company, Inc., 1943, p. 500.

98. Ibid., p. 489.

99. Townes and Schawlow, op. cit., pp. 273 ff.

100. Margenau and Murphy, op. cit., p. 373.

101. Townes and Schawlow, op. cit., p. 266.

102. Gordy et al., op. cit., p. 164.

VITA

Lorimer Clayton, Jr. was born July 28, 1929, in Atlanta, Georgia. He attended public schools in Atlanta and in Clearwater, Florida. In 1947 he graduated from Boys' High School in Atlanta. He married Miss Grace Anne Rosselot in 1950; they now have three children.

Mr. Clayton received the B. S. (1951) and M. S. (1954) degrees in physics from the Georgia Institute of Technology. From 1951 to 1957 he worked at the Georgia Tech Engineering Experiment Station as Research Assistant and Research Physicist. Since 1957 he has been employed by Scientific-Atlanta, Inc., where he is now Assistant Director of Engineering.

Mr. Clayton is a member of Sigma Xi, Phi Kappa Phi, Tau Beta Pi, Sigma Pi Sigma, and the Institute of Radio Engineers.